SYNCHRONIZATION OF LINEARLY AND NONLINEARLY COUPLED HARMONIC OSCILLATORS

A THESIS SUBMITTED TO
THE GRADUATE SCHOOL OF NATURAL AND APPLIED SCIENCES
OF
MIDDLE EAST TECHNICAL UNIVERSITY

BY

ALİ YETKİN PENBEGÜL

IN PARTIAL FULLFILLMENT OF THE REQUIREMENTS
FOR
THE DEGREE OF MASTER OF SCIENCE
IN
ELECTRICAL AND ELECTRONICS ENGINEERING

MAY 2011

Approval of the thesis:

SYNCHRONIZATION OF LINEARLY AND NONLINEARLY COUPLED HARMONIC OSCILLATORS

submitted by **ALİ YETKİN PENBEGÜL** in partial fulfillment of the requirements for the degree of **Master of Science in Electrical and Electronics Engineering Department, Middle East Technical University** by,

Prof. Dr. Canan Özgen
Dean, Graduate School of **Natural and Applied Sciences** _____

Prof. Dr. İsmet Erkmen
Head of Department, **Electrical and Electronics Engineering** _____

Assist. Prof. Dr. S. Emre Tuna
Supervisor, **Electrical and Electronics Engineering Dept., METU** _____

Examining Committee Members:

Prof. Dr. Mübeccel Demirekler
Electrical and Electronics Engineering Dept., METU _____

Assist. Prof. Dr. S. Emre Tuna
Electrical and Electronics Engineering Dept., METU _____

Assist. Prof. Dr. Afşar Saranlı
Electrical and Electronics Engineering Dept., METU _____

Prof. Dr. Kemal Leblebicioğlu
Electrical and Electronics Engineering Dept., METU _____

Dr. Volkan Nalbantoğlu
ASELSAN INC. _____

Date: 25.05.2011

I hereby declare that all information in this document has been obtained and presented in accordance with academic rules and ethical conduct. I also declare that, as required by these rules and conduct, I have fully cited and referenced all material and results that are not original to this work.

Name, Last name : ALİ YETKİN PENBEGÜL

Signature :

ABSTRACT

SYNCHRONIZATION OF LINEARLY AND NONLINEARLY COUPLED HARMONIC OSCILLATORS

Penbegül, Ali Yetkin

M. Sc., Department of Electrical and Electronics Engineering

Supervisor: Assist. Prof. Dr. Sezai Emre Tuna

May 2011, 101 pages

In this thesis, the synchronization in the arrays of identical and non-identical coupled harmonic oscillators is studied. Both linear and nonlinear coupling is considered. The study consists of two main parts. The first part concentrates on theoretical analysis and the second part contains the simulation results.

The first part begins with introducing the harmonic oscillators and the basics of synchronization. Then some theoretical aspects of synchronization of linearly and nonlinearly coupled harmonic oscillators are presented. The theoretical results say that linearly coupled identical harmonic oscillators synchronize for any frequency of oscillation. For nonlinearly coupled identical harmonic oscillators, synchronization is shown to occur at large enough frequency values.

In the second part, the simulator and simulation results are presented. A GUI is designed in MATLAB to run the simulations. In the simulations, synchronization

of coupled harmonic oscillators are studied according to different coupling strength values, different frequency values, different coupling graph types (e.g. all-to-all, ring, tree) and different coupling function types (e.g. linear, saturation, cubic). The simulation results do not only support the theoretical part of the thesis but also give some idea about the part of the synchronization of coupled harmonic oscillators uncovered by theory.

Keywords: Synchronization, coupled harmonic oscillators, linear and nonlinear coupling, coupling graph.

ÖZ

HARMONİK OSİLATÖRLERİN DOĞRUSAL VE DOĞRUSAL OLMAYAN BAĞLAŞIM İLE SENKRONİZASYONU

Penbegül, Ali Yetkin

Yüksek Lisans, Elektrik Elektronik Mühendisliği Bölümü

Tez Yöneticisi: Yrd. Doç. Dr. Sezai Emre Tuna

Mayıs 2011, 101 sayfa

Bu tezde, eş ve eş olmayan bağlaşık harmonik osilatör dizilerinin senkronizasyonu üstünde çalışılmıştır. Çalışmalarda hem doğrusal hem de doğrusal olmayan bağlaşım kullanılmıştır. Tez iki ana bölümden oluşmaktadır. İlk bölümde teorik analizlere ağırlık verilmekte, ikinci bölüm ise simülasyon sonuçlarından oluşmaktadır.

İlk bölüm harmonik osilatörler ve senkronizasyonun temelleri tanıtımı ile başlamıştır. Sonra doğrusal ve doğrusal olmayan bağlaşıma sahip harmonik osilatörler teorik açıdan tanıtılmıştır. Teorik sonuçlar, doğrusal bağlaşıma sahip eş harmonik osilatörler salınım frekans değerinden bağımsız olarak senkronize olduklarını göstermektedir. Doğrusal olmayan bağlaşıma sahip eş harmonik osilatörlerin ise yeterince yüksek frekans değerleri için senkronize oldukları gösterilmiştir.

İkinci bölümde, simülatör tanıtılmış ve simülasyon sonuçları verilmiştir. MATLAB'da bir kullanıcı arayüzü "GUI" tasarlanmış ve tüm simülasyonlar GUI'nin altında koşturulmuştur. Simülasyonlarda bağlaşık harmonik osilatörlerin değişik bağlaşım güçlerine, frekans değerlerine, bağlaşım grafiklerine (örneğin tümü tümüne, çember, ağaç) ve bağlaşım fonksiyonlarına (örneğin doğrusal, saturasyon, kübik) göre çalışılmıştır. Simülasyon sonuçları sadece tezin teorik bölümünü desteklemekle kalmayıp bağlaşık harmonik osilatörlerin senkronizasyonu konusunda teorinin kapsamadığı bölümleri hakkında da fikir vermektedir.

Anahtar Kelimeler: Senkronizasyon, bağlaşık harmonik oscilatörler, doğrusal ve doğrusal olmayan bağlaşım, bağlaşım grafiği.

To My Father,

ACKNOWLEDGEMENTS

First and foremost I offer my sincerest gratitude to my supervisor, Emre Tuna, who has supported me throughout my M.Sc. study with his patience, knowledge, encouragement and belief. He was always there to listen and assist when I needed and without his supervision, this thesis would not have been completed or written.

I would like to express my special thanks to my friends Özsel Kılınç, Şule Akdoğan, Zeynep Kireçci, Önder Altan and all other friends who have been with me during this period. Their friendship, support and encouragement are always significant for me.

I would like to thank my manager Alper Ünsoy and all my other colleagues in Aselsan, for their continuous encouragement, helpfulness and support during the whole process.

I would also like to express gratitude to TÜBİTAK Science Fellowships and Grant Programs Department (BİDEB) for their financial support.

Last but not the least; I would like to thank my beloved family, my mother Esin and my brother Ekin and my fiancée Çiler Akyüz for their continuous support, but especially for their trust in me. I always feel very lucky to be with them.

TABLE OF CONTENTS

LIST OF FIGURES

FIGURES

CHAPTER 1

INTRODUCTION

1.1 GENERAL IDEA ABOUT SYNCHRONIZATION

The word "synchronous" which is often used in the daily life language and in different areas of science (such as synchronous machines, synchronous generators, synchronous communication, synchronous counters and synchronous learning) comes from Greek "$\sigma\acute{\upsilon}\nu$: *syn* = the same, common" and "$\chi\rho\acute{o}\nu\varsigma$: *chronos* = time". If it is translated directly, it means "happening at the same time". Synchronization is the noun form of "synchronous" and it is also related to the different fields such as astronomy, engineering, chemistry, biology, and physics. At first glance synchronization in each different field seems different, but the reality is they usually obey the same universal rules [1].

If we look around carefully, we can see that we are surrounded by full of synchronized objects. For instance, in a concert when people start applauding, initially there is no synchrony but then after a while we can easily recognize the synchrony of applauding audience. Another example is violinists in a concert, they hear the tone of each others' instruments and they start to play synchronously. A biological example is the menstruation period of women. The women, who spend long time together with other women, for example students living in the same room, start to have their menstruation periods in the same days. There are many more examples such as cardiac pacemaker cells and flashing fireflies [1-4]. All aforementioned examples contain an adjustment of the rhythms based on some interaction and this is the basics of the synchronization [1].

1.1.1 Historical Evolution of Synchronization Theory

The very first written description about synchronization is given by Alexander the Great. In the fourth century B.C., while the soldiers were on the way to conquer India, he noticed that the leaves of trees are open in the day time and closed at the night time. Of course, at that time it was just an observation and there was nothing to do with science [3].

There are lots of examples for synchronization in life. People sing and dance together, applause in unison, soldiers march in step. Some people may think that all this synchrony comes from the intelligence of human or any other living organism. Moreover, it can be thought that it is because of the evolution and natural selection in billions of years. However, Cristiaan Huygens, Dutch physicists, showed that this is not the right explanation by observing the process of lifeless synchronization: synchronization of two pendulum clocks [3].

In 1665 Cristiaan Huygens, sitting in his bed for several days because of his illness, had observed the behavior of the two pendulum clocks hanged on the same wooden stick. Huygens was the inventor of these clocks and was working on a solution for longitude measurements that would help seamen find their way. While he was observing the clocks in his bed, he noticed the synchrony in the two clocks. He disturbed rhythms of the clocks, but in half an hour the synchrony was established again. When he put two clocks away from each other, the agreement did not occur. He thought the agreement in the rhythms was due to the interaction of clocks via air. Then he put the clocks close again and put a kind of wall between two clocks to prevent the interaction between clocks. The synchronization was observed again, concluding he was wrong. The air had nothing to do with the synchronization. Therefore, he understood that the synchronization was due to the interaction of clocks through the wooden stick which they were hanged on [1-4].

Although he didn't give a quantitative explanation; Huygens did a great job by explaining the mutual synchronization between two lifeless objects. He correctly understood that the reason of the "sympathy of the clocks" was because of interaction by the help of a common support. In modern terminology this would

mean two clocks are synchronized due to the *coupling* through the wooden beam [1].

Thus, the synchronization of clocks taught us that the reason behind synchronization need not be intelligence or natural selection [3].

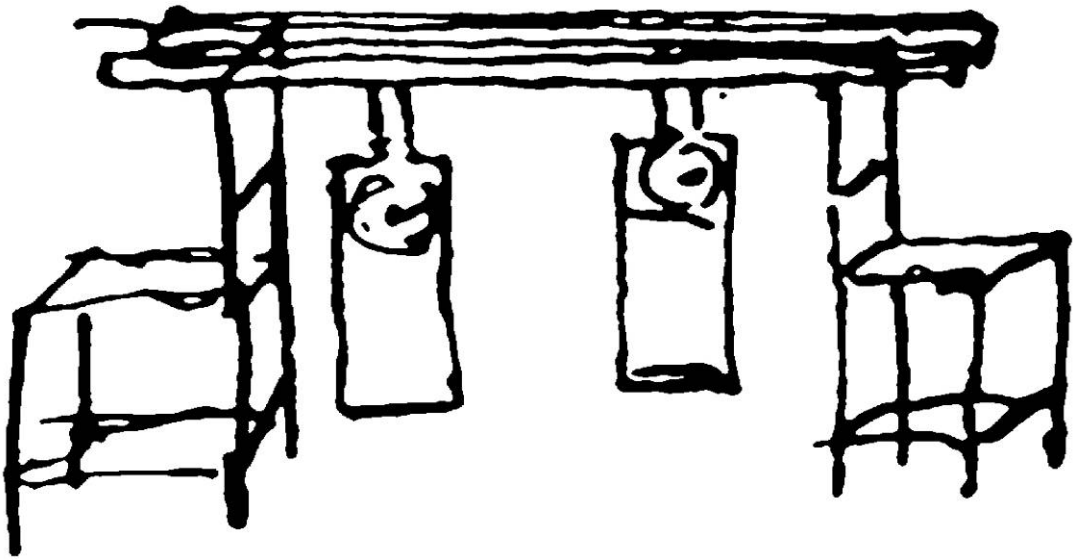

Figure 1.1: An original drawing of Huygens illustrating his experiments with pendulum clocks [1].

Until twentieth century, there has been no big step in understanding synchronization. The development in radio and electrical engineering led people study oscillation in electrical circuits. In 1920 W.H. Eccles and J.H. Vincent discovered the synchronization in triode generators. They coupled two generators with different but close frequencies and they saw that due to the coupling, generators reached the same frequency. A few years later Edward Appleton and Balthasar Van Der Pol improved the studies on the triode generators and came up with first theoretical results. [2, 3]. Nowadays, we can see that synchronization of coupled oscillators is involved in many fields. One example is the ring laser gyroscope used in many application fields including navigation and motion control. At low frequencies two counter-propagating laser beams are synchronized which results in a null output. This example shows that synchronization does not always have good results.

1.1.2 Synchronization: Description and Constraints

As mentioned before, we can define synchronization as *the adjustment of rhythms of mutually and weakly interacting oscillating objects.* What does the description tell us? The description gives the constraints for occurrence of synchronization. These constraints are:

- At least two oscillating objects,
- Weak interaction,
- Adjustment of rhythms.

An oscillating object is any system that performs a periodic behavior. Some examples for oscillating objects are a pendulum clock, a flashing firefly, a triode generator. All those oscillating objects, namely self sustained oscillators, are active systems. They have their own internal energy and their own rhythms. This means even if a flashing firefly is separated from its group and put into a room alone; it will continue to flash due to its internal rhythm. Second property of the self-sustained objects is the oscillation type that is independent of initial values. Last characteristic of the oscillating objects is that small disturbances don't destroy the oscillation. Although the oscillation is disturbed for a while, it will return to its previous periodic movement [1, 4].

What does "weak interaction" or "weak coupling" mean? In the example of Huygens' clocks, the interaction is due to the wooden beam and the wooden beam helps the clocks feel each other by the vibrations through it. In this example "weak" interaction means wooden beam is not fully rigid. If the wooden beam was rigid, there would be a strong coupling which makes the two clocks nondecomposable. Then, the clocks would either stop or move synchronously as one system. However, to talk about synchronization, we need at least two systems. In other words, in strong coupling oscillating objects start to behave as if they are one system and for one system we can not talk about synchronization. Therefore, weak coupling is necessary for occurrence of the synchronization [1].

Adjustment of rhythms in oscillators can be explained as follows. If two uncoupled oscillators have different natural frequency values, f_1 and f_2, and if they are coupled, after some time they will meet in the same frequency value between f_1 and f_2. Of course, there is a limit for $|f_1 - f_2|$ which we call "synchronization region". Outside of this region the synchronization does not occur [1].

1.2 SYNCHRONIZATION vs. CONSENSUS

In the previous section, basics of synchronization and synchronization criteria are introduced. There is another topic which is highly related with synchronization. It is called "consensus". Synchronization and consensus are quite similar topics. However, they still have some differences.

In synchronization one of the criteria is the oscillating objects. However, in consensus, the states or agents do not need to be oscillating. Therefore, in synchronization the individual dynamics of the agents play an important role, but in consensus in the absence of coupling, agents usually have no dynamics. Therefore, in consensus, the emphasis is on the coupling rather than the individual agent [5, 6].

As a result of the differences mentioned above, the consensus is reached at a point and this point has zero or constant velocity. However the equilibrium of synchronization has a time-varying velocity [6].

Although there are some differences between two topics in literature, it is not wrong to use the word "synchronization" instead of "consensus". Consensus can be thought as the special case of synchronization. In the rest of the thesis, consensus examples will be usually stated as synchronization.

1.3 SYNCHRONIZATION IN LIFE

In section 1.1, living synchronization, namely biological synchronization, is mentioned by a few examples. Some other examples about biological synchronization are introduced in this section and by these examples importance of the synchronization in life is explained.

It is essential to note that even if we do not notice, synchronization is always in our life and we sometimes enjoy it. People dance Halay, a kind of Anatolian folk dancing, in Turkey which is a good example of people dancing in synchrony. In addition to that, people sing together in a choir or play music in an orchestra or soldiers march in unison. All these synchronization examples result from practice and intelligence. Therefore, there seems nothing miraculous about these examples. However, pacemaker cells in the heart or nervous system have no intelligence or planning. The fascination is based on the unconsciousness of the synchronizing entities, like crickets chirping in unison, collectively oscillating pancreatic beta cells or fireflies flashing in unison [3].

Nowadays, study of biological clocks is getting more and more popular. Therefore, research related to the internal and external synchronization of human body is very crucial. The lowest and first level synchronization starts in the cells of organs in human body. Cardiac pacemaker cells which are controlling the heart rate are one of the most marvelous examples to the first level synchronization. Second level is the synchrony between organs even if the function of each organ is different. The synchrony between organs means they have the same period and they keep the same beat. These two levels of synchronization are self-sustained, namely endogenous. Therefore, it is called internal synchronization. The last level of synchronization is the circadian rhythm, which means the approximately 24 hours cycle of any living organism, animal, plant or human being. This is the synchronization of the body with outside world parameters like sunshine, food or temperature. This process of synchronization occurring with the adjustment of an external cue is called entrainment.

From the beginning of the thesis, a lot of examples are introduced about both living and non-living synchronization. At this point important question is “in which field does synchronization have to be studied?”: Biology, physics, mathematics, engineering, sociology? The answer is: the topic is related to all and many other fields. The intersection of all these studies is “coupled oscillators”. Crickets that chirp in unison, synchronously flashing fireflies, firing pacemaker cells or coupled pendulum clocks are all group of oscillators and they are interconnected to each

other physically, chemically or in another natural way. These interconnected oscillators are called coupled oscillators.

The simplest type of oscillator is the harmonic oscillator, which constitutes the main study focus of this thesis. Therefore, in the next section, initially, harmonic oscillators are introduced by some examples and then the behavior of coupled harmonic oscillators will be explained.

For more examples and researches about circadian rhythms, see [7-9]; and for more examples about living synchronization, see [3, 10-12].

1.4 HARMONIC OSCILLATORS

Oscillation is the repetition of a measure (e.g. displacement, angle, voltage, current, etc.) in time about an equilibrium value or between two or more states [13]. Oscillation phenomena have wide application range related to physics, biology, mechanics, electronics, optics, etc. For example, circadian rhythms, neural oscillation and insulin release oscillations are biological and human-related oscillations. Periodical motion of the planets in a fixed trajectory which is related to astronomy is also an oscillating system. In fact, oscillators are frequently encountered in the everyday life.

Harmonic oscillator is the simplest type of oscillator. In electronics, it is a circuit generating a sinusoidal signal. In mechanics, it is a system that, when it is disturbed q units from its equilibrium point, generates a force, F=-kq, where k is a positive constant. In general, harmonic oscillator is a system which has a state q varying in time and the solution of state is of the form

$$q(t) = A\sin(wt + \alpha) \tag{1.1}$$

where A is the peak value and w is the frequency of the periodic behavior, i.e. $w = \frac{2\pi}{T}$ where T is the period. See Figure 1.2 [14].

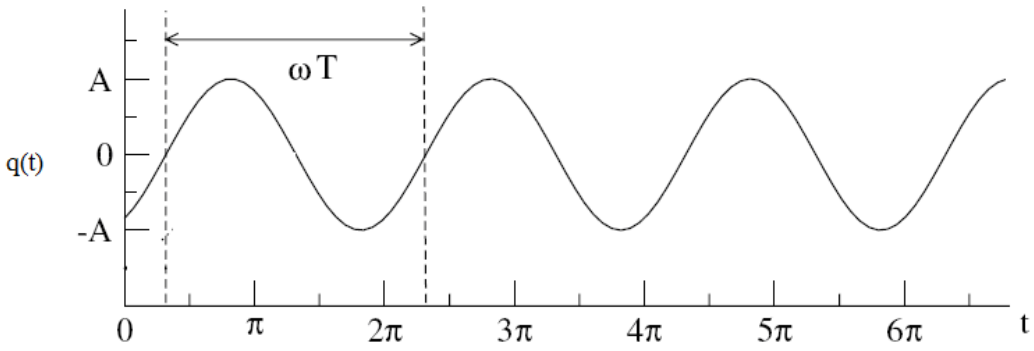

Figure 1.2: Sinusoidal motion of a harmonic oscillator [14].

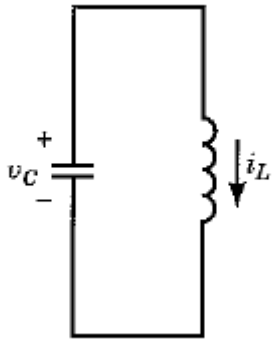

Figure 1.3: Harmonic oscillator circuit [15].

In electronics, an ideal capacitor and an ideal inductor together form a harmonic oscillator, see Figure 1.3. In this circuit, if there is no initial voltage or current, nothing will happen, but if there is initial voltage in the capacitor, then the capacitor voltage will create a current over inductor. As voltage value decreases the energy stored on the capacitors decreases, as well and this energy starts to be stored in the inductor until capacitor voltage value is zero. At this time, inductor has maximum magnetic flux energy. From this time everything goes backwards and current value starts to decrease and capacitor voltage value increases. As current in inductor reaches zero value, voltage in current reaches its maximum value. Moreover, since the capacitor and inductor are ideal and assuming no other losses, the oscillation goes on forever.

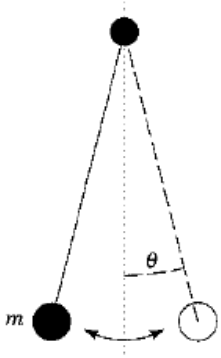

Figure 1.4: Pendulum with very small maximum angle deviation [15].

Pendulum which has a small angle of oscillations, see Figure 1.4, or a mass connected to a spring moving on a frictionless surface, see Figure 1.5, are other examples of harmonic oscillators.

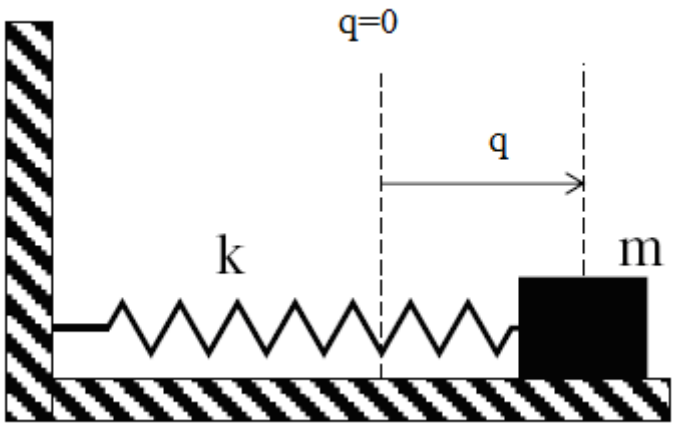

Figure 1.5: Mass-spring system [10].

The differential equation describing the harmonic oscillator is

$$\ddot{q} + w^2 q = 0\,. \tag{1.2}$$

For pendulum model w^2=g/L with g: standard gravitational acceleration and L: length of the pendulum and for spring model w^2=k/m with k: spring constant and m: mass. According to the equation, it is obvious that the internal parameters such as spring constant and length of pendulum of the oscillating system affect the

solution. Apart from these parameters, solution also depends on the initial values of q and $\dot{q}$.

1.4.1 Coupled Harmonic Oscillators

It is not really interesting to work on a free harmonic oscillator doing the same repetitive movement all the time. The interesting case is the coupling of two or more harmonic oscillators. See Figure 1.6.

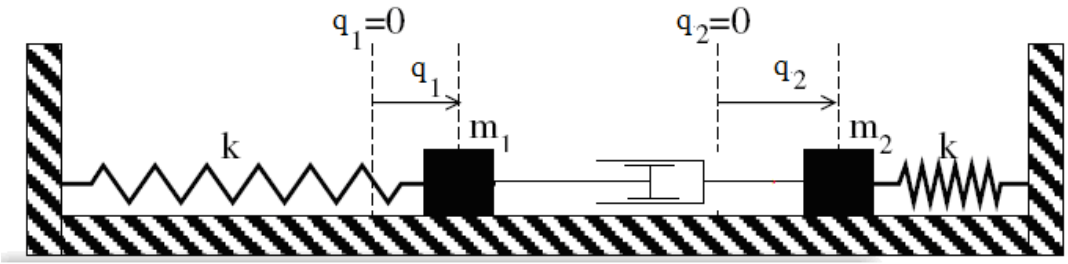

Figure 1.6: Two spring-mass systems (harmonic oscillators) coupled with a damper [10].

1.4.1.1 Identical Coupled Harmonic Oscillators

Consider the following system which is the array of coupled harmonic oscillators

$$\ddot{q}_i = -w^2 q_i + \sum_{i \neq j} \gamma_{ij}(\dot{q}_j - \dot{q}_i) \qquad \text{i=1, 2,…, N} \qquad (1.3)$$

where, natural frequency w>0 and $\gamma_{ij}(.)$ denotes the interconnection between the harmonic oscillators. Rewriting (1.3)

$$\dot{q}_i = w p_i \qquad (1.4\text{-a})$$

$$\dot{p}_i = -w q_i + \sum_{i \neq j} \gamma_{ij}(p_j - p_i), \qquad \text{i=1, 2,…, N} \qquad (1.4\text{-b})$$

where q_i and p_i are the states of each harmonic oscillator is obtained.

Let N= 4, w= 1 rad/sec, $\gamma_{ij}(s) = s$ for all i and j=1, 2, 3, 4 and let the initial conditions be $\varepsilon(0) = [-5 \quad 1 \quad 2 \quad 1 \quad 8 \quad 5 \quad 15 \quad 7]^T$ where $\varepsilon_i = [q_i \quad p_i]^T$ and

$\varepsilon = \begin{bmatrix} \varepsilon_1^T & \varepsilon_2^T & \cdots & \varepsilon_N^T \end{bmatrix}^T$. Then as time goes to ∞, all the states will synchronize to a common amplitude and phase. See Figure 1.7 and Figure 1.8.

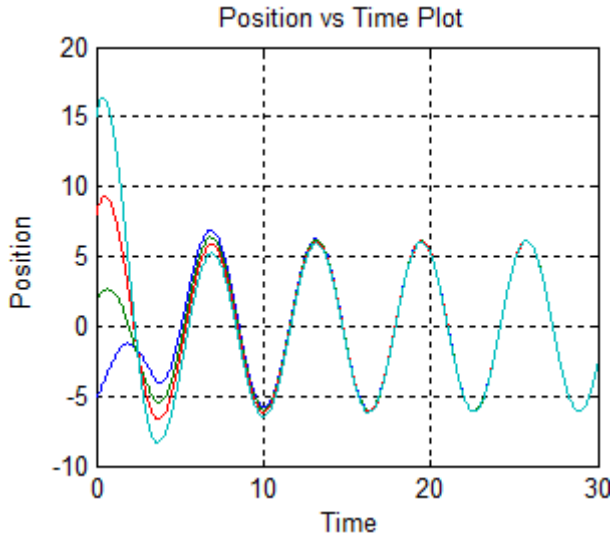

Figure 1.7: Position vs. time graph of identical harmonic oscillators.[1]

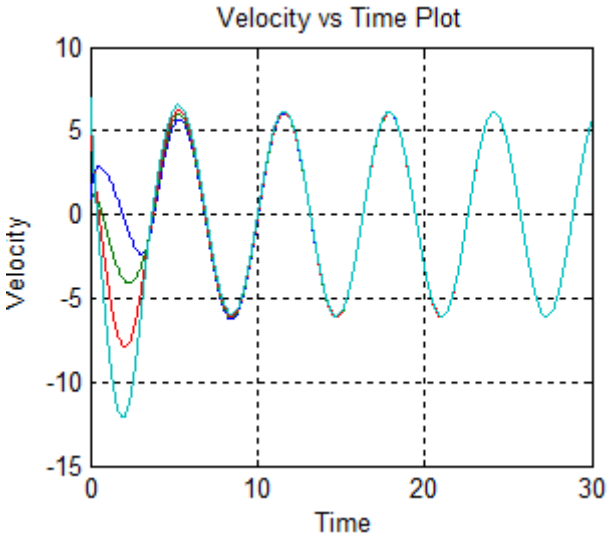

Figure 1.8: Velocity vs. time graph of identical harmonic oscillators.[2]

---

[1] In Figure 1.7 and in the rest of the thesis state q_i is denoted as position with unit meter (m).

[2] In Figure 1.8 and in the rest of the thesis state $p_i = \dot{q}_i / w$ is denoted as velocity with unit meter per second (m/sec).

1.4.1.2 Non-identical Coupled Harmonic Oscillators

In real life, it is almost impossible to obtain identical oscillators. Therefore, it is worthwhile to see what happens if the natural frequency values of the oscillators, w_i, are slightly different from each other. In other words, the natural frequency of the uncoupled oscillators does not match and they are different. This phenomenon, mismatch of frequencies of the uncoupled harmonic oscillators, is called frequency detuning.

A good assumption for frequency detuning may be $0.95w_j \le w_i \le 1.05w_j$ for $i \neq j$. According to this assumption, the equation (1.4) changes accordingly.

$$\dot{q}_i = w_i p_i \tag{1.5-a}$$

$$\dot{p}_i = -w_i q_i + \sum_{j \neq i} \gamma_{ij}(p_j - p_i), \qquad \text{i=1, 2,…,N} \tag{1.5-b}$$

Let N= 4, w_1=1 rad/sec, w_2=1.02 rad/sec, w_3=1.04 rad/sec, and w_4=1.05 rad/sec, $\gamma_{ij}(s) = s$ for all i and j=1, 2, 3, 4 and let the initial conditions be $\varepsilon(0) = \begin{bmatrix} -5 & 1 & 2 & 1 & 8 & 5 & 15 & 7 \end{bmatrix}^T$. We again observe that as time goes to ∞, all the states will synchronize to a common frequency and amplitude. However, it takes much longer than the synchronization of identical harmonic oscillators. See Figure 1.9 and Figure 1.10. In the example, the oscillators with different natural frequencies start to oscillate with same frequency due to coupling, it is called frequency locking. Moreover, the phase differences come to either zero or to a constant value different from zero and this phenomenon is called phase locking [2].

For detailed information and extra examples about non-identical harmonic oscillators, see section 4.2.4.

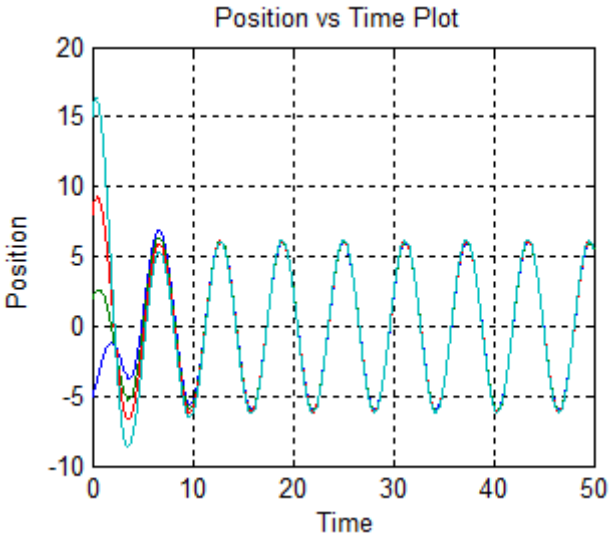

Figure 1.9: Position vs. time graph of non-identical harmonic oscillators.

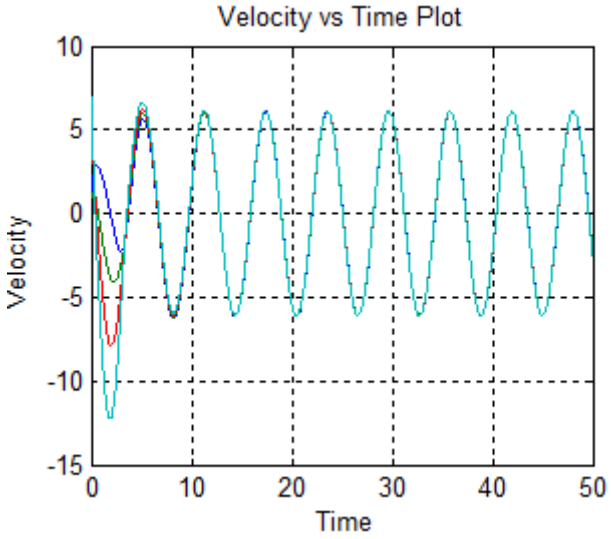

Figure 1.10: Velocity vs. time graph of non-identical harmonic oscillators.

1.5 OBJECTIVES AND ORGANIZATION OF THE THESIS

The aim of the thesis is to investigate the sufficient conditions for the convergence of solutions of coupled identical and non-identical harmonic oscillators to a common trajectory. There are two main parts of the thesis: Theoretical part and simulations. Initially, the theory of synchronization of harmonic oscillators will be

introduced. Next, the user interface of MATLAB will be used to simulate the coupled harmonic oscillators. The simulations run by GUI will give information about the behavior of the coupled harmonic oscillators for various different conditions.

The remainder of the thesis is organized as follows. In Chapter 2, linearly coupled harmonic oscillators are studied in detail. Moreover, important concepts and theorems about synchronization theory and harmonic oscillators are introduced. In Chapter 3 the basics of the nonlinearly coupled harmonic oscillators are given. Nonlinear coupling functions are introduced. Furthermore, relevant theorems and the procedure to show the synchronization of nonlinearly coupled harmonic oscillators are illustrated. Chapter 4 is the simulation part of the thesis. It contains brief information about the simulator, GUI-user interface of MATLAB, the algorithms running behind the GUI and the simulation results. The simulation results about synchronization of coupled harmonic oscillators are categorized and presented according to the different type of criteria such as coupling graph, coupling function, and coupling strength. Finally, the conclusion and future work is given in Chapter 5. All of the algorithms and simulations throughout the thesis are implemented on MATLAB.

CHAPTER 2

BASIC THEORY OF SYNCHRONIZATION

In this chapter, some basic examples are presented to give a better feel about the theory. Some important definitions and concepts are introduced. Moreover, by some theorems, the basics of synchronization theory are explained.

2.1 SYNCHRONIZATION OF DYNAMICAL SYSTEMS

In the first chapter, some examples have been given about synchronization. In this section, a simple consensus example is illustrated and it is worked on to better understand the behavior. The example is about the capacitors connected to each other by resistors, see Figure 2.1. Each capacitor has capacitance C_i, where i=1, 2, 3. The resistances are $1/\alpha_{12}$ and $1/\alpha_{23}$. In the circuit, the capacitors are supposed to reach to the same voltage value by the help of connection elements, resistors.

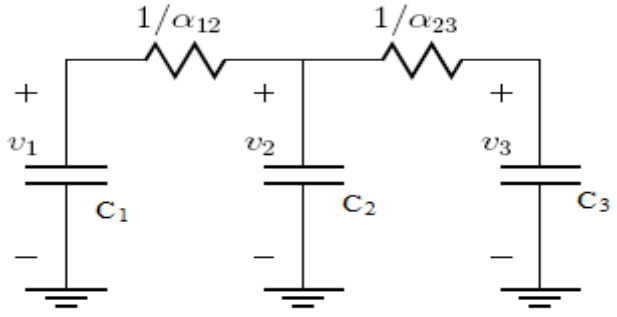

Figure 2.1: Capacitors connected via resistors.

Writing Kirchoff's Current Law at each node, the following set of equations is obtained.

$$
\begin{aligned}
C_1\dot{v}_1 &= \alpha_{12}(v_2 - v_1) \\
C_2\dot{v}_2 &= \alpha_{12}(v_1 - v_2) + \alpha_{23}(v_3 - v_2) \\
C_3\dot{v}_3 &= \alpha_{23}(v_2 - v_3).
\end{aligned} \tag{2.1}
$$

In matrix form,

$$
\dot{v} = \begin{bmatrix} -C_1^{-1}\alpha_{12} & C_1^{-1}\alpha_{12} & 0 \\ C_2^{-1}\alpha_{12} & -C_2^{-1}(\alpha_{12}+\alpha_{23}) & C_2^{-1}\alpha_{23} \\ 0 & C_3^{-1}\alpha_{23} & -C_3^{-1}\alpha_{23} \end{bmatrix} v \tag{2.2}
$$

where $v = \begin{bmatrix} v_1 & v_2 & v_3 \end{bmatrix}^T$.

In this example it is known that all capacitor voltages reach to the same value since they are coupled by the resistors.

One other example is the masses connected via dampers. In this example the masses are C_i, where i = 1, 2, 3 and the damping factors are $1/\alpha_{12}$ and $1/\alpha_{23}$, see Figure 2.2.

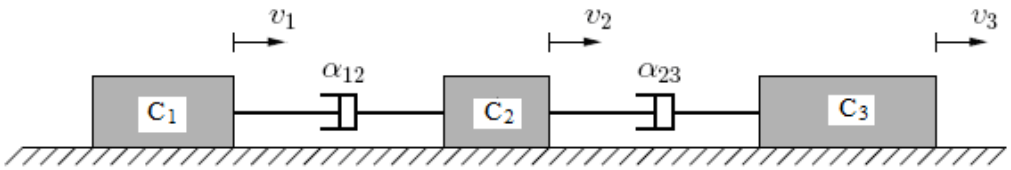

Figure 2.2: Masses connected via dampers.

Here the velocities, v_1, v_2 and v_3, will behave as the capacitance voltages of the previous example and they will become equal.

Another example can be the thermal synchronization by heat flow between 3 boxes which have different temperature values. All boxes are attached to each other. Therefore due to connection, there will be heat flow between each other and in the end all boxes will reach the same temperature. Undoubtedly, heat transfer has more complex mathematical model than the equation of the previous examples.

However, in the heat transfer system, the temperature also plays the role of voltage or velocity of the previous examples.

All these aforementioned examples, where states of interacting systems converge to each other, lies at the heart of the field named *synchronization of dynamical systems.*

2.2 COUPLING MATRIX

The matrix appearing in (2.2) plays a very important role in synchronization. In a system, synchronization of the oscillators highly depends on this matrix. This matrix is called the coupling or interconnection matrix and usually denoted by Γ. Looking at the matrix in (2.2), the following observations on Γ are obtained:

i. The off-diagonal entries are non-negative.

ii. Sum of the entries of any row is equal to zero.

Those two observations are true for all coupling matrices. And as the matrix is generalized for NxN coupling matrix, the following form of Γ (where $\Gamma \in R^{NxN}$) is obtained:

$$\Gamma := \begin{bmatrix} -\sum_{j\neq 1}\gamma_{1j} & \gamma_{12} & \cdots & \gamma_{1N} \\ \gamma_{21} & -\sum_{j\neq 2}\gamma_{2j} & \cdots & \gamma_{2N} \\ \vdots & \vdots & \ddots & \vdots \\ \gamma_{N1} & \gamma_{N2} & \cdots & -\sum_{j\neq N}\gamma_{Nj} \end{bmatrix}$$

where $\gamma_{ij} \geq 0$ for $i \neq j$.

In the following pages **1** will denote the column vector in R^N with all entries equal to 1. That is, $\mathbf{1}=\begin{bmatrix}1 & 1 & \cdots & 1\end{bmatrix}^T$. Using this vector the second observation can be rewritten as follows:

$$\Gamma\mathbf{1} = 0. \tag{2.3}$$

Equation (2.3) tells that $\lambda=0$ is the eigenvalue of the matrix with eigenvector v=**1** satisfying $\Gamma v = \lambda v$. Therefore, one of the eigenvalues is known. The remaining eigenvalues of the matrix are not exactly known. However, the capacitor example can give an idea about the remaining eigenvalues. It is known that there is no way that the capacitor voltages increase to a larger value than the largest initial capacitor voltage. This observation assures that the solution of the system is bounded. Therefore, it is guaranteed that the other N-1 eigenvalues of Γ have zero or negative values. The explanation below will make it clearer.

The differential equation describing each state variable (it is called an "agent", as well) of the system $\dot{x} = \Gamma x$ is

$$\dot{x}_i = \sum_{j \neq i} \gamma_{ij} (x_j - x_i), \text{ i=1, 2,..., N.} \tag{2.4}$$

Figure 2.3: Agents on the real line.

Each agent x_i will be represented as points on the real line R as it is shown in Figure 2.3. At some time $t=t_0$, the leftmost state variable will be labeled as x_ℓ and rightmost state variable as x_r where x_ℓ and $x_r \in \{x_1, x_2, \ldots, x_N\}$. That is,

$$x_\ell(t_0) = \min_i x_i(t_0),$$

$$x_r(t_0) = \max_i x_i(t_0).$$

Since $x_j(t_0) - x_\ell(t_0) \geq 0$ for all j, by (2.3) it can be deduced that $\dot{x}_l(t_0) \geq 0$. Similarly, $\dot{x}_r(t_0) \leq 0$. This means velocity vector of leftmost agent, $x_\ell(t_0)$, is either zero or pointing to the right and in the same way the velocity vector of rightmost agent, $x_r(t_0)$, is either zero or pointing to the left, see Figure 2.3.

As a result, it is obvious that the interval between leftmost and rightmost agents can never expand. This result shows that the solution of the system is bounded and Γ is a marginally stable matrix[3].

2.3 COUPLING GRAPH

In this part, the graph of the coupling matrix will be generated. First, some definitions about graphs will be introduced.

(a) Graph-1 (b) Graph-2

Figure 2.4: Graph-1 is undirected graph and Graph-2 is directed graph [16].

A *graph* is an ordered pair (N,E) where N is a set of vertices or nodes together with a set E of edges or lines (n_i,n_j), where n_i and n_j are the nodes of N. An *undirected graph* has no orientation on its edges, see Figure 2.4 Graph-1. A *directed graph* has directed edges, see Figure 2.4 Graph-2. A *directed path* from n_1 to n_ℓ is a sequence of nodes $(n_1, n_2, \ldots n_\ell)$ such that (n_i,n_{i+1}) is an edge for $i \in \{1, 2, \ldots, \ell - 1\}$ with direction from n_i to n_{i+1}. A graph is said to be *connected* if it has a node to which there exists a directed path from all the remaining nodes.

[3] A matrix is marginally stable if and only if all the eigenvalues of the matrix are zero or have negative real parts and all eigenvalues with zero real value are simple roots.

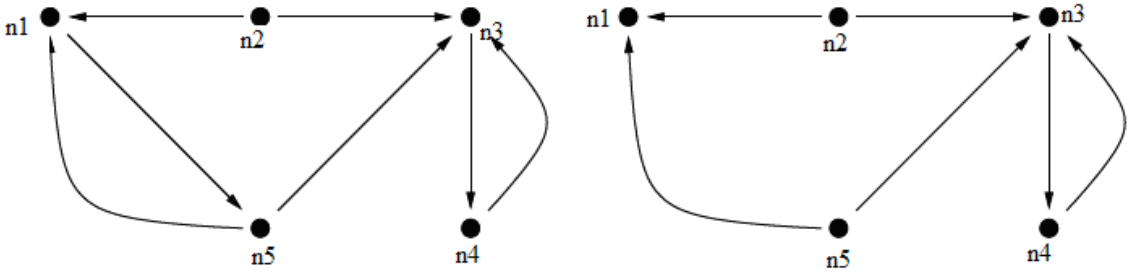

(a) Graph-1 (b) Graph-2

Figure 2.5: Graph-1 is connected and Graph-2 is unconnected.

In Figure 2.5, a connected graph, Graph-1, and an unconnected graph, Graph-2, are shown. In the connected graph, there is a directed path from all nodes to one node, n_4. However, as one edge is removed from Graph-1 (the edge directed from n_1 to n_5), the unconnected graph, Graph-2, is obtained.

The graph of coupling matrix, $\Gamma=[\gamma_{ij}]$, is the pair (N,E) where $N=\{n_1, n_2,\ldots,n_N\}$ is the set of nodes together with a set E of edges (n_i,n_j), such that $(n_i,n_j)\in E$ if and only if $\gamma_{ij} > 0$.When the graph is connected, the coupling matrix is said to be *connected*, as well. An example will be given to explain how to obtain the graph from interconnection matrix.

$$\Gamma = \begin{bmatrix} -2 & 0 & 0 & 0 & 2 \\ 3 & -4 & 1 & 0 & 0 \\ 0 & 0 & -6 & 6 & 0 \\ 0 & 0 & 3 & -3 & 0 \\ 2 & 0 & 3 & 0 & -5 \end{bmatrix} \tag{2.5}$$

The matrix appearing in (2.5) has the graph shown in Figure 2.6.

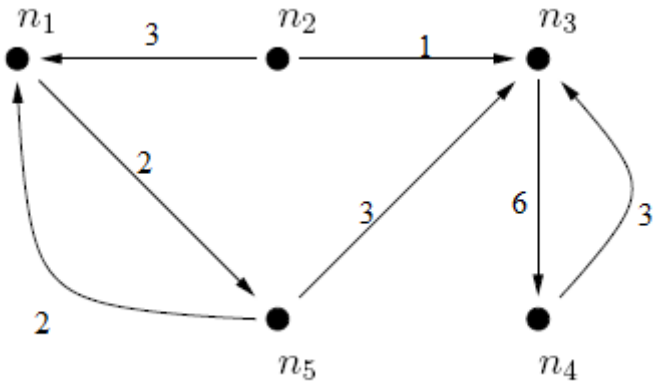

Figure 2.6: Graph of coupling matrix Γ.

In Figure 2.6, it is easily seen that all nodes lead to n_4 directly or indirectly. In other words, the motion of agents represented by n_1, n_2, n_3 and n_5 are affected by n_4. Hence, we can express connectedness in a slightly different way: connectedness of the graph of interconnection matrix is equivalent to that there is at least one agent that influences the motion of the remaining agents.

Having given the basic, it is now time to give some fundamental results of the synchronization theory.

Theorem 2.1 Consider the agents in (2.4) associated with coupling matrix Γ. The agents synchronize, that is, there exists $\bar{x} \in R$ such that $\lim_{t\to\infty} x_i(t) = \bar{x}$ for i=1, 2,…,N for all initial conditions if and only if the interconnection graph is connected.

Theorem 2.1 implies the following theorem.

Theorem 2.2 Let $\lambda_1, \lambda_2, \lambda_3 \ldots, \lambda_N$ be the eigenvalues of the interconnection matrix Γ and $\lambda_1 = 0 \geq \mathrm{Re}(\lambda_2) \geq .... \geq \mathrm{Re}(\lambda_N)$ .The graph of Γ is connected, if and only if $\mathrm{Re}(\lambda_2)<0$.

To sum up, coupling matrix Γ is said to be *connected* if its graph is connected. For connected Γ, eigenvalue λ = 0 is distinct and all the other eigenvalues have real parts strictly negative.

2.4 A LEFT EIGENVECTOR OF COUPLING MATRIX

Scalar $\lambda \in C$ is an eigenvalue of matrix $A \in R^{NxN}$ if there exists a nonzero vector $v \in C^N$ satisfying $Av=\lambda v$. Vector $v \in C^N$ is called the right eigenvector corresponding to the eigenvalue, λ, which we already mentioned earlier. There is yet another vector $r \in C^N$ associated to λ. It is called the left eigenvector of λ and satisfies $r^T A=\lambda r^T$.

Theorem 2.1 tells us that if the coupling graph is connected, agents converge to a point $\bar{x} \in R$ for all initial conditions. Theorem doesn't tell what $\bar{x}$ exactly is. However, observing the mathematical model it can be seen that $\bar{x}$ depends on the coupling matrix Γ and the initial condition vector $\begin{bmatrix} x_1(0) & x_2(0) & \cdots & x_N(0) \end{bmatrix}$. Since the system is linear, the point that the agents converge to has to be a linear function of the initial conditions. That is, $\bar{x} = r_1 x_1(0) + r_2 x_2(0) + \cdots + r_N x_N(0)$ for some real numbers r_i. Letting $r \in R^N$ and $r= [r_1 \ r_2 \ \ldots \ r_N]^T$, the equation becomes

$$\bar{x} = r^T x(0). \tag{2.7}$$

Equation (2.7) can be generalized to

$$\bar{x} = r^T x(t) \ \text{ for all t.} \tag{2.8}$$

Using (2.8), it can be shown that r is a left eigenvector of Γ.

Since $r^T x(t)$ is constant $0 = \dfrac{d}{dt}\{r^T x(t)\}$

$$= r^T \dot{x}$$

$$= r^T \Gamma x(t) \quad \text{for all t.} \tag{2.9}$$

The equation (2.9) includes $r^T \Gamma x(0)=0$. Moreover, since x(0) can be arbitrarily set, $r^T \Gamma x(0)=0$ can be written as $r^T \Gamma v = 0$, where $v \in R^N$. Thus, $r^T \Gamma x(0)=0$ can only be true if

$$r^T \Gamma = 0. \tag{2.10}$$

It is already mentioned that left eigenvector satisfies $r^T A = \lambda r^T$ and equation (2.10) shows that r^T is the left eigenvector corresponding to eigenvalue λ=0. Yet, r^T is not known exactly, since it is not unique. There are infinitely many r^T forming a line in R^N passing through origin. There needs to be one more equation for unique r^T and the Lemma 2.1 will be used to find it.

Lemma 2.1: If initial condition vector $[x_1(0)\ x_2(0)\ \ldots.\ x_N(0)]$ is changed to $[\,(x_1(0) + a)\ \ (x_2(0) + a)\ \ldots.\ (x_N(0) + a)]$, the agents will converge to $\bar{x} + a$.

By using Lemma 2.1, we can write as $r^T(x(0) + a\,\mathbf{1}) = \bar{x} + a$. And by (2.4), $ar^T\mathbf{1} = a$ is determined. Thus,

$$r^T\mathbf{1} = 1. \tag{2.11}$$

Equations (2.10) and (2.11) determine the unique left eigenvector. Using Theorem 2.1, (2.10), and (2.11) the following theorem can be stated.

Theorem 2.3: Consider the agents in (2.4) associated with coupling matrix Γ. The agents synchronize for all initial conditions if and only if the graph is connected. More specifically, for i=1, 2,…, N, the systems moreover converge to

$$\lim_{t\to\infty} x_i(t) = r^T x(0)$$

where $r \in R^N$ satisfies (2.10) and (2.11).

2.5 SYNCHRONIZATION IN R^2

In previous sections synchronization is only considered in one dimensional medium, namely on the line. This special and relatively easy case is a good way to understand the synchronization theory. However, in real life most remarkable phenomena (for example synchronization of harmonic oscillators) occur in plane R^2 or in space R^3 or even in higher dimensions.

The next definition will be helpful in the following parts of the thesis.

Definition 2.1 Kronecker Product of $A \in R^{mxn}$ and $B \in R^{pxq}$ is defined as

$$A \otimes B := \begin{bmatrix} a_{11}B & a_{12}B & \cdots & a_{1n}B \\ a_{21}B & a_{22}B & \cdots & a_{2n}B \\ \vdots & \vdots & \ddots & \vdots \\ a_{m1}B & a_{m2}B & \cdots & a_{mn}B \end{bmatrix}.$$

The properties of the Kronecker Product are

- If the products AC and BD are allowed, then $(A \otimes B)(C \otimes D) = (AC \otimes BD)$.
- $(A \otimes B) + (A \otimes C) = A \otimes (B + C)$ for B and C that are of the same size.
- $(A \otimes B)^T = A^T \otimes B^T$.

The next example will be on plane (R^2).

Assume there are four agents on the plane and each having as neighbor one of the other agents and no two agents having the same neighbor. Let the scenario be such that each agent wants to approach to its neighbor and does this directly, meaning; its velocity vector at any instant directly points toward its neighbor. See Figure 2.7.

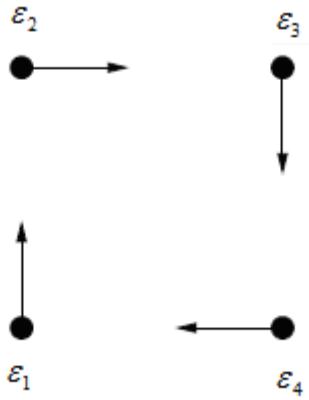

Figure 2.7: Four Agents on R^2.

Similar to the previous examples, in this example the coupling is linear. For simplicity, the weights of all coupling edges are equal to 1.

Therefore the mathematical model is

$$\dot{\varepsilon}_1 = \varepsilon_2 - \varepsilon_1$$

$$\dot{\varepsilon}_2 = \varepsilon_3 - \varepsilon_2$$

$$\dot{\varepsilon}_3 = \varepsilon_4 - \varepsilon_3 \tag{2.12}$$

$$\dot{\varepsilon}_4 = \varepsilon_1 - \varepsilon_4$$

where $\varepsilon_i \in R^2$. Define $\varepsilon := \left[\varepsilon_1^T \varepsilon_2^T \varepsilon_3^T \varepsilon_4^T\right]^T$ where $\varepsilon \in R^8$, then

$$\dot{\varepsilon} = \begin{bmatrix} -I & I & 0 & 0 \\ 0 & -I & I & 0 \\ 0 & 0 & -I & I \\ I & 0 & 0 & -I \end{bmatrix} \varepsilon \tag{2.13}$$

where I is the identity matrix in R^2. More compactly,

$$\dot{\varepsilon} = (\overline{\Gamma} \otimes I)\varepsilon \tag{2.14}$$

where $\overline{\Gamma} = \begin{bmatrix} -1 & 1 & 0 & 0 \\ 0 & -1 & 1 & 0 \\ 0 & 0 & -1 & 1 \\ 1 & 0 & 0 & -1 \end{bmatrix}$ is the coupling matrix.

Since the synchronization is in two dimensions in the example, it is as easy to estimate the behavior of the agents as in the one dimensional example. Two dimensional equation will be decomposed into vertical and horizontal coordinates. Let $\varepsilon_i = \left[x_i y_i\right]^T$, where $x_i \in R$ is the horizontal coordinate and $y_i \in R$ is the vertical coordinate of ith agent. From geometrical aspect, the decomposition is the (orthogonal) projection of the agents onto horizontal and vertical axes. Then, (2.12) implies

$$\begin{aligned} \dot{x}_1 &= x_2 - x_1 & \dot{y}_1 &= y_2 - y_1 \\ \dot{x}_2 &= x_3 - x_2 & \dot{y}_2 &= y_3 - y_2 \\ \dot{x}_3 &= x_4 - x_3 \quad \& & \dot{y}_3 &= y_4 - y_3 \\ \dot{x}_4 &= x_1 - x_4 & \dot{y}_4 &= y_1 - y_4 \end{aligned} \tag{2.15}$$

Theorem 2.3 and the connectedness of the coupling matrix $\overline{\Gamma}$, together, tell that $x_i(t) \to r^T x(0)$ and $y_i(t) \to r^T y(0)$ where r satisfies (2.10) and (2.11). Thus,

$$\varepsilon_i(t) \to \begin{bmatrix} r^T x(0) \\ r^T y(0) \end{bmatrix}$$

$$= (r^T \otimes I)\varepsilon(0). \tag{2.16}$$

Obviously, this result can be generalized for the agents in any dimensions. Therefore, picking medium as R^n, the generalized result is given in Theorem 2.4.

Theorem 2.4 Consider the array of agents satisfying

$$\dot{\varepsilon}_i = \sum_{i \neq j} \gamma_{ij}(\varepsilon_j - \varepsilon_i) \quad \text{for i=1,2, …, N} \tag{2.17}$$

where $\varepsilon_i \in R^n$ and coupling matrix $\Gamma = [\gamma_{ij}] \in R^{NxN}$ is connected. Then agents synchronize for all initial conditions. In particular,

$$\lim_{t \to \infty} \varepsilon_i(t) = (r^T \otimes I) \begin{bmatrix} \varepsilon_1(0) \\ \vdots \\ \varepsilon_p(0) \end{bmatrix} \tag{2.18}$$

where $r \in R^N$ satisfies $r^T \Gamma = 0$ and r^T **1**=1.

In (2.15), orthogonal projection method is used to solve the synchronization problem. Next, projection matrix is introduced.

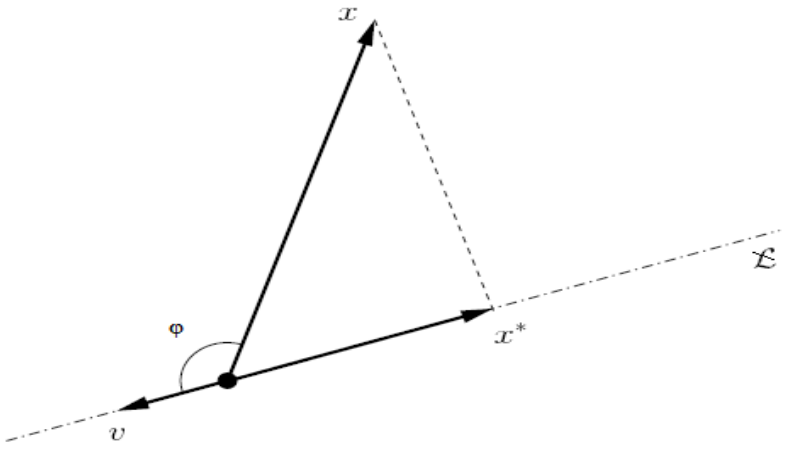

Figure 2.8: Projection on the line.

Projection Matrix: Consider a line *Ł* passing through the origin in R^n. Let *v* be a point other than the origin on the line Ł. Then the following description can be given Ł=$\{\lambda v : \lambda \in R\}$. Let *x* be a vector on R^n. Then, the orthogonal projection of *x* on *v* is

$$x^* = \frac{v}{|v|}|x|\cos\varphi \tag{2.19}$$

where $|v| = \sqrt{v^T v}$ and φ is the angle between vectors *v* and x . Figure 2.8 gives the the visualization of the projection. Let P := vv^T / ($v^T v$), using the definition $v^T x$=|*x*| |*v*| cosφ and (2.19) the following equation can be obtained.

$$x^* = \frac{v}{|v|}|x|\cos\varphi$$

$$x^* = \frac{v}{|v|^2}|x||v|\cos\varphi$$

$$x^* = \frac{v}{v^T v}v^T x$$

$$x^* = Px$$

Therefore, P is the orthogonal projection matrix onto line *Ł*. Namely, a projection matrix P is an *n x n* matrix that projects a vector from R^n to subspace W, where W is the image of P. Moreover, P is an orthogonal projection matrix if and only if $P=P^2$ and $P=P^T$ [17].

It is already mentioned that in (2.17) there is a projection in both x and y axes. Although P matrix is not easily seen in (2.17), it exists and it is identity matrix. Therefore, it does not need to be written explicitly. Slightly changing (2.17),

$$\dot{\varepsilon}_i = \sum_{i \neq j} \gamma_{ij} P(\varepsilon_j - \varepsilon_i) \qquad \text{i=1, 2,…, N} \tag{2.20}$$

is obtained. According to the P matrix, the projection is going to be applied and the solution will change.

Next simulations will give better intuition about the projection mechanism and it will be a good step for moving on to the harmonic oscillators. In the simulations number of agents, N will be 10, and $\varepsilon_i \in R^2$ which implies $P \in R^{2X2}$. Let $\Gamma \in R^{10X10}$ be linear and connected and the entries of Γ are

$$\Gamma = \begin{bmatrix} -4.3 & 0.9 & 0.4 & 0.5 & 0.7 & 0.5 & 0.2 & 0.9 & 0.1 & 0.2 \\ 0.3 & -3.9 & 0.1 & 0.6 & 0.4 & 0.9 & 0.2 & 0 & 0.7 & 0.7 \\ 0.6 & 0.8 & -4.4 & 0.4 & 0.1 & 0.6 & 0.7 & 0.5 & 0.5 & 0.2 \\ 0.3 & 0.3 & 0.5 & -4.1 & 0.3 & 1 & 0.8 & 0.4 & 0.2 & 0.3 \\ 0.8 & 0.6 & 0.7 & 0.7 & -4.2 & 0.2 & 0.3 & 0.5 & 0.3 & 0.1 \\ 1 & 0 & 0.7 & 1 & 0.2 & -5.5 & 0.7 & 0.8 & 0.6 & 0.5 \\ 0.7 & 0.4 & 0.6 & 0.5 & 0.5 & 0.3 & -4.2 & 0.3 & 0.2 & 0.7 \\ 0.4 & 0.3 & 0 & 0.3 & 0.5 & 0.6 & 0 & -3.3 & 0.7 & 0.5 \\ 0.6 & 0.1 & 0 & 0.1 & 0.5 & 0.7 & 0.6 & 0.4 & -3.4 & 0.4 \\ 0.1 & 0.2 & 0.3 & 0.6 & 0.8 & 0 & 0.4 & 0 & 0.9 & -3.3 \end{bmatrix}$$

Let the initial values of the agents be as shown in Figure 2.9 and take P=$\begin{bmatrix} 1 & 0 \\ 0 & 0 \end{bmatrix}$ such that the projection will be onto the horizontal axis. Then $\lim_{t\to\infty} \varepsilon_i(t)$ will be as in Figure 2.10.

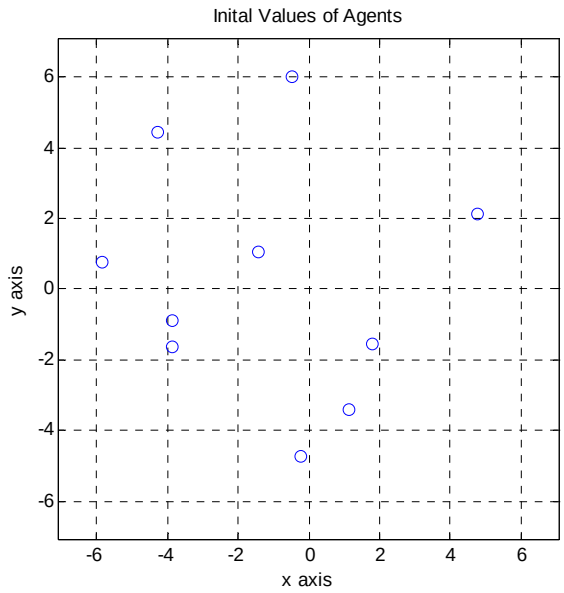

Figure 2.9: Initial Values of agents.

If the same simulation is carried out for P=$\begin{bmatrix} 0 & 0 \\ 0 & 1 \end{bmatrix}$, the projection will be on the y-axis. Different from x and y axes, for P=$\begin{bmatrix} 1/2 & 1/2 \\ 1/2 & 1/2 \end{bmatrix}$ the result will be as shown in Figure 2.11 which is all the agents are projected along the x=y line direction.

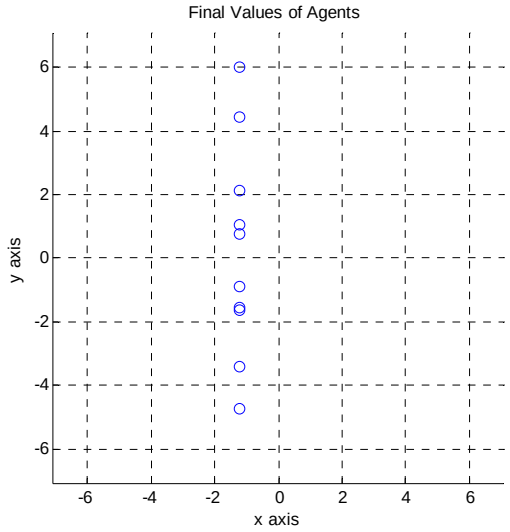

Figure 2.10: Agents as $t \to \infty$ for P=$\begin{bmatrix} 1 & 0 \\ 0 & 0 \end{bmatrix}$.

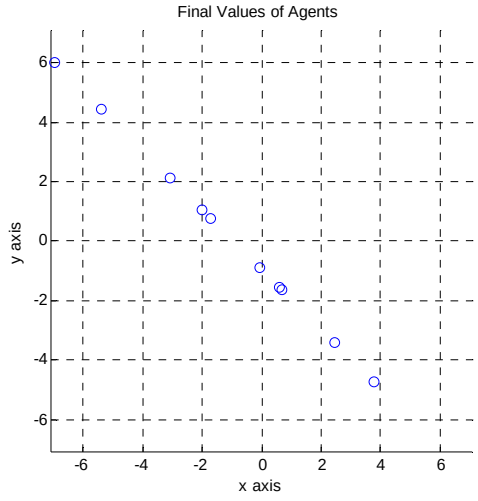

Figure 2.11: Agents as $t \to \infty$ for P=$\begin{bmatrix} 1/2 & 1/2 \\ 1/2 & 1/2 \end{bmatrix}$.

So far in the examples P has been picked as time-invariant. What happens if the projection matrix is time-varying? Let the projection matrix be

$$P(t)=v(t)^{T}v(t) \qquad \text{where } v(t)=[\ \cos(t)\ \sin(t)\ ]\,. \tag{2.21}$$

Note that the requirements $P(t)=P^{2}(t)$ and $P(t)=P^{T}(t)$ are satisfied. Therefore P(t) selection is correct and can be used in (2.20). If the simulation is started again for the same initial values as in Figure 2.9 and same Γ, as $t \to \infty$ the agents will approach each other and they will meet at one point. The qualitative reason for this result is that P(t) is time-varying and the projection is done in infinitely many lines. As the result of the time-varying projection all agents reach a consensus. See Figure 2.12.

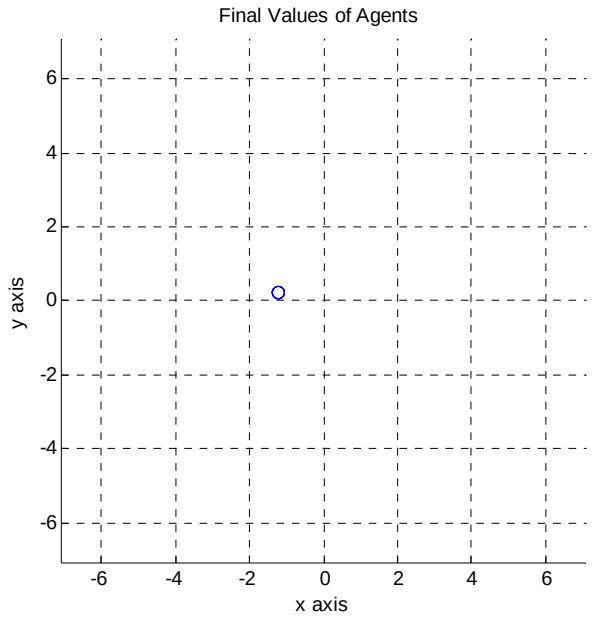

Figure 2.12: Agents as $t \to \infty$ for time-varying P(t).

In the same time-varying projection matrix, consensus of agents holds for any connected graph. Moreover, consensus occurs regardless of agent number and initial values of the agents.

2.6 LINEARLY COUPLED HARMONIC OSCILLATORS

In first chapter harmonic oscillators are mentioned and the equation of coupled harmonic oscillators is already given. The equation of linearly coupled harmonic oscillators can be generalized as

$$\dot{\varepsilon}_i = S\varepsilon_i + H^T H \sum_{j=1}^{N} \gamma_{ij}(\varepsilon_j - \varepsilon_i), \qquad \text{i=1, 2,…, N} \tag{2.22}$$

where $\varepsilon_i \in R^n$ is the agent of the i[th] system, $S \in R^{nxn}$ and $H \in R^{mxn}$. Moreover,

i. S is skew-symmetric,

ii. (H,S) is observable,

iii. Γ is connected where Γ=[γ_{ij}].

The following theorem holds for system (2.22).

Theorem 2.5 Consider the system in (2.22). Solutions $\varepsilon_i(.)$ synchronize to

$$\lim_{t\to\infty} \varepsilon_i(t) = (r^T \otimes e^{St}) \begin{bmatrix} \varepsilon_1(0) \\ \vdots \\ \varepsilon_N(0) \end{bmatrix}$$

where $r \in R^N$ satisfies $r^T \Gamma = 0$ and $r^T \mathbf{1}$=1.

In system (2.22) $S\varepsilon_i$ is the generalized rotation term and H^TH is the projection matrix of the agents. Even though the H^TH matrix is time-invariant, rotating term ensures the synchronization of the coupled systems. For proof of the theorem, see [18].

For $\varepsilon = \left[\varepsilon_1^T \varepsilon_2^T \cdots \varepsilon_N^T\right]$ with $\varepsilon_i \in R^n$ let $A := \{\varepsilon \in R^{nN} : \varepsilon_i = \varepsilon_j$ for all i, j} be synchronization manifold. Note that Theorem 2.5 implies that synchronization manifold A is asymptotically stable.

As a result of Theorem 2.5, the following corollary about harmonic oscillators holds.

Corollary 2.1 Consider the following array of coupled harmonic oscillators in R^2

$$\dot{q}_i = wp_i \tag{2.23-a}$$

$$\dot{p}_i = -wq_i + \sum_{j \neq i} \gamma_{ij}(p_j - p_i) \quad \text{for} \quad \text{i=1, 2,…, N.} \tag{2.23-b}$$

where w>0. The oscillators synchronize for all connected coupling matrix $[\gamma_{ij}]$.

In Section 1.4.1, an example about Corollary 2.1 is already given. Figure 1.7 and Figure 1.8 show the synchronization of the agents with linear coupling function. More examples about linearly coupled harmonic oscillators will be given in Chapter 4.

In this chapter, we started with some basic examples to give a better feel about the synchronization of dynamical systems. Then, we gave some basic definitions such as coupling matrix, coupling graph and projection matrix. After presenting some important theorems, finally we reached an important result: Provided that coupling matrix is connected, linearly coupled identical harmonic oscillators synchronize for any frequency.

In the next chapter, we will introduce nonlinearly coupled harmonic oscillators.

CHAPTER 3

NONLINEARLY COUPLED HARMONIC OSCILLATORS

In synchronization literature, linear coupling has a great research area; for example [19-22]. However, linear coupling does not have the capability to contain all phenomena in the nature. Nonlinear coupling is needed for modeling of some phenomena such as synchronously flashing fireflies and cardiac pacemaker cells. Winfree is one of the first researchers who found a model, named Winfree model, with nonlinear interactions in 1967. Then, Kuramoto simplified the Winfree model and he obtained another good model for nonlinearly coupled synchronization, see [23, 24]. Although these two models are quite successful to an extent, since these models assume that the coupling between two oscillators is always smooth, a more realistic model was needed. Peskin found another model about nonlinear oscillators using integrate-and-fire oscillators. The problem of this model was that the mathematics was too complex to solve for large number of oscillators. Finally, Mirollo and Strogatz extended and generalized Peskin's model. Although they have some differences, all four models are good and famous approaches to realize nonlinearly coupled oscillators and they can be used to model biological synchronization in nature such as a group of women, whose menstrual periods are synchronized, synchronously flashing fireflies or crickets that chirp in unison. For more nonlinear coupling examples, see [25, 26].

In this thesis since we are working on harmonic oscillators, we will not use any of the models mentioned above. We will provide the nonlinear model by selecting the coupling function between harmonic oscillators as nonlinear.

In previous chapters, linearly coupled harmonic oscillators are already introduced; mathematical models and examples illustrating those models are given. In this chapter, the coupling between harmonic oscillators will be taken as nonlinear. The mathematical model and solution method for nonlinearly coupled harmonic oscillators will be introduced. Moreover some definitions and important concepts, which are hoped to help the reader to understand the topic better, will be given.

3.1 MATHEMATICAL MODEL

Let $|\cdot|$ denote the Euclidean norm and $R_{\geq 0}$ the set of nonnegative real numbers. A set of functions, $\gamma_{ij} : R \to R$ where i, j= 1, 2,…, p and $i \neq j$, describes a interconnection if the following properties are satisfied for all $s \in R$:

I. $\gamma_{ij}(0) = 0$ and $s\gamma_{ij}(s) \geq 0$

II. Either $\gamma_{ij}(s) \equiv 0$ or $|\gamma_{ij}(s)| \geq \beta(|s|)$ where $\beta: R_{\geq 0} \to R_{\geq 0}$ is a continuous, zero at zero, and strictly increasing function.

Namely, the interconnection function, $\gamma_{ij}(.)$, is either zero or the graph of $\gamma_{ij}(.)$ takes place only in the first and third quadrants. Some possible graphs of $\gamma_{ij}(.)$ are shown in Figure 3.1

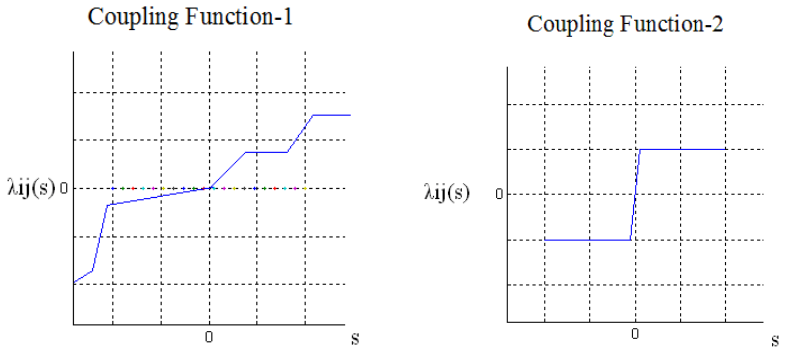

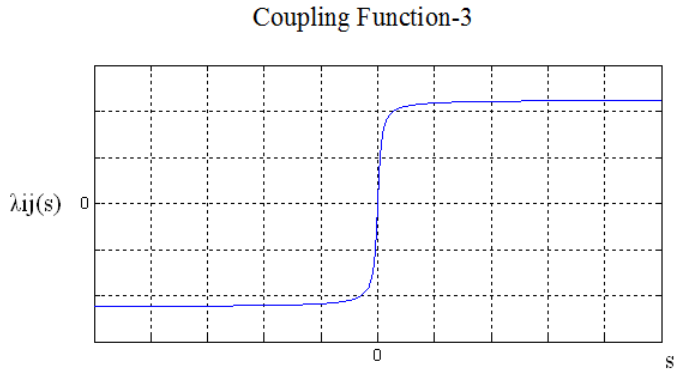

Figure 3.1: Some possible nonlinear coupling function examples

To mean $\gamma_{ij}(s) \equiv 0$ we write $\gamma_{ij} = 0$. Otherwise we write $\gamma_{ij} \neq 0$. The graph of interconnection $\{\gamma_{ij}\}$ is pair (N, E), where N = $\{n_1, ..., n_p\}$ and E is such that $(n_i, n_j) \in E$ iff $\gamma_{ij} \neq 0$. An interconnection (coupling) is said to be *connected* when its graph is connected. [27]

Following equations will be used as the mathematical model of nonlinearly coupled harmonic oscillators.

$$\dot{q}_i = wp_i \tag{3.1-a}$$

$$\dot{p}_i = -wq_i + \sum_{j \neq i} \gamma_{ij}(p_j - p_i), \qquad i=1, 2,\ldots, N \tag{3.1-b}$$

where w>0 and $\{\gamma_{ij}\}$ is a *connected* coupling.

In Corollary 2.1, it is already stated that if γ_{ij} is linear, then identical harmonic oscillators synchronize for all w. When γ_{ij} is nonlinear, it is not straightforward to show whether oscillators synchronize or not for all w. In this chapter we will try to find a solution for the following problem.

Problem definition: Do the nonlinearly coupled identical harmonic oscillators synchronize for any w provided that coupling graph is connected?

In other words, the aim is to understand the behavior of coupled identical harmonic oscillators provided that graph is connected and coupling γ_{ij} is nonlinear. In the next section a solution procedure will be introduced for the given problem.

3.2 SOLUTION PROCEDURE

The procedure, see Figure 3.2, that will be followed to reach the answer is

i. Change of coordinates: Since solution of an uncoupled harmonic oscillator is a rotating vector on R^2 with frequency w rad/sec, solution of the coupled harmonic oscillators contains a rotation term, as well. Therefore, we will apply a change of coordinates to the system and we will define the system with respect to a rotating coordinate frame. After applying the change of coordinates, the time-invariant system will turn into the system whose righthand side is periodic in time with period $T=2\pi / w$.

ii. Averaging: Theory of perturbations [29] tells us that, starting from close initial conditions, the solution of a system with a periodic righthand side and the solution of the time-average approximate system stay close for a long time provided that the period is small enough. Therefore, to use the perturbation theory, we will take the average of the system.

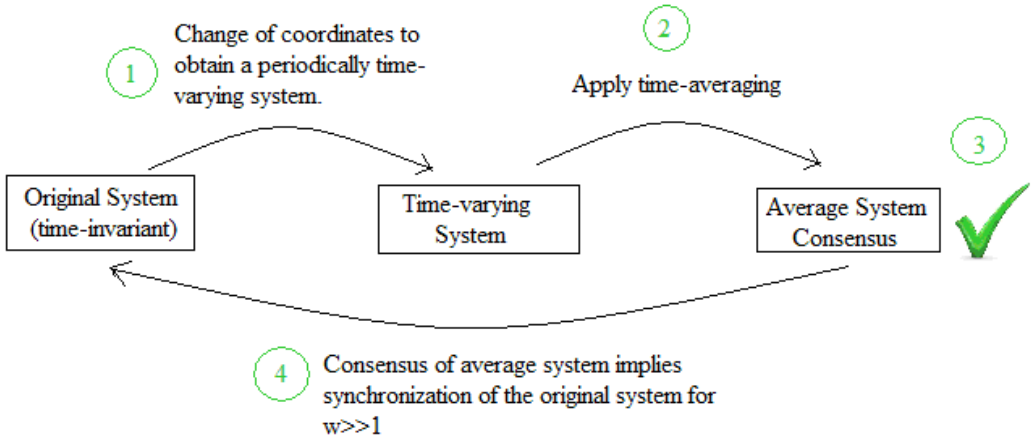

Figure 3.2: Solution procedure for proof of synchronization of nonlinearly coupled harmonic oscillators with high frequency.

iii. Showing consensus for average system: After applying averaging to the system, the problem turns out to be a consensus problem, see [28]. In this step, we will show that the average system reaches to a consensus.

iv. Returning to the original system: In final step, we will show that consensus of average system implies synchronization of the original system provided that the rotation is rapid enough.

3.2.1 Time-varying Change of Coordinates

Let $\varepsilon_i \in R^2$, $S(w) \in R^{2x2}$, $H \in R^{1x2}$ and they have the following definitions:

$\varepsilon_i = [q_i p_i]^T$, $S(w)=\begin{bmatrix} 0 & w \\ -w & 0 \end{bmatrix}$ and H=[0 1].

According to the given definitions, (3.1) can be rewritten as

$$\dot{\varepsilon}_i = S(w)\varepsilon_i + H^T \sum_{j=1}^{N} \gamma_{ij}(H(\varepsilon_j - \varepsilon_i)). \tag{3.2}$$

In (3.2), "$S(w)\varepsilon_i$" term defines a rotation with frequency w rad/sec and "$H^T \sum_{j=1}^{N} \gamma_{ij}(H(\varepsilon_j - \varepsilon_i))$" term defines the consensus of coupled states along the projection term H^T, namely vertical axis. It is easy to understand the geometrical meaning of each separate term in (3.2). However, it may not be so easy to visualize what happens when two terms are added together. Therefore, a change of coordinates will be applied and system (3.2) will be simplified.

Let $x_i(t) := e^{-S(w)t}\varepsilon_i(t)$ where $e^{-S(w)t}$ defines a rotation matrix. Then, rewriting (3.2) in terms of x_i, the following equation is achieved.

$$\dot{x}_i = e^{S(w)^T t} H^T \sum_{j=1}^{N} \gamma_{ij}(He^{S(w)t}(x_j - x_i)) \tag{3.3}$$

In equation 3.3, inserting $e^{S(w)t} = \begin{bmatrix} \cos(wt) & \sin(wt) \\ -\sin(wt) & \cos(wt) \end{bmatrix}$ and H=[0 1]

$$\dot{x}_i = \begin{bmatrix} -\sin(wt) \\ \cos(wt) \end{bmatrix} \sum_{j=1}^{N} \gamma_{ij} \left([-\sin(wt) \quad \cos(wt)](x_j - x_i) \right). \tag{3.4}$$

The change of coordinates using rotation matrix eliminates the first term in (3.2). In other words, system (3.2) is observed from a rotating reference frame which has the same rotation frequency with the system. Moreover, since change of coordinates is performed by the rotation matrix $e^{-S(w)t}$, changing the coordinates does not change the relative distances between the states, mathematically $\left|x_i(t) - x_j(t)\right| = \left|\varepsilon_i(t) - \varepsilon_j(t)\right|$ for all t and all i, j [27].

The first step of the solution procedure is completed. However, system (3.4) is still far from yielding. Therefore, time average of the righthand side of (3.4) will be taken to understand the behavior of the system.

3.2.2 Averaging and Returning to the Original System

Average of all coupling functions, $\overline{\lambda}_{ij} : R^2 \to R^2$ can be written as follows:

$$\overline{\lambda}_{ij}(y) = \frac{1}{2\pi}\int_0^{2\pi}\begin{bmatrix}-\sin\alpha\\ \cos\alpha\end{bmatrix}\gamma_{ij}\left(\begin{bmatrix}-\sin\alpha & \cos\alpha\end{bmatrix}y\right)d\alpha\,. \tag{3.5}$$

Then the time average of the system becomes

$$\dot{x}_i = \sum_{j=1}^{N}\overline{\gamma}_{ij}(x_j - x_i)\,. \tag{3.6}$$

Realizing that the right-hand side of (3.4) is periodic in time, we give the following result of perturbation theory. Let a system have a periodic righthand side, then the solution of the system stays close to the solution of time-average approximate system for a long time provided that the starting conditions are not far away and the frequency is large enough [27]. The theory says that for large frequency values, the approximation applied in (3.5) and (3.6) will help to get information about the original system.

Equation (3.6) does not tell much if the meaning of the average coupling function $\overline{\gamma}_{ij}$ is not understood. To give a better intuition, Lemma 3.1 is introduced.

Lemma 3.1: $\overline{\lambda}_{ij}(y) = \beta_{ij}(|y|)\dfrac{y}{|y|}$ where $\beta_{ij} := R_{\geq 0} \to R_{\geq 0}$ is

$$\beta_{ij}(r) := \frac{1}{2\pi}\int_0^{2\pi} \gamma_{ij}(r\sin\alpha)\sin\alpha d\alpha .$$

For the proof of Lemma 3.1, see [27]. The following mathematical concept, convex hull, will be used to explain Lemma 3.1.

Convex Hull: A set $C \subset R^n$ is said to be convex if for any two points x, y in *C,* the line segment [x, y] connecting two points entirely lies in *C,* that is $[x, y] \subset C$. For example, circle or a solid cube is convex, but crescent shape is not convex. In Figure 3.3, both convex and non-convex sets are introduced.

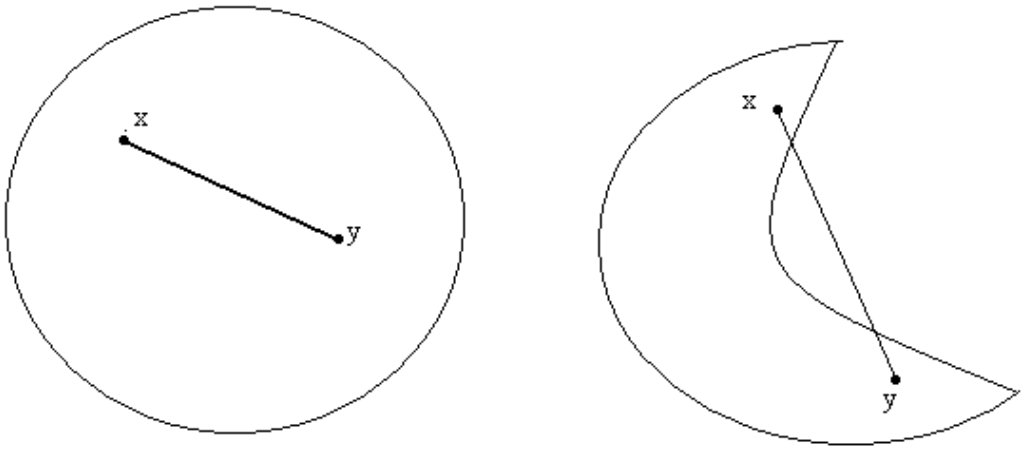

(a) Set-1 (b) Set-2

Figure 3.3: Set-1 is convex and Set-2 is non-convex.

Given a set of points $\{x_1, x_2, ..., x_N\}$ in R^n, their convex hull, denoted by $co\{x_1, x_2, ..., x_N\}$, is the smallest convex set that contains them. A set of points on plane and their convex hull is depicted in Figure 3.4.

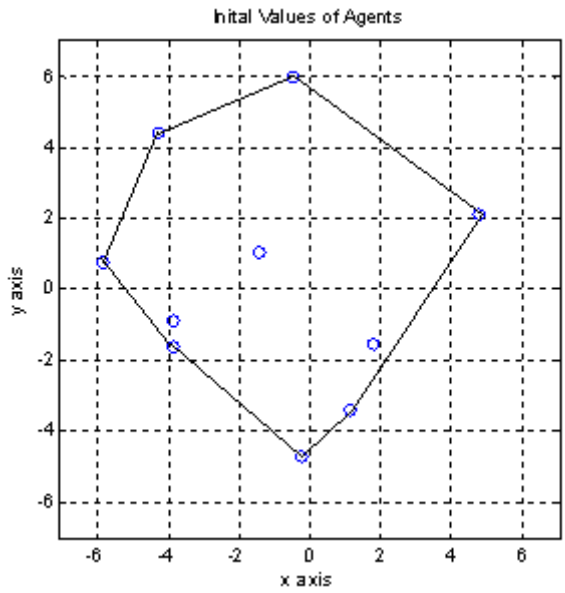

Figure 3.4: Convex hull of initial values of the agents, see Figure 2.9

Lemma 3.1 tells that the vectors $\bar{\lambda}_{ij}(y)$ and y are always in the same direction. Taking Lemma 3.1 into consideration, it is easily seen that the velocity vectors which are at the boundary of the convex hull of the agents never points outside the convex hull. See Figure 3.4. Hence the following result.

Theorem 3.1: Consider the system (3.2) where coupling is not necessarily connected. Then, $\varepsilon_i(t) \in co\{\varepsilon_1(0),\cdots,\varepsilon_N(0)\}$ for all $t \geq 0$ and i.

Theorem 3.1 implies that $co\{\varepsilon_1(t+T),\cdots,\varepsilon_N(t+T)\} \subset co\{\varepsilon_1(t),\cdots,\varepsilon_N(t)\}$ for all $T, t \geq 0$. Moreover, when the coupling graph is connected, the convex hull shrinks to one point, which means the consensus of the agents is satisfied. For the proof of the shrinkage of the agents to a single point, see [28]. We now give the formal application of this result to our case.

For $x = \left[x_1^T x_2^T \cdots x_N^T\right]$ with $x_i \in R^n$ let $A := \{x \in R^{nN} : x_i = x_j$ for all i, j$\}$ be synchronization manifold. Define

$$\gamma_{av}(x) = \begin{bmatrix} \sum \bar{\gamma}_{1j}(x_j - x_1) \\ \vdots \\ \sum \bar{\gamma}_{Nj}(x_j - x_N) \end{bmatrix},$$

Then we express (3.6) as

$$\dot{x} = \gamma_{av}(x). \tag{3.7}$$

Now we have the following theorem.

Theorem 3.2: Consider system (3.7). Synchronization manifold A is globally asymptotically stable [27].

To sum up, by the help of Lemma 3.1 and [28], the consensus of average system is shown. Therefore first three steps of the procedure are accomplished. However, we are not finished yet. Going back to the original system is needed.

In the previous pages we have talked about perturbation theory [29] and according to the perturbation theory, we can say that consensus of the average system implies the consensus of the time varying system on condition that the frequency is large enough. Since changing the coordinates, in other words moving from the original system to time varying system, is performed by the rotation matrix $e^{-S(w)t}$, the relative distances between the states are preserved, mathematically $\left|x_i(t) - x_j(t)\right| = \left|\varepsilon_i(t) - \varepsilon_j(t)\right|$ for all t and all i, j. Therefore, from synchronization point of view the original system and the time varying system are the same. This means consensus of time-varying system implies the synchronization of the original system. At this point final step of the procedure is accomplished and synchronization of the original system for large frequency values is shown.

To sum up, we applied a solution procedure to show the synchronization of nonlinearly coupled harmonic oscillators for large frequency values. First, we changed the coordinates by a rotation matrix and obtain the time-varying system. Then we obtained the approximate system via averaging. In step three, we showed that average system reaches to a consensus. In last step, we returned to the original time-invariant system and showed synchronization of the original system. Hence, the result of overall procedure is that; nonlinearly coupled identical harmonic oscillators synchronize for large frequencies provided that coupling graph is connected and the coupling function, $\gamma_{ij}(.)$, is either zero or the graph of $\gamma_{ij}(.)$ takes place only in the first and third quadrants.

In this chapter, synchronization of the nonlinearly coupled identical harmonic oscillators is shown for large frequency values. In the next chapter, the simulation results will suggest that the synchronization occurs for any w.

CHAPTER 4

SIMULATIONS

In Chapter 4, simulations will be used to analyze the coupled harmonic oscillators. In section 4.1, the simulator will be introduced. The inputs and outputs of the simulator and the general idea about the algorithms of the simulations will be given. In the rest of the Chapter 4, simulation results will be initially used to support the theoretical results obtained in previous chapters and then simulations will suggest us the results about the unproved part of synchronization of coupled harmonic oscillators.

4.1 SIMULATOR

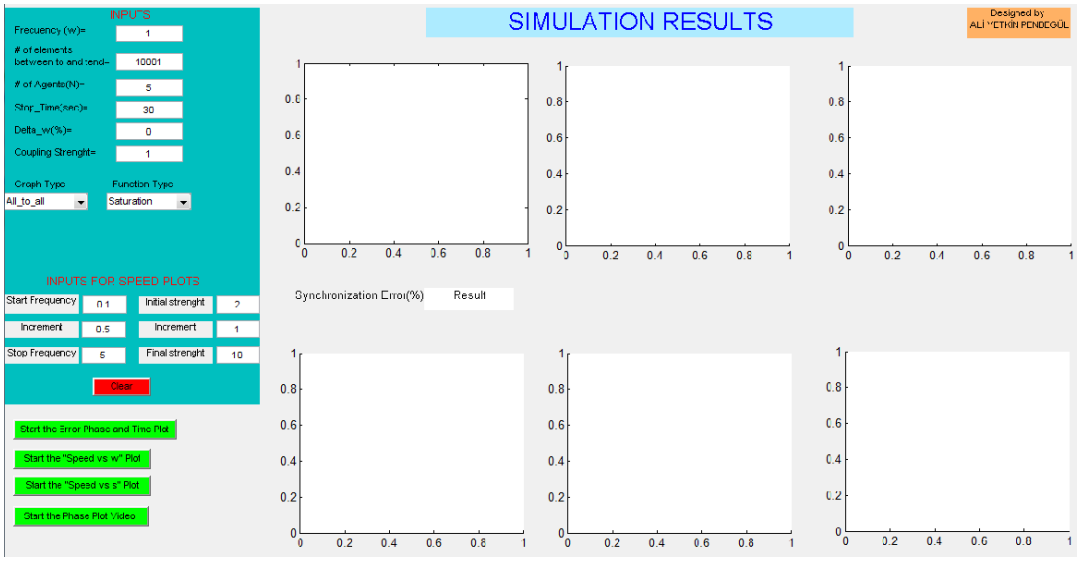

Figure 4.1: GUI.

All simulations are run in the GUI, the user interface of MATLAB. The simulator has various input values which can be entered by the user. There are four different start buttons to start different algorithms. Since visual aids give a better understanding to the user, the results of all algorithms are plotted and shown by the graphs.

4.1.1 Inputs

The inputs in the GUI are as follows:

- Frequency (w rad/sec): The rotation frequency of the harmonic oscillators is entered. This is the frequency value of the first agent. The frequency values of the other agents are calculated by the help of Δw (delta_w). If Δw is zero, all agents have the same frequency.

- Number of elements between t_o and t_{end}: The number of calculations between start and end time during the solution of the differential equations inside the algorithms is entered.

- Number of agents (N): Agent number of the system is entered.

- Stop time: The length of the process.

- Delta_w (Δw%): This input gives the percentage differences between the frequency values of the agents. For example, let w=1 rad/sec, Δw=5% and N=4, then the frequency values of the agents are w_1=1 rad/sec, w_2=1.05 rad/sec, w_3 and w_4 are selected randomly between 1 rad/sec and 1.05 rad/sec or let w=3 rad/sec, Δw=3% and N=5, then the frequency values of the agents are w_1=3 rad/sec, w_2=3.09 rad/sec, w_3, w_4, and w_5 are selected randomly between 3 rad/sec and 3.09 rad/sec.

- Coupling strength (s): The strength of the coupling value is entered. If s is small, the coupling is weak and as s increases, the coupling gets stronger. To be more clear, the mathematical model including the strength term, s, is

$$\dot{q}_i = wp_i \qquad (4.1\text{-a})$$

$$\dot{p}_i = -wq_i + \sum_{i \neq j} s\gamma_{ij}(p_j - p_i), \qquad \text{i=1, 2,…N} \qquad (4.1\text{-b})$$

• Coupling graph: There are 3 type of coupling graphs. User can select any of them.

✓ All-to-all: This graph type has bidirectional coupling and each edge behaves like dampers in mass-damper systems. See Figure 2.2.

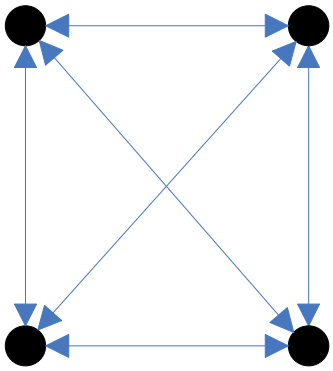

Figure 4.2: All-to-all graph for N=4.

✓ Ring: This graph type has unidirectional coupling. Therefore, the edges behave as special dampers having effect only on one direction.

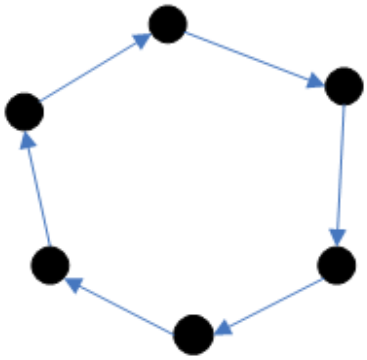

Figure 4.3: Ring graph for N=6.

✓ Tree: This graph type has unidirectional coupling, as well. Moreover, there is a leader agent affecting all other agents.

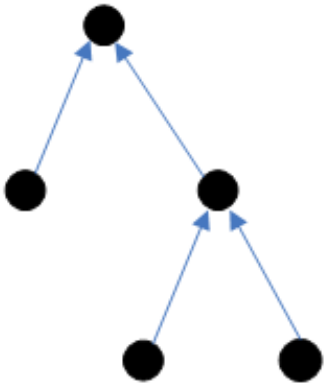

Figure 4.4: Tree graph for N=5.

• Function type: There are 3 type of coupling functions. User can select any of them.

✓ Saturation:

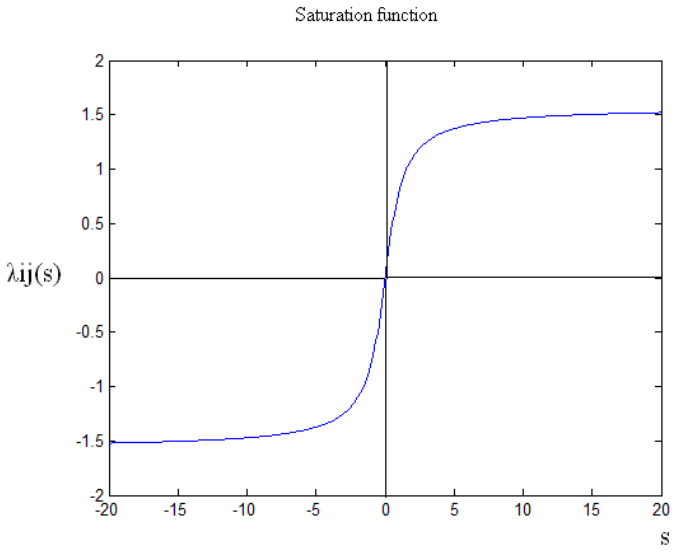

Figure 4.5: Saturation function.

✓ x^3:

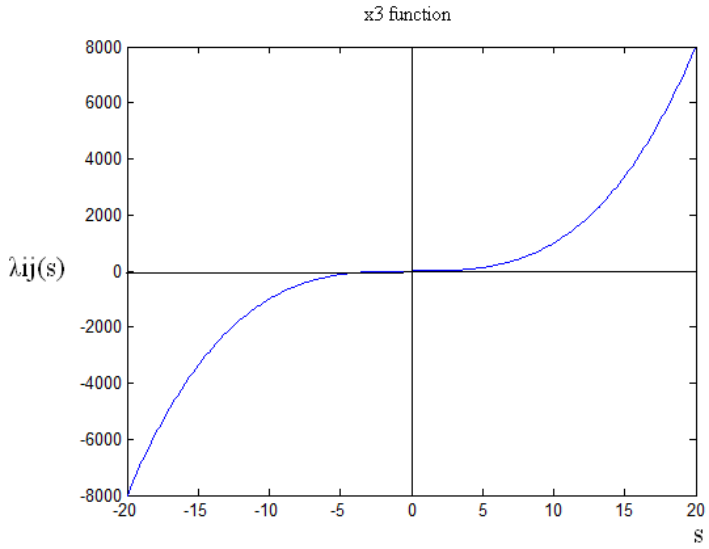

Figure 4.6: x^3 function.

✓ Linear

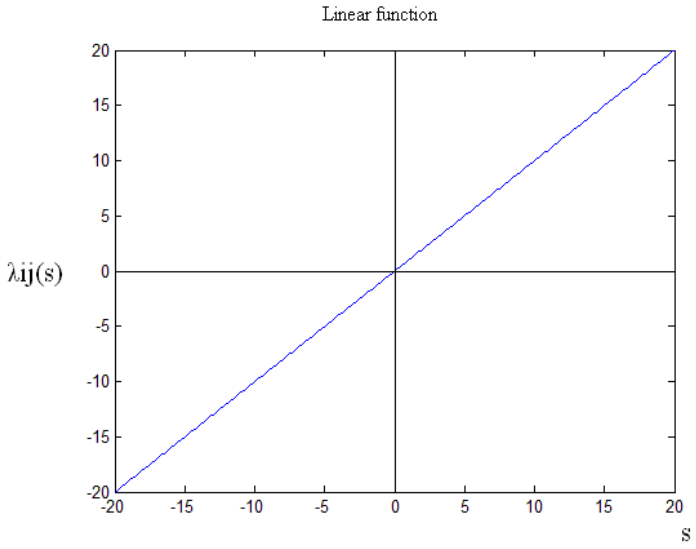

Figure 4.7: Linear function.

• Start frequency, increment, and stop frequency: These inputs are used only to plot synchronization speed vs. frequency graph.

• Initial strength, increment, and final strength: These inputs are used only to plot synchronization speed vs. coupling strength graph.

4.1.2 Start Buttons and Algorithms

- ✓ **"Start the error, phase and time plot" Button**

There are four different algorithms running inside the button. The first algorithm runs for "the error vs. time plot". In this algorithm, the synchronization error is taken as $\sum_{j \neq i} \sqrt{(p_j - p_i)^2 + (q_j - q_i)^2}$ where i=1, 2,…,N and N is the total agent number. Then, initial error value is normalized to 100. Therefore, the synchronization error value in the simulator is the percentage value of the initial error. At the beginning synchronization error is always 100% and as time goes on, it gets smaller. In other words, as the states of harmonic oscillators come closer, the error approaches zero.

The second algorithm runs for the phase space plot. Phase space plot gives the "velocity vs. position" values of the agents changing with time. Since the oscillations are periodic, the graph is a closed curve. Moreover, since the graph contains both state and derivative of the state, it gives us full information about the synchronization of agents.

The third and fourth algorithms give the "position vs. time" and "velocity vs. time" plots. These plots separately do not give complete information. Two plots, together, are needed to understand the complete behavior of the agents. Using these two plots we can observe the synchronization of the states of the agents, position and velocity separately.

- ✓ **"Start the phase plot video" Button**

This button plots the phase space; "velocity vs. position" plot, as well. The difference from the phase plot algorithm in **"**Start the error, phase and time plot" button is in this button the phase space is plotted as a video. It is a good way to observe behavior of the agents second by second.

- ✓ **"Start the speed vs. w" Button**

"Start the speed vs. w" button shows the change in the synchronization speed with respect to different frequency values. Synchronization speed is defined as $1/T$

where *T* is the time needed for the synchronization error to reach 1/1000 of the initial error value. For each frequency value, the synchronization speed is calculated and plotted.

- ✓ **"Start the speed vs. s" Button**

"Start the speed vs. s" button shows the change of synchronization speed with respect to different coupling strength values. Synchronization speed is defined as 1/*T* where *T* is the time needed for the synchronization error to reach 1/1000 of the initial error value. For each coupling strength value, the synchronization speed is calculated and plotted.

4.2 SIMULATION RESULTS

4.2.1 Frequency vs. Synchronization Relation

In this section, during the analysis agent number N is taken as 5, initial conditions are selected randomly in the region of [0, 20], t_{end} is changing according to the frequency, number of elements between t_o and t_{end}, n, is 10001 and all the agents have exactly same frequency.

Simulation results are synchronization error of the harmonic oscillators, phase plot, "position vs. time" and "velocity vs. time" plots. For large frequency values complete time scale of the position and velocity versus time plots do not tell much about the synchronization. Therefore, for w=100 rad/sec we zoom to the starting time and finishing time of these two plots. In this case synchronization error plot and final error value also gives the relevant information about the behavior of the agents.

4.2.1.1 Linear Coupling

In section 2.6, it is stated that linearly coupled harmonic oscillators synchronize for any frequency provided that the coupling graph is connected. In the following graphs simulation results of linearly coupled harmonic oscillators for various frequency values are illustrated. The simulations are run for

-graph types: all-to-all and tree,

-coupling function: linear,

-frequency values: 1 rad/sec, 10 rad/sec, and 100 rad/sec,

-coupling strength: 1.

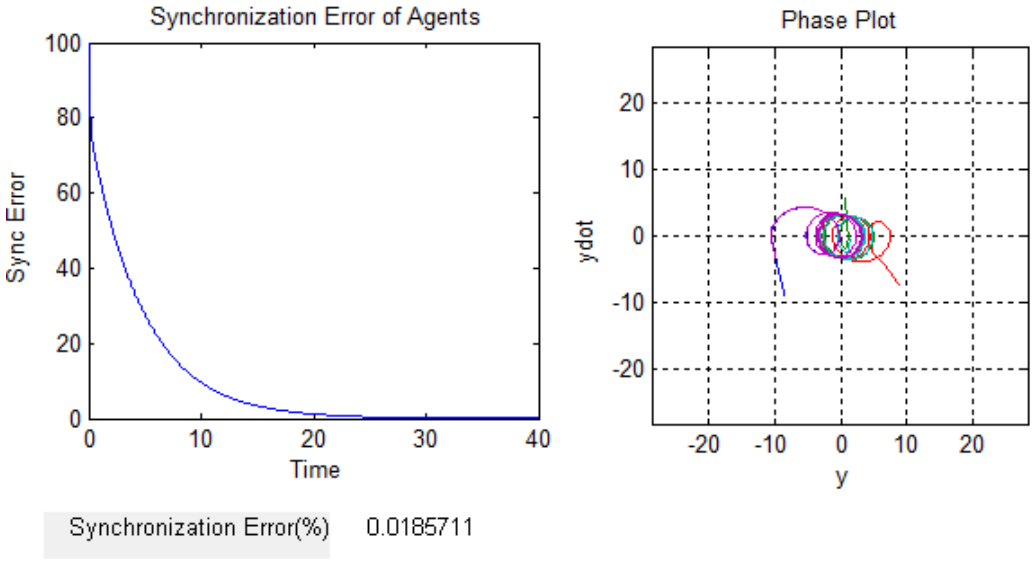

Figure 4.8: Synchronization error and phase plot for graph type: all-to-all, coupling function: linear, w=1 rad/sec.

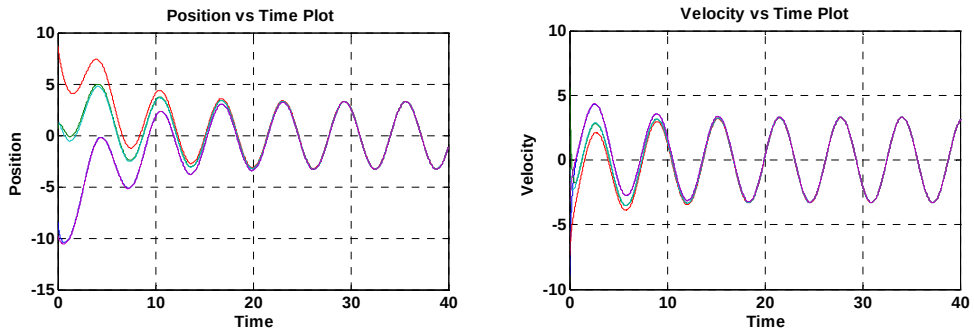

Figure 4.9: “Position vs. time” and “velocity vs. time” plots for graph type: all-to-all, coupling function: linear, w=1 rad/sec.

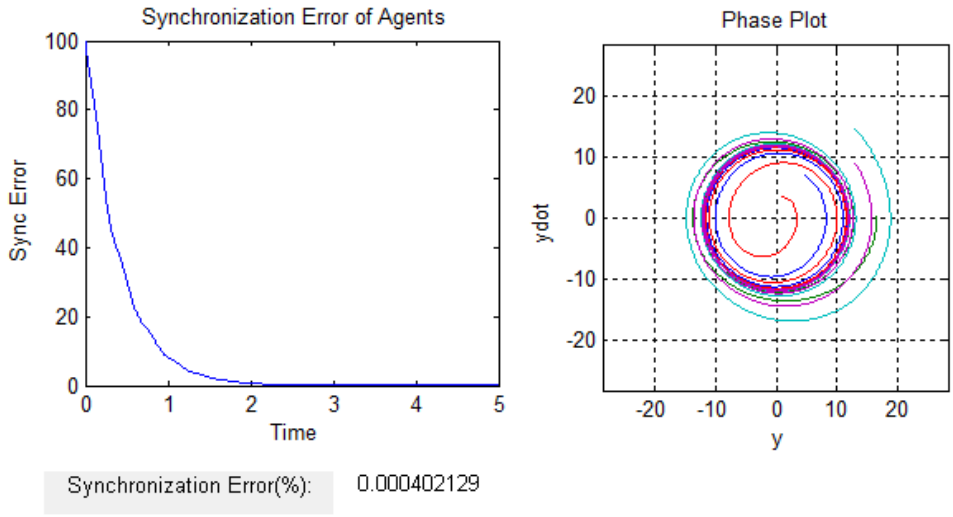

Figure 4.10: Synchronization error and phase plot for graph type: all-to-all, coupling function: linear, w=10 rad/sec.

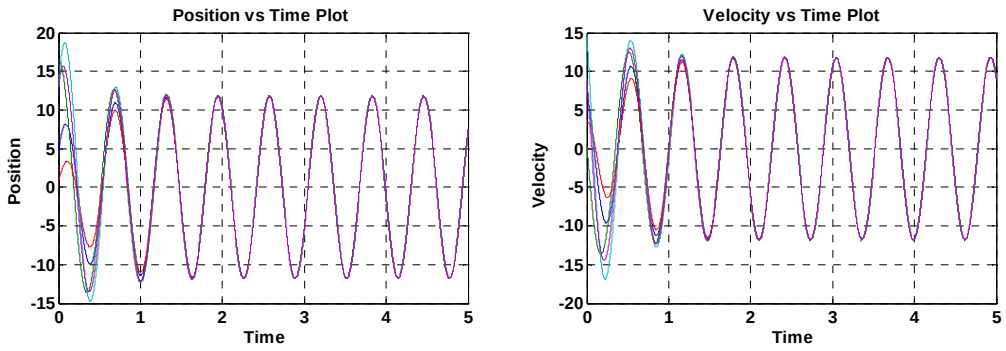

Figure 4.11: "Position vs. time" and "velocity vs. time" plots for graph type: all-to-all, coupling function: linear, w=10 rad/sec.

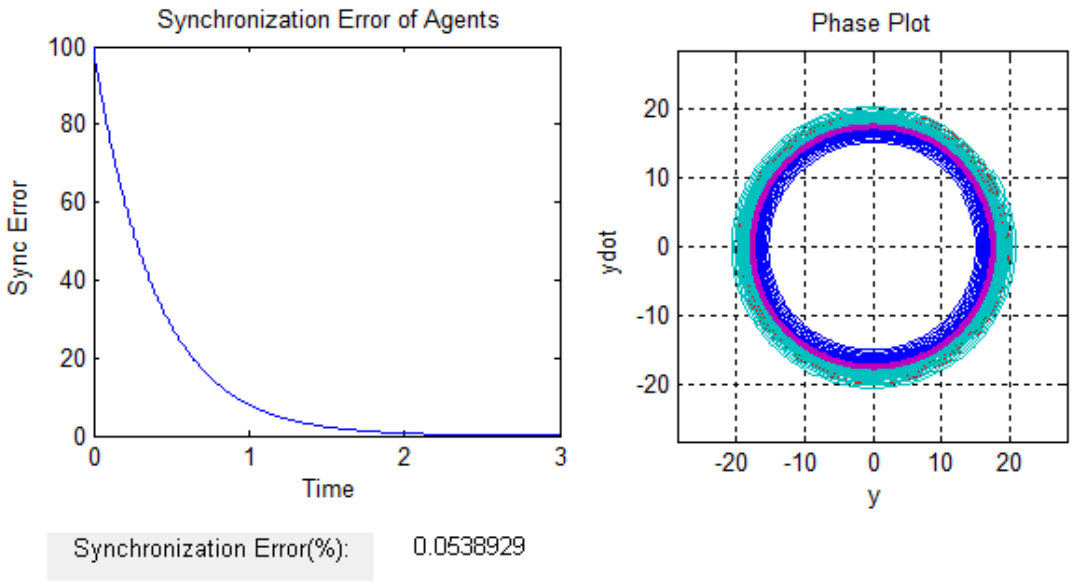

Figure 4.12: Synchronization error and phase plot for graph type: all-to-all, coupling function: linear, w=100 rad/sec.

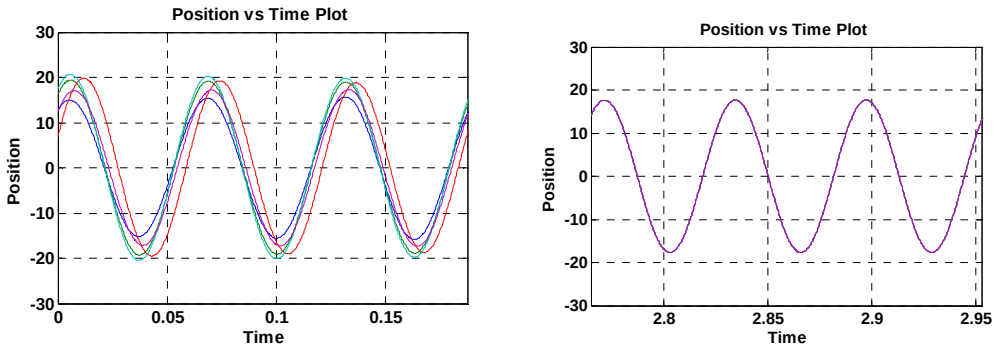

Figure 4.13: “Position vs. time” plots for graph type: all-to-all, coupling function: linear, w=100 rad/sec.

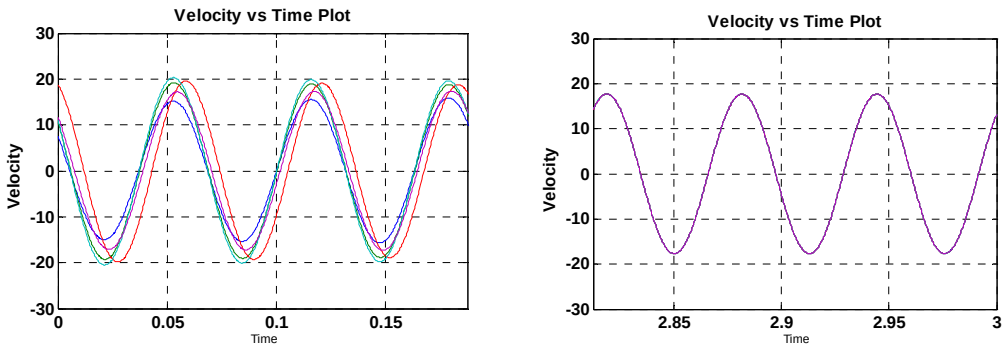

Figure 4.14: "Velocity vs. time" plots for graph type: all-to-all, coupling function: linear, w=100 rad/sec.

When we analyse the simulation results from synchronization point of view, the simulation results of linearly coupled harmonic oscillators for "all-to-all" coupling confirm the theoretical results, which means the synchronization is achieved independent of frequency value. Only difference between the plots for different frequency values are the synchronization speed. For w=10 rad/sec and 100 rad/sec, synchronization is achieved in less than 5 seconds. When w=1 rad/sec, since the frequency of the agents is not large, the synchronization is a bit slower and synchronization of the agents takes about 30-40 seconds. This issue is related to synchronization speed and we will give the simulation results about synchronization speed in later pages.

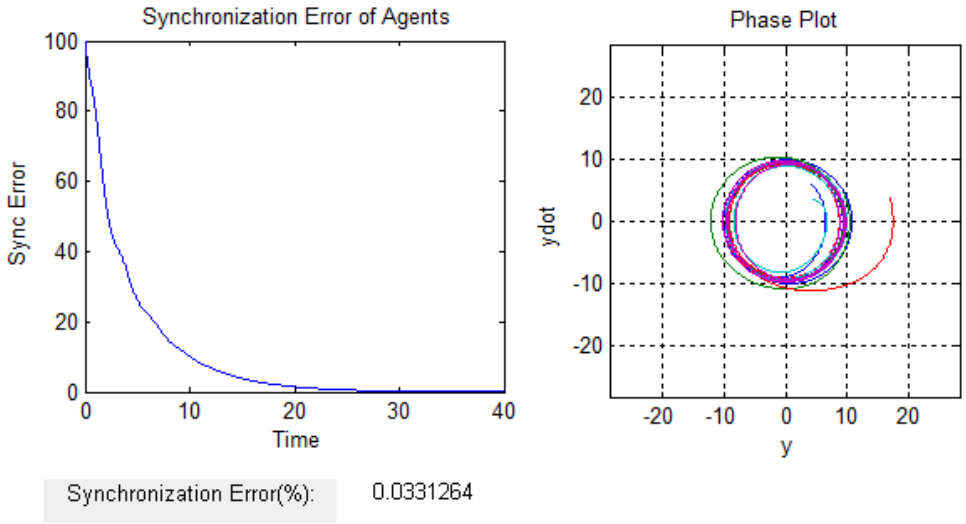

Figure 4.15: Synchronization error and phase plot for graph type: tree, coupling function: linear, w=1 rad/sec.

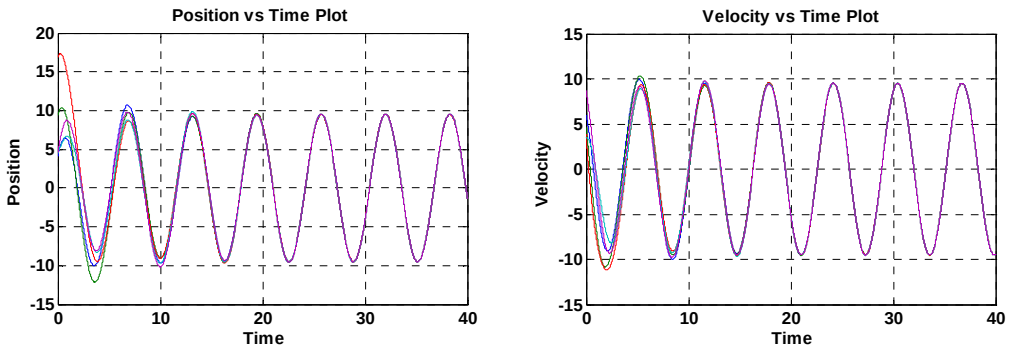

Figure 4.16: “Position vs. time” and “velocity vs. time” plots for graph type: tree, coupling function: linear, w=1 rad/sec.

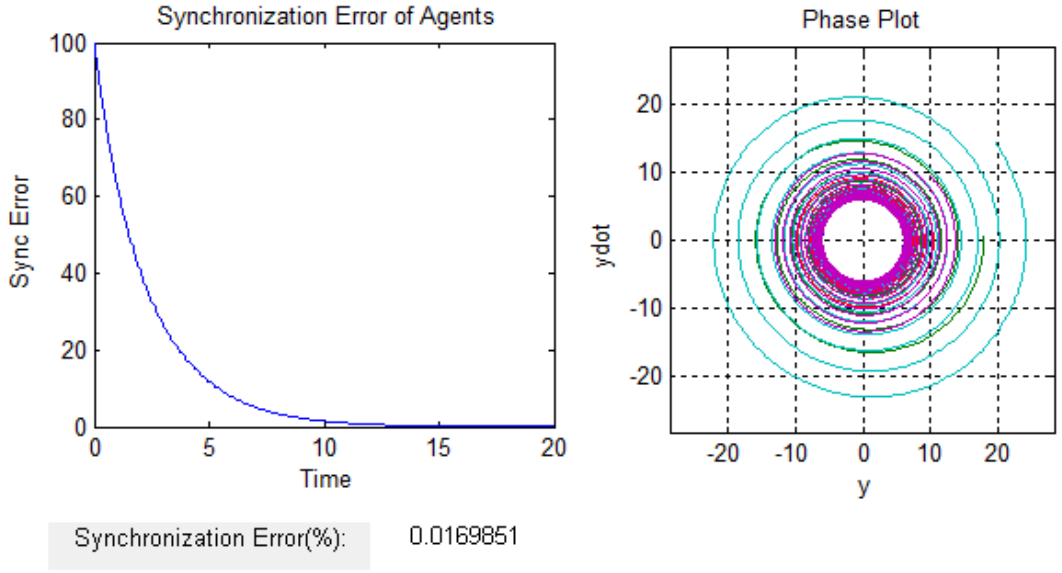

Figure 4.17: Synchronization error and phase plot for graph type: tree, coupling function: linear, w=10 rad/sec.

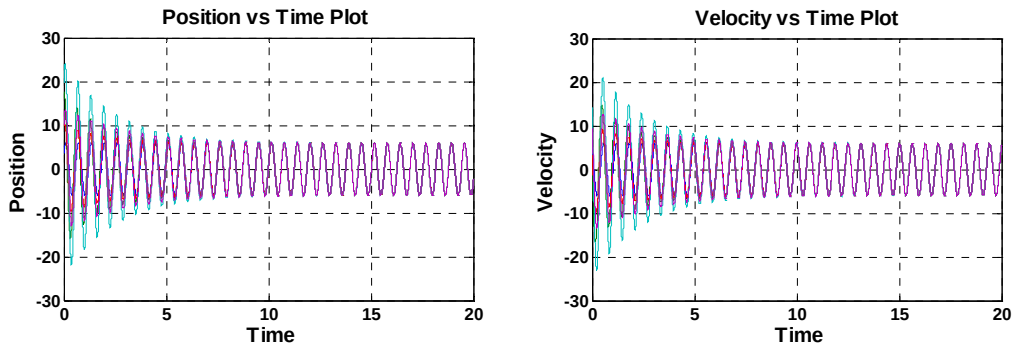

Figure 4.18: “Position vs. time” and “velocity vs. time” plots for graph type: tree, coupling function: linear, w=10 rad/sec.

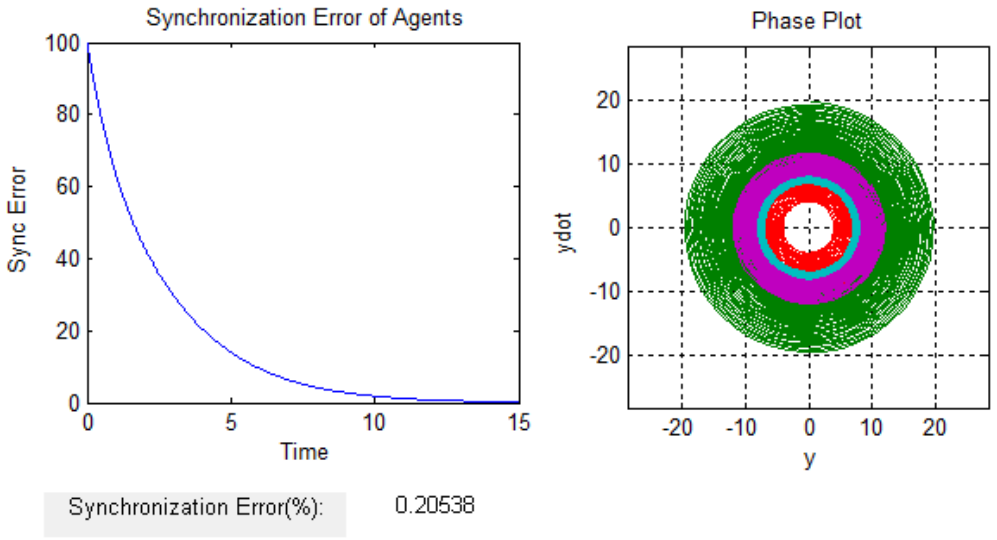

Figure 4.19: Synchronization error and phase plot for graph type: tree, coupling function: linear, w=100 rad/sec.

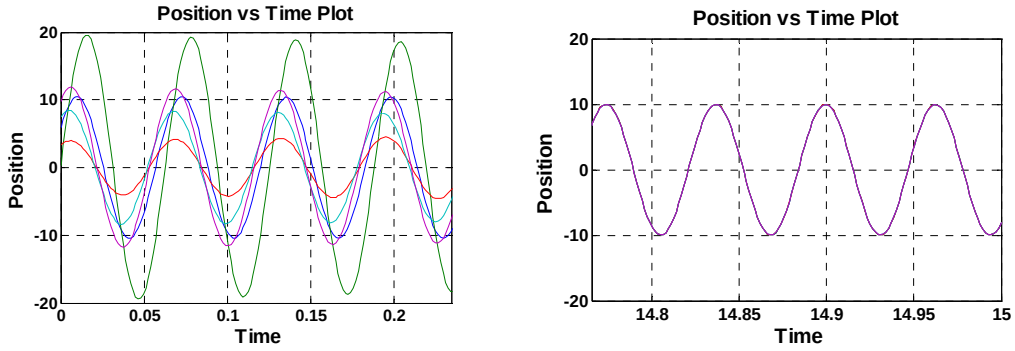

Figure 4.20: “Position vs. time” plots for graph type: tree, coupling function: linear, w=100 rad/sec.

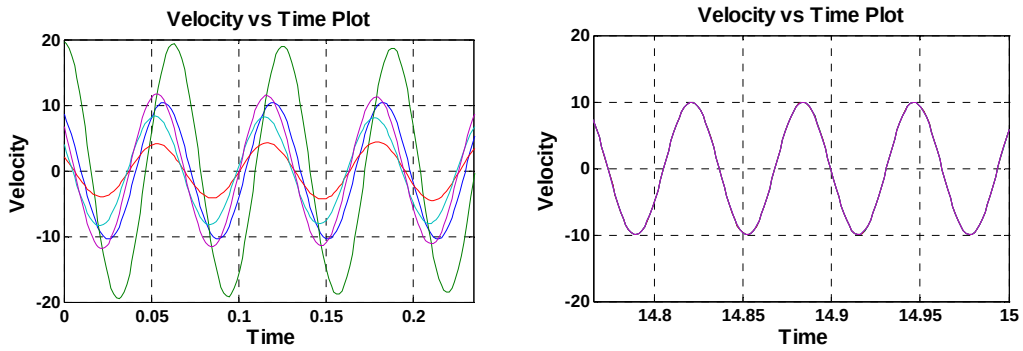

Figure 4.21: "Velocity vs. time" plots for graph type: tree, coupling function: linear, w=100 rad/sec.

When the coupling graph is selected as "tree", linearly coupled harmonic oscillators synchronize for all frequency values just like in the case of "all-to-all" coupling.

As a result, we can say that simulation results are pretty much close to the expected results. In other words, theoretical results of the synchronization of linearly coupled harmonic oscillators are supported by the simulation results.

The nonlinear coupling of harmonic oscillators is relatively more complicated than linear coupling case. In the following section nonlinear coupling will be studied.

4.2.1.2 Nonlinear Coupling

In Chapter 3, we have argued that nonlinearly coupled harmonic oscillators synchronize if the coupling graph is connected and frequency is large enough. However, when the frequency of harmonic oscillators is not large enough, the synchronization of harmonic oscillators is not proved (or disproved) for nonlinear coupling. In this part we will observe the simulations of nonlinearly coupled harmonic oscillators for different frequency values. The simulations are run for

-graph types: all-to-all and ring,

-coupling function: saturation and x^3,

-frequency values: 1 rad/sec, 10 rad/sec, and 100 rad/sec,

-coupling strength: 1.

We could have run more simulations and enlarge the simulation results for any other graph or function type. However, these parameters will be enough to make a good generalization about the synchronization of the nonlinearly coupled harmonic oscillators. Therefore, we limited the simulations with these parameters.

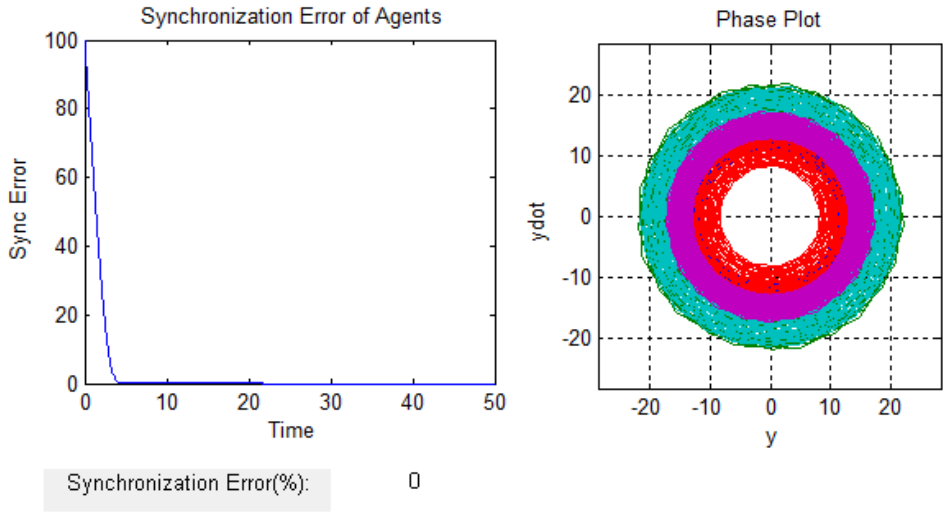

Figure 4.22: Synchronization error and phase plot for graph type: all-to-all, coupling function: saturation, w=100 rad/sec.

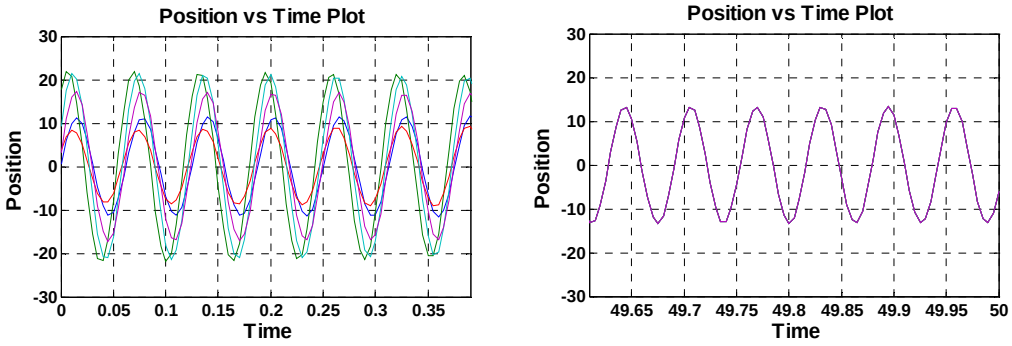

Figure 4.23: “Position vs. time” plots for graph type: all-to-all, coupling function: saturation, w=100 rad/sec.

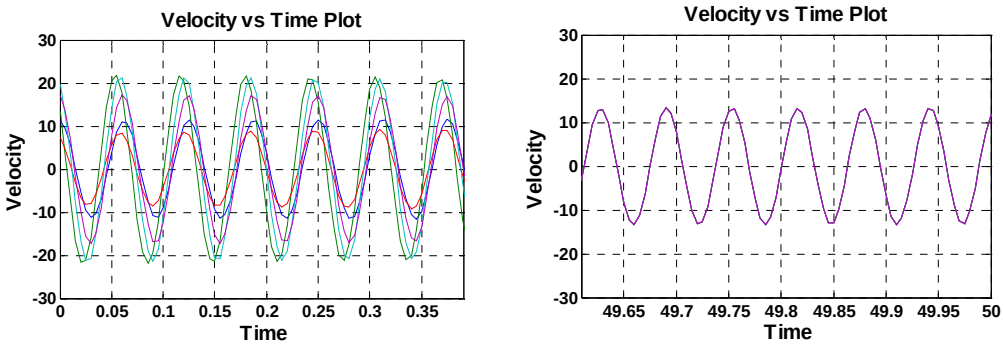

Figure 4.24: "Velocity vs. time" plots for graph type: all-to-all, coupling function: saturation, w=100 rad/sec.

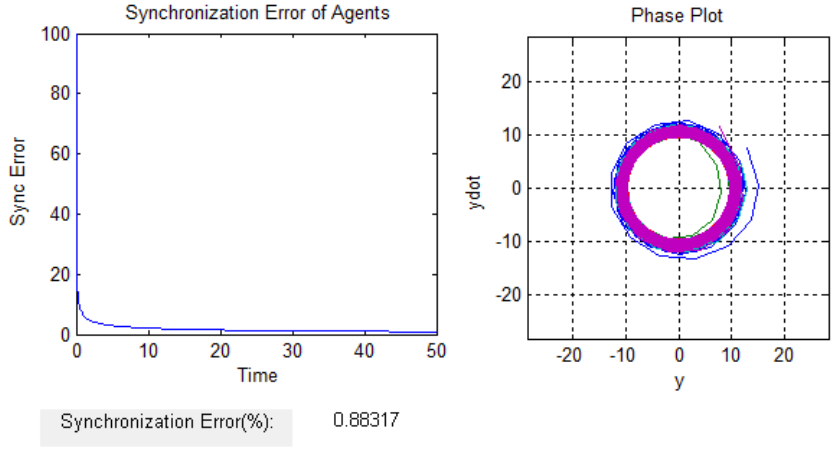

Figure 4.25: Synchronization error and phase plot for graph type: all-to-all, coupling function: x^3, w=100 rad/sec.

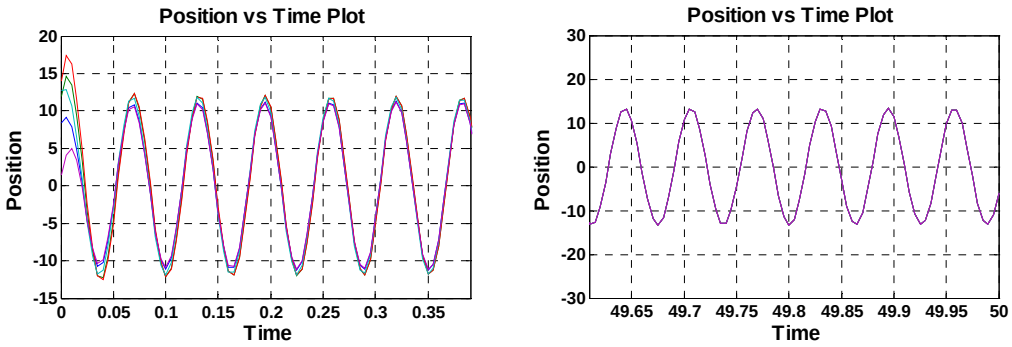

Figure 4.26: "Position vs. time" plots for graph type: all-to-all, coupling function: x^3 , w=100 rad/sec.

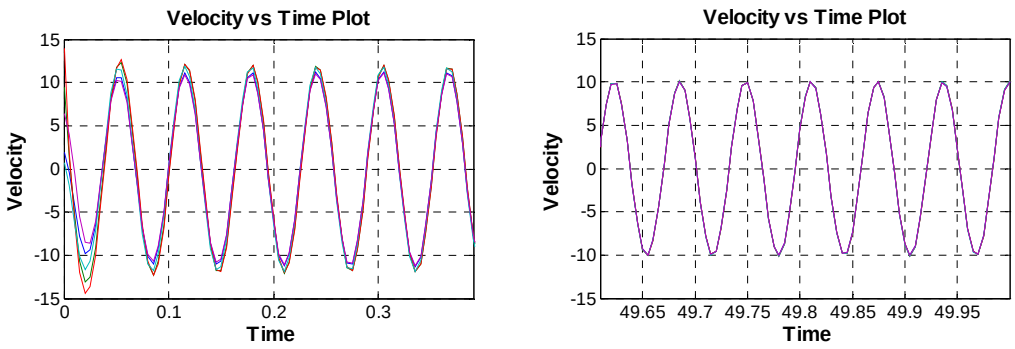

Figure 4.27: "Velocity vs. time" plots for graph type: all-to-all, coupling function: x^3, w=100 rad/sec.

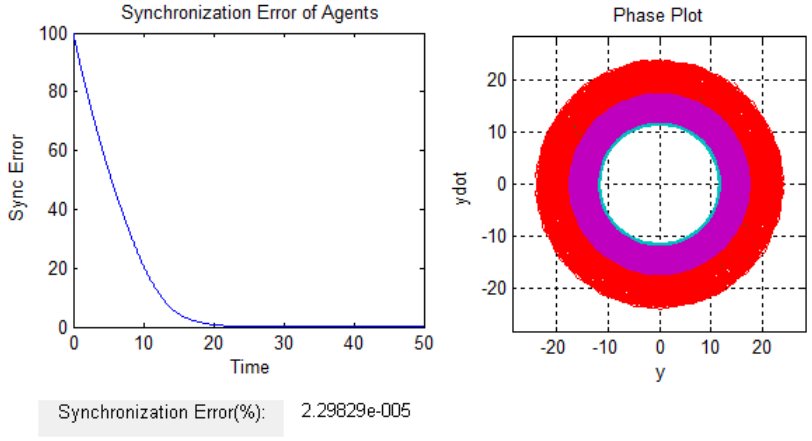

Figure 4.28: Synchronization error and phase plot for graph type: ring, coupling function: saturation, w=100 rad/sec

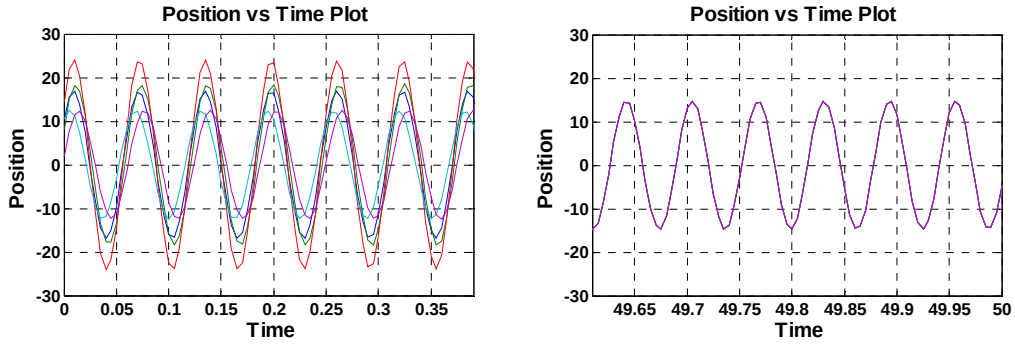

Figure 4.29: "Position vs. time" plots for graph type: ring, coupling function: saturation, w=100 rad/sec.

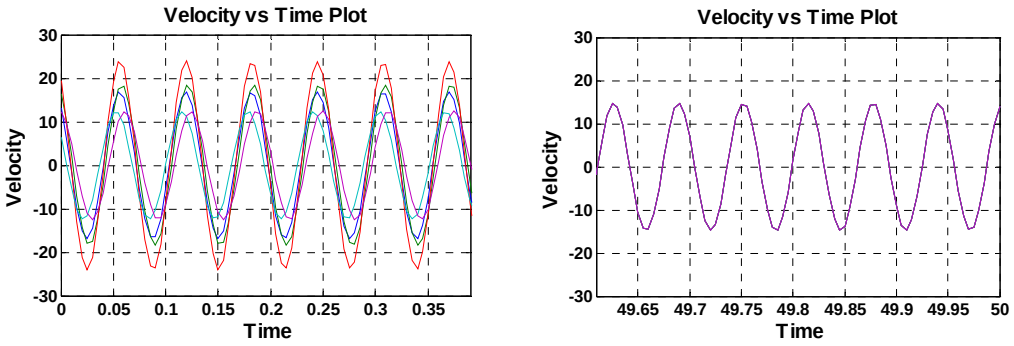

Figure 4.30: "Velocity vs. time" plots for graph type: ring, coupling function: saturation, w=100 rad/sec.

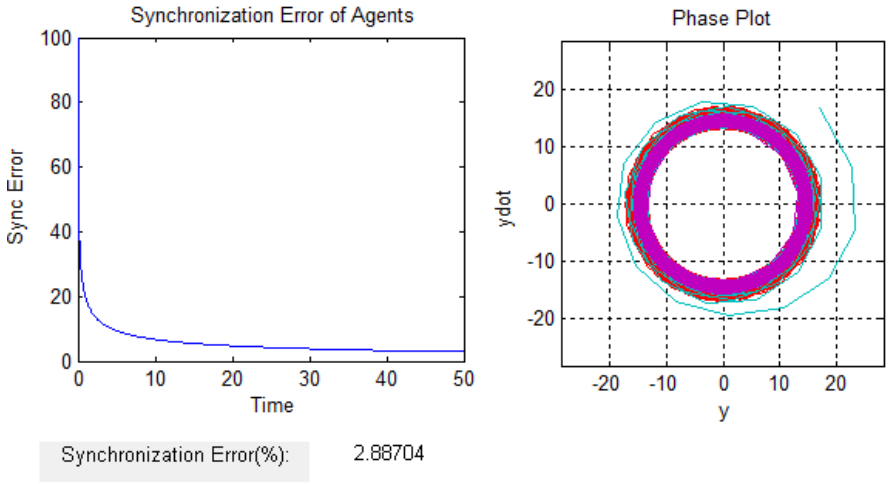

Figure 4.31: Synchronization error and phase plot for graph type: ring, coupling function: x^3, w=100 rad/sec.

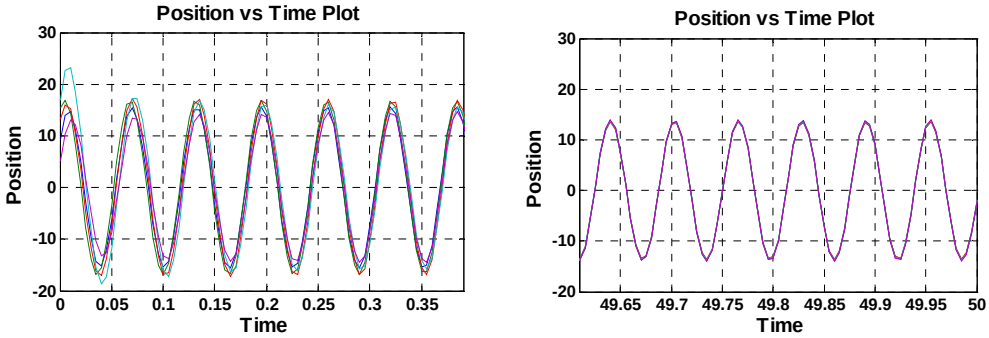

Figure 4.32: "Position vs. time" plots for graph type: ring, coupling function: x^3, w=100 rad/sec.

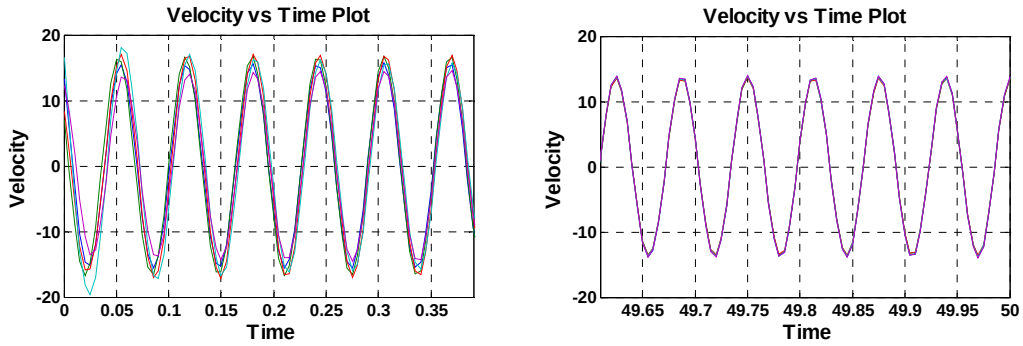

Figure 4.33: "Velocity vs. time" plots for graph type: ring, coupling function: x^3, w=100 rad/sec.

Between Figure 4.22 and Figure 4.33 the synchronization observations are done for w=100 rad/sec, graph types "all-to-all" and "ring" and coupling function types "saturation" and "x^3". Since the frequency is large, phase plots do not tell much about the synchronization. However, position vs. time, velocity vs. time, and synchronization error plots give the enough information about the behavior of the coupled oscillators.

By the help of position and velocity versus time plots we observe that harmonic oscillators are initially are not synchronized. However, they are almost synchronized in 50 seconds regardless of coupling graph and coupling function type. It is also good to analyze error plots. Figure 4.22 and Figure 4.28, although the coupling function is "saturation", error plot decreases linearly and synchronization is achieved immediately. The reason of the linearity is initial conditions of the agents are close to each other and only linear part of the saturation function is used. In Figure 4.25 and Figure 4.31, since the coupling function is "x^3", error plot is decreasing very fast in a second, but after error value is under 10%, the speed is getting slower. However, it does not stop and in each plot the synchronization is finally achieved. In the previous chapter, we already showed that nonlinearly coupled harmonic oscillators synchronize for that large frequency values provided that coupling graph is connected. Therefore, it is not wrong to say that the simulation results shown between Figure 4.22 and Figure 4.33 verify the theoretical results given in Chapter 3.

The simulations shown between Figure 4.22 and Figure 4.33 give us an intuition about the synchronization of nonlinearly coupled harmonic oscillators for large frequencies. However, they do not show that synchronization is provided for all frequency values. The following simulations will be for w=10 rad/sec and w=1 rad/sec and these simulation results will be combined with the previous results, which are obtained for w=100 rad/sec. Finally we will obtain complete information about frequency vs. synchronization relation of nonlinear coupling case.

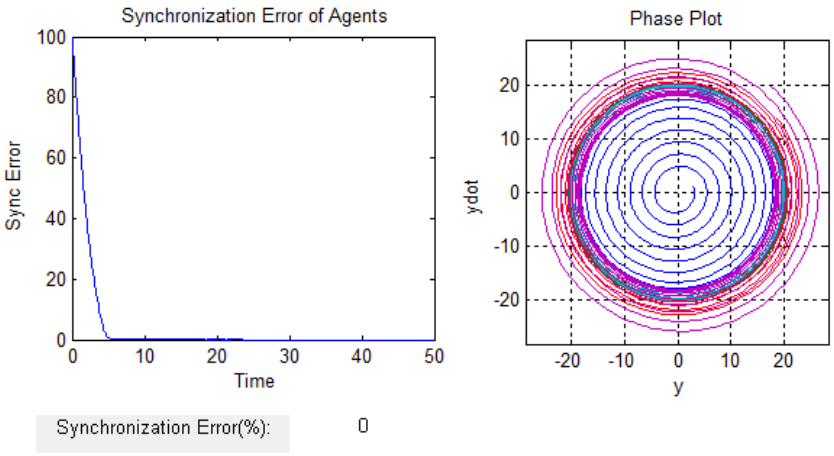

Figure 4.34: Synchronization error and phase plot for graph type: all-to-all, coupling function: saturation, w=10 rad/sec.

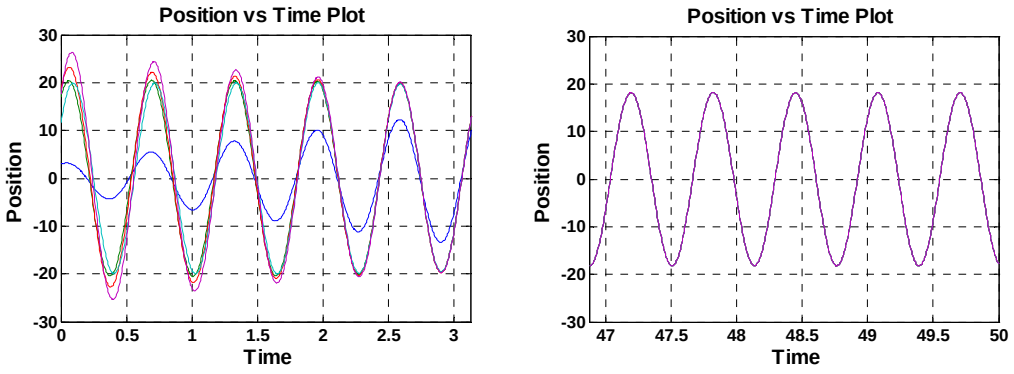

Figure 4.35: “Position vs. time” plots for graph type: all-to-all, coupling function: saturation, w=10 rad/sec.

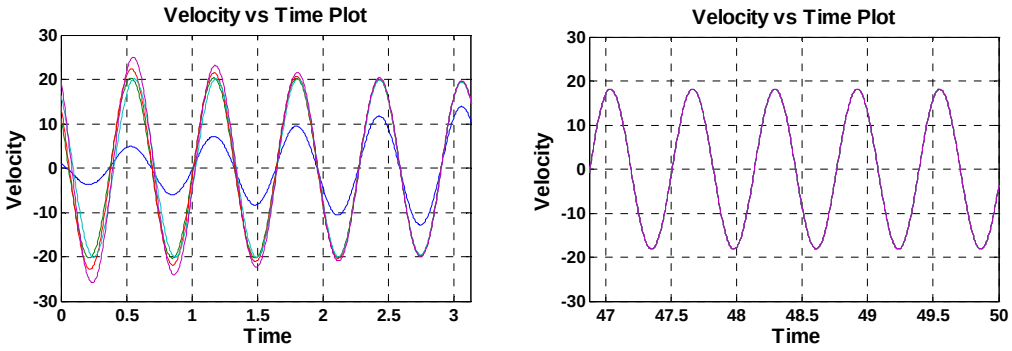

Figure 4.36: "Velocity vs. time" plots for graph type: all-to-all, coupling function: saturation, w=10 rad/sec.

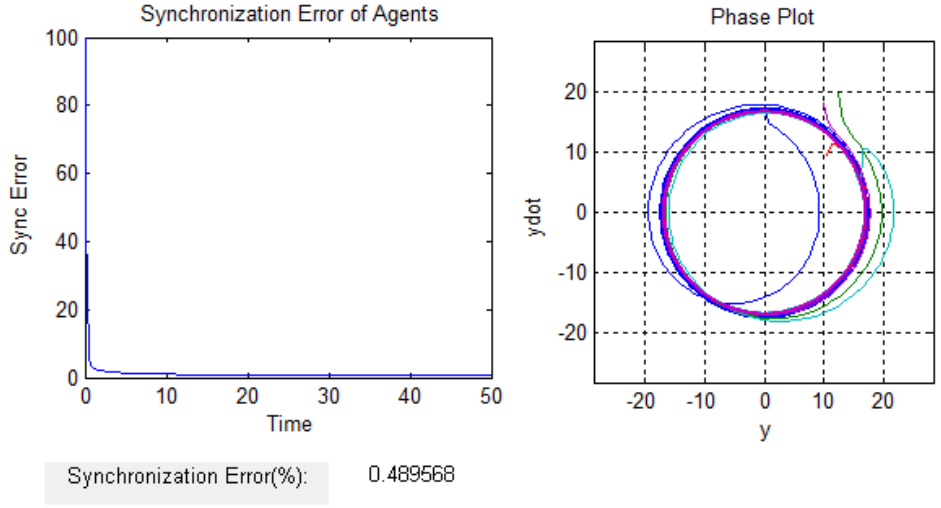

Figure 4.37: Synchronization error and phase plot for graph type: all-to-all, coupling function: x^3, w=10 rad/sec.

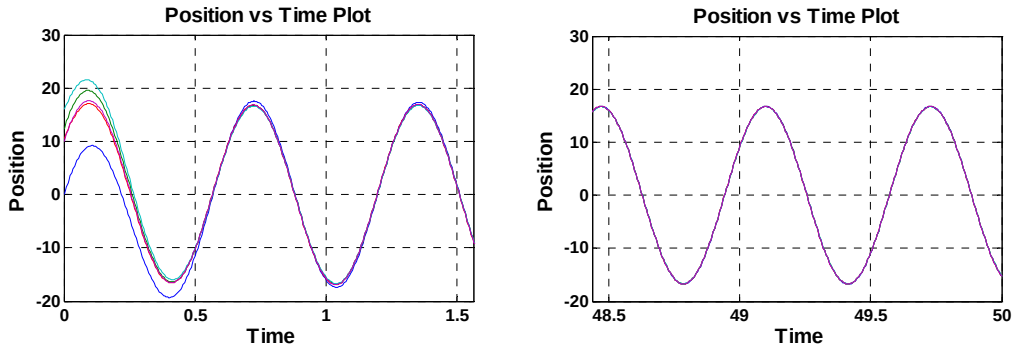

Figure 4.38: "Position vs. time" plots for graph type: all-to-all, coupling function: x^3, w=10 rad/sec.

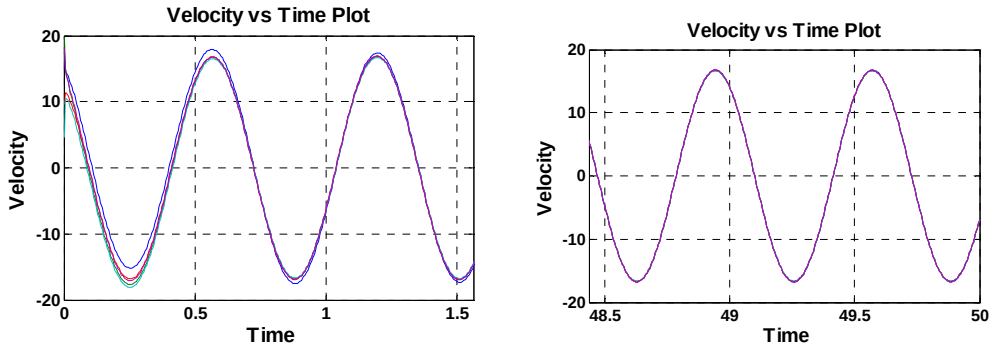

Figure 4.39: "Velocity vs. time" plots for graph type: all-to-all, coupling function: x^3, w=10 rad/sec.

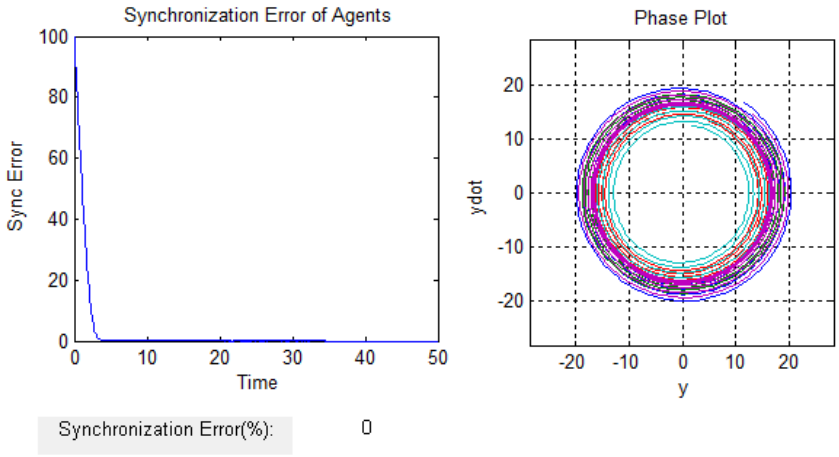

Figure 4.40: Synchronization error and phase plot for graph type: ring, coupling function: saturation, w=10 rad/sec.

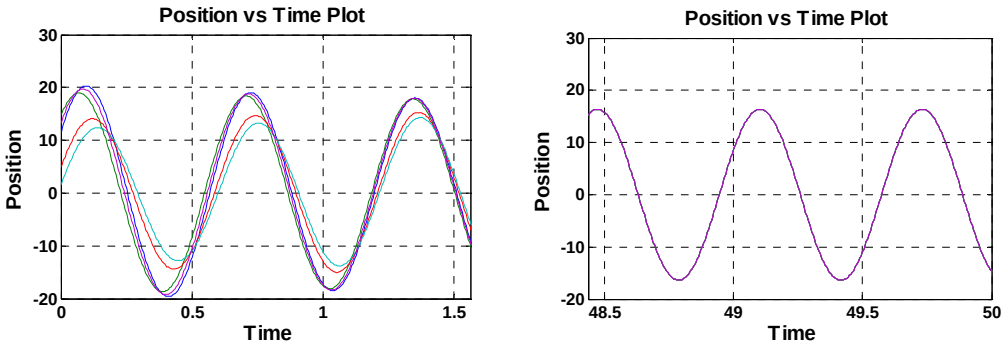

Figure 4.41: "Position vs. time" plots for graph type: ring, coupling function: saturation, w=10 rad/sec.

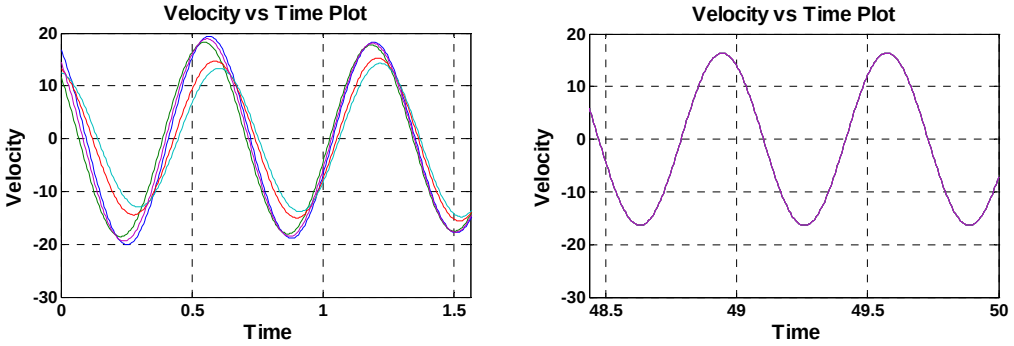

Figure 4.42: "Velocity vs. time" plots for graph type: ring, coupling function: saturation, w=10 rad/sec.

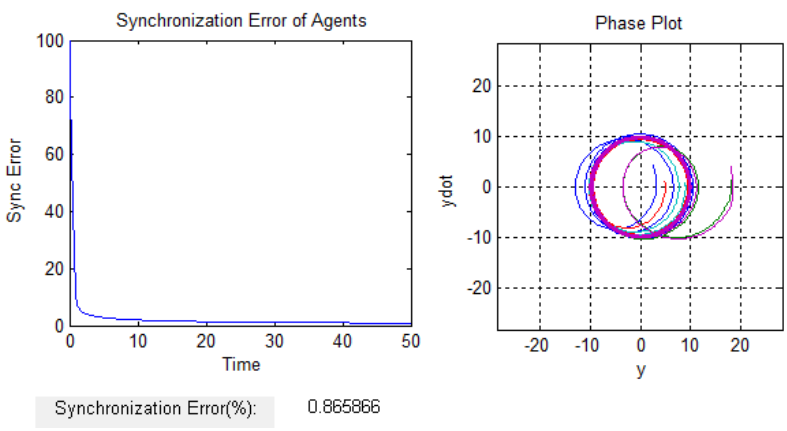

Figure 4.43: Synchronization error and phase plot for graph type: ring, coupling function: x^3, w=10 rad/sec.

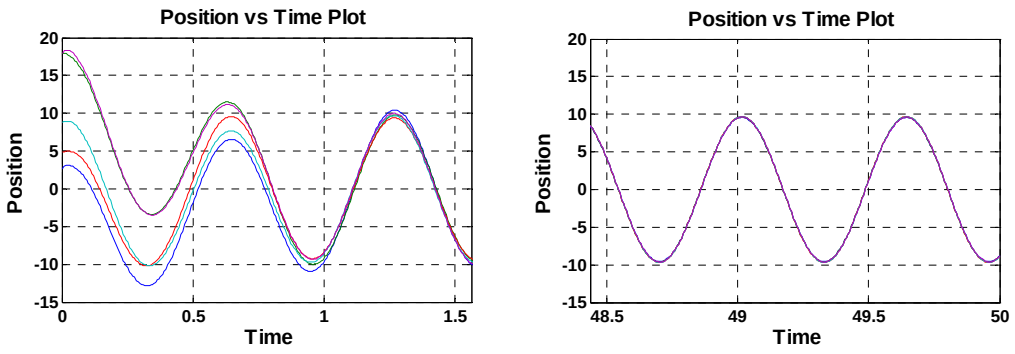

Figure 4.44: "Position vs. time" plots for graph type: ring, coupling function: x^3, w=10 rad/sec.

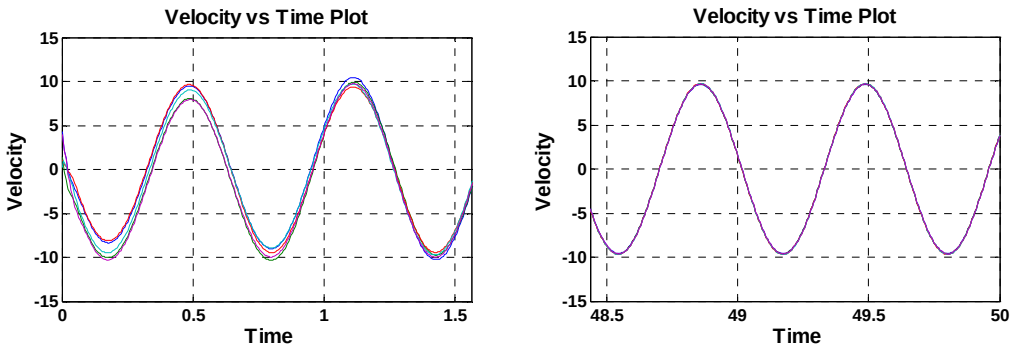

Figure 4.45: "Velocity vs. time" plots for graph type: ring, coupling function: x^3, w=10 rad/sec.

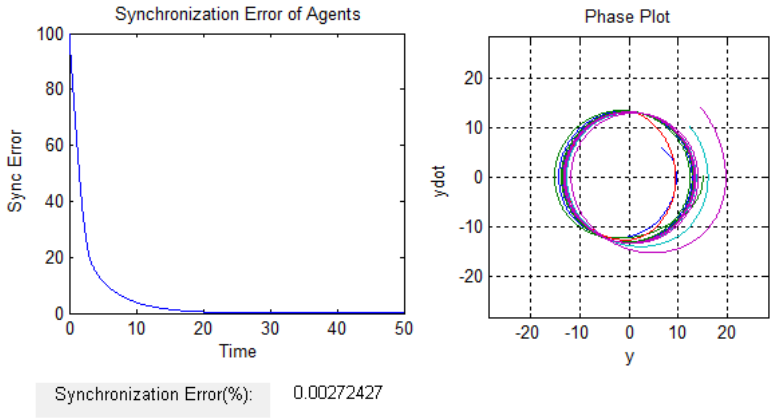

Figure 4.46: Synchronization error and phase plot for graph type: all-to-all, coupling function: saturation, w=1 rad/sec.

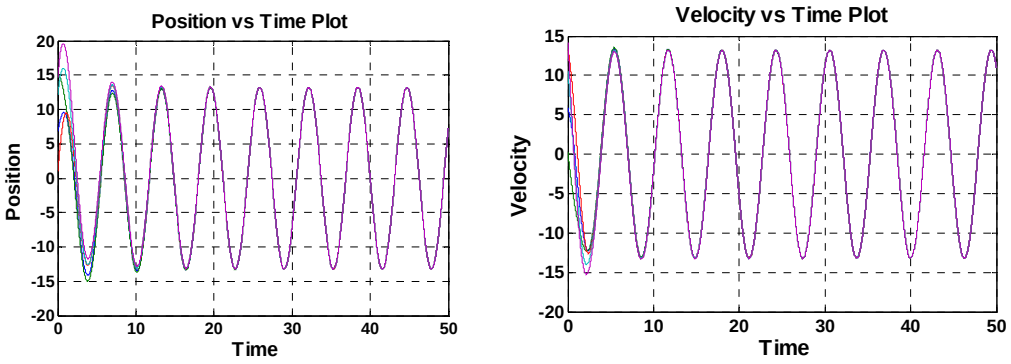

Figure 4.47: "Position vs. time" and "velocity vs. time" plots for graph type: all-to-all, coupling function: saturation, w=1 rad/sec.

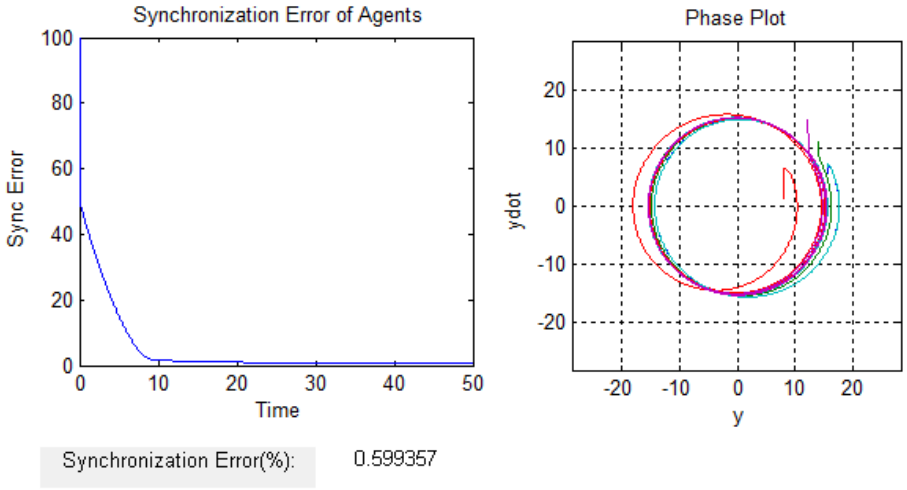

Figure 4.48: Synchronization error and phase plot for graph type: all-to-all, coupling function: x^3, w=1 rad/sec.

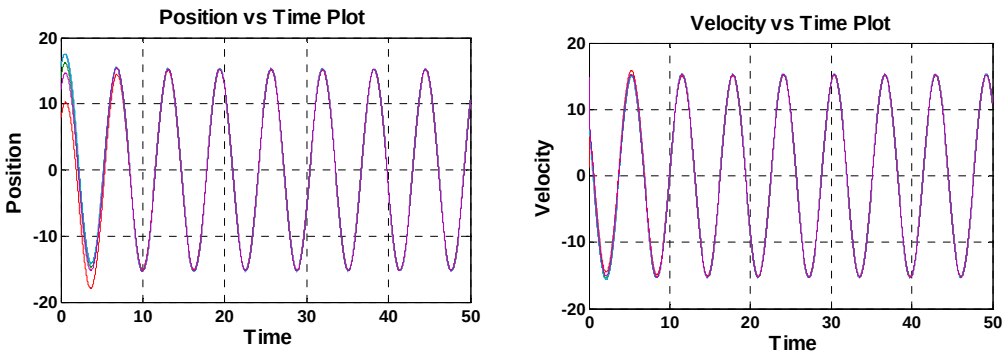

Figure 4.49 : "Position vs. time" and "velocity vs. time" plots for graph type: all-to-all, coupling function: x^3, w=1 rad/sec.

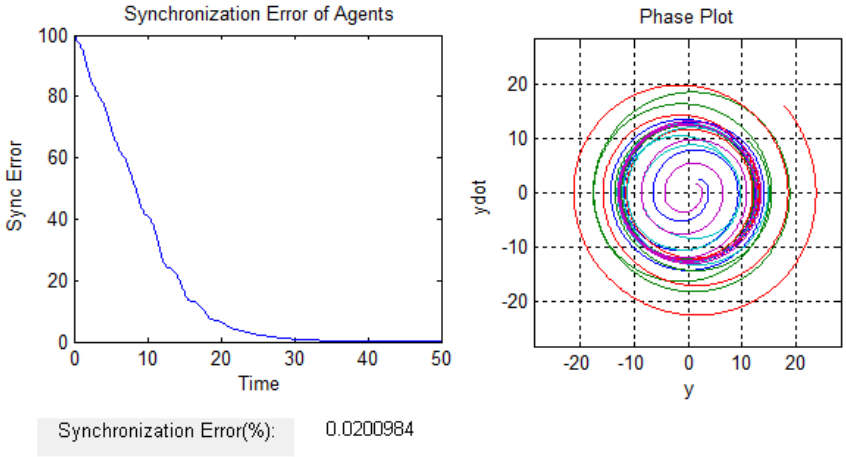

Figure 4.50: Synchronization error and phase plot for graph type: ring, coupling function: saturation, w=1 rad/sec.

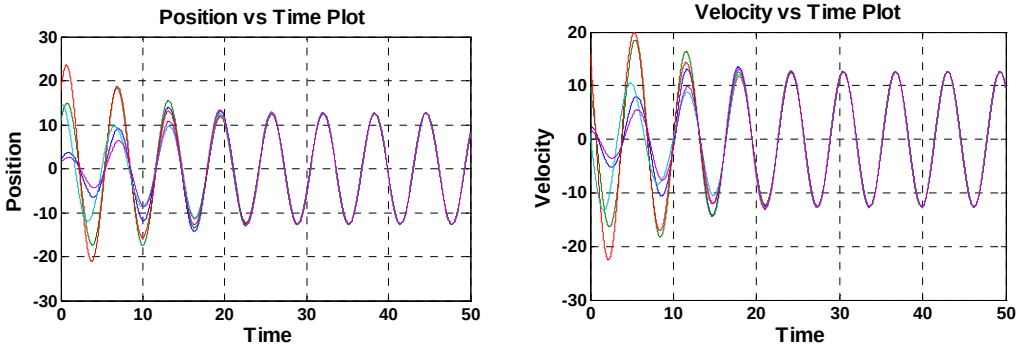

Figure 4.51: "Position vs. time" and "velocity vs. time" plots for graph type: ring, coupling function: saturation, w=1 rad/sec.

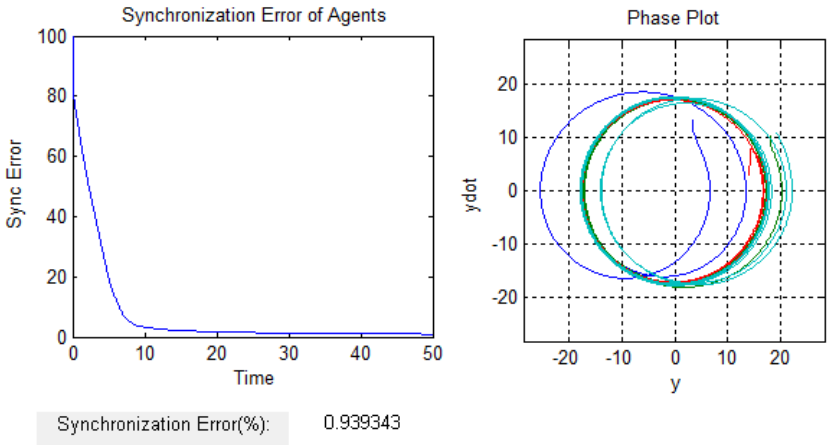

Figure 4.52: Synchronization error and phase plot for graph type: ring, coupling function: x^3, w=1 rad/sec.

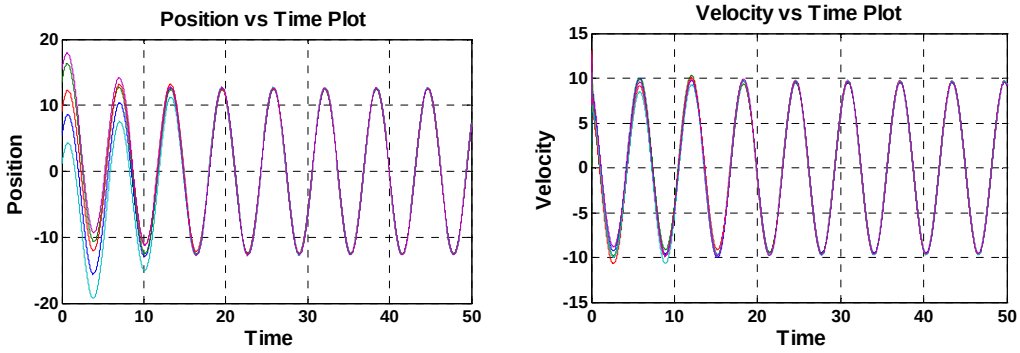

Figure 4.53: "Position vs. time" and "velocity vs. time" plots for graph type: ring, coupling function: x^3, w=1 rad/sec.

From Figure-4.34 to Figure-4.53, the simulation results for w=10 rad/sec and w=1 rad/sec are shown. The figures show that synchronization is achieved for w=10 rad/sec and w=1 rad/sec regardless of graph type and coupling function. Since there is no proof about synchronization of nonlinearly coupled harmonic oscillators for frequency values that are not large, the results of these simulations are very important. In all graphs between Figure 4.34 and Figure 4.53, it is observed that all agents synchronize with each other and they reach to the same position and velocity value. Therefore, we can say that even though it is not proved (or disproved), simulation results tell that harmonic oscillators synchronize for frequency values that are not large, as well.

To sum up, the result of all the simulations run in the section 4.2.1.2 suggest that nonlinearly coupled identical harmonic oscillators synchronize for all frequency values provided that coupling graph is connected.

4.2.2 Synchronization Speed vs. Coupling Strength Relation

Synchronization speed is also an important concept to study. In this section we try to observe the effect of coupling strength on synchronization speed. The simulations are run for

-graph types: all-to-all and tree, and ring,

-coupling function: linear and saturation,

-frequency values: 1 rad/sec and 10 rad/sec.

In this section, for each plot we obtain ten different results according to ten randomly chosen initial conditions in the region of [0, 20]. Then, we take the average of the results and plot the average result. The simulation results are as follows:

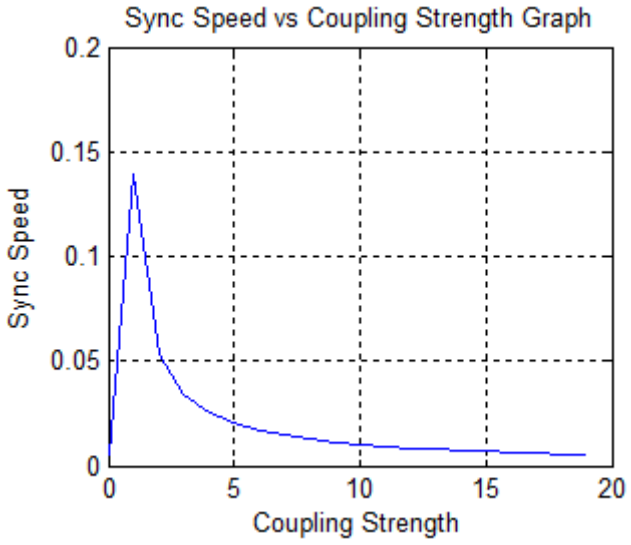

Figure 4.54: “Synchronization speed vs. coupling strength” plot for graph type: all-to-all, coupling function: saturation, w=1 rad/sec.

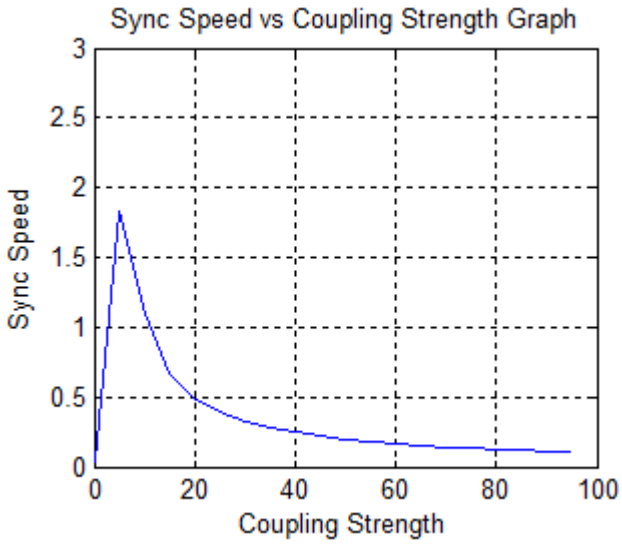

Figure 4.55: “Synchronization speed vs. coupling strength” plot for graph type: all-to-all, coupling function: saturation, w=10 rad/sec.

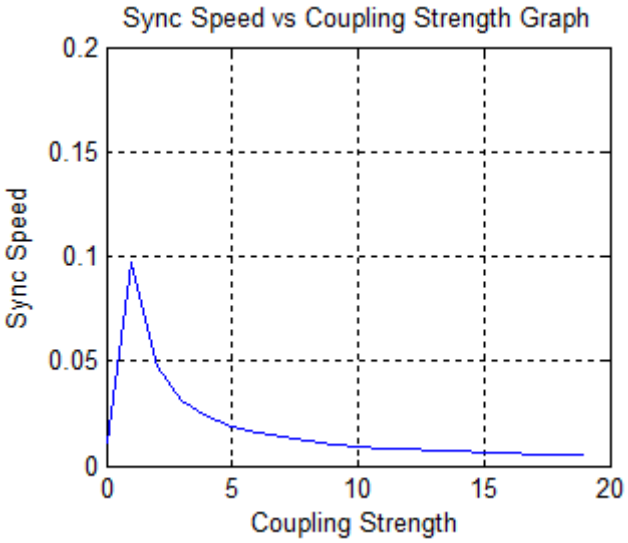

Figure 4.56: “Synchronization speed vs. coupling strength” plot for graph type: all-to-all, coupling function: linear, w=1 rad/sec.

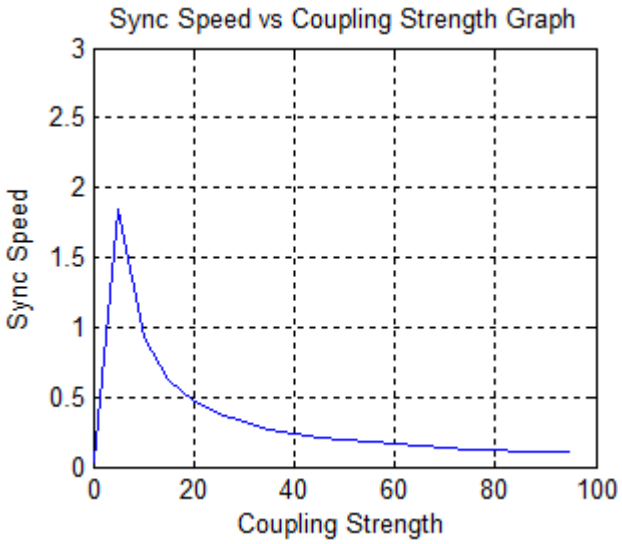

Figure 4.57: "Synchronization speed vs. coupling strength" plot for graph type: all-to-all, coupling function: linear, w=10 rad/sec.

Between Figure-4.54 and Figure-4.57 "all-to-all" coupling graph is used. In these plots we observe that synchronization speed increases up to a point and then it starts to decrease and finally it nearly reaches to the saturation. Comparing the plots with different frequency values, w=1 rad/sec and w=10 rad/sec, it is understood that the coupling strength value where the upper limit of the synchronization speed occurs is affected by the frequency of the agents. Taking coupling function linear, for w=1 rad/sec the upper speed limit is obtained around strength s=0.3 and for w=10 rad/sec the upper speed limit is obtained around strength s=3.

Let $\varepsilon_i = [q_i \, p_i]^T$, $S(w) = \begin{bmatrix} 0 & w \\ -w & 0 \end{bmatrix}$, H=[0 1] and s is the coupling strength. Then

$$\dot{\varepsilon}_i = S(w)\varepsilon_i + sH^T \sum_{j=1}^{N} \lambda_{ij}(H(\varepsilon_j - \varepsilon_i)) \tag{4.2}$$

In Chapter 3, we already mentioned that the frequency part, $S(w)\varepsilon_i$, is the rotation term and $sH^T \sum_{j=1}^{N} \lambda_{ij}(H(\varepsilon_j - \varepsilon_i))$ term is the coupling or consensus term. When the frequency is much larger than the coupling, it means the rotation is rapid, but the coupling is weak. Hence, synchronization speed will be slow. When frequency

value is not large and coupling term is high, the rotation is slow and coupling is strong. In this case the synchronization speed is slow again. Therefore, we can conclude that the synchronization speed is related not only to coupling strength but also to frequency. We will analyze the "synchronization speed vs. frequency" relation in the next section, but first it is good to see the simulation results of "synchronization speed vs. coupling strength" relation for other graph types: tree and ring.

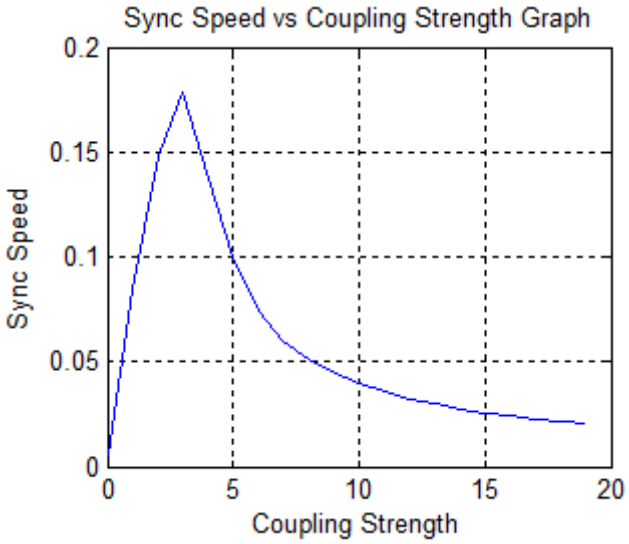

Figure 4.58: "Synchronization speed vs. coupling strength" plot for graph type: tree, coupling function: saturation, w=1 rad/sec.

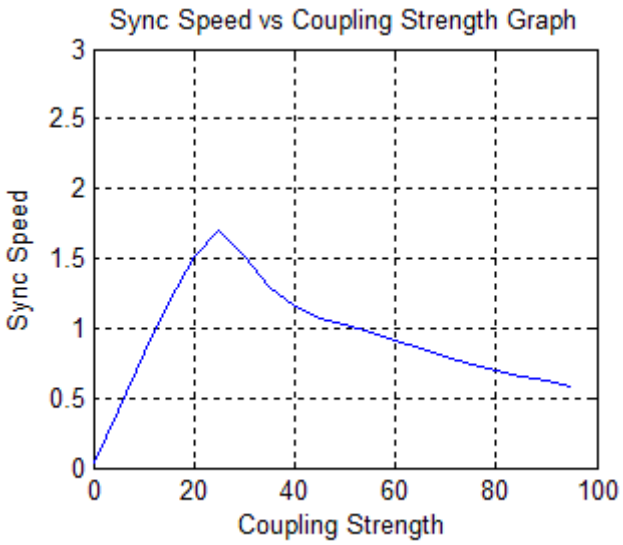

Figure 4.59: “Synchronization speed vs. coupling strength” plot for graph type: tree, coupling function: saturation, w=10 rad/sec.

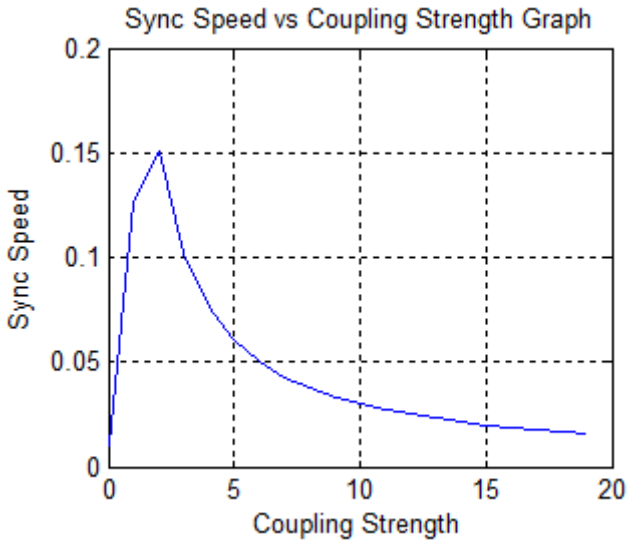

Figure 4.60: “Synchronization speed vs. coupling strength” plot for graph type: tree, coupling function: linear, w=1 rad/sec.

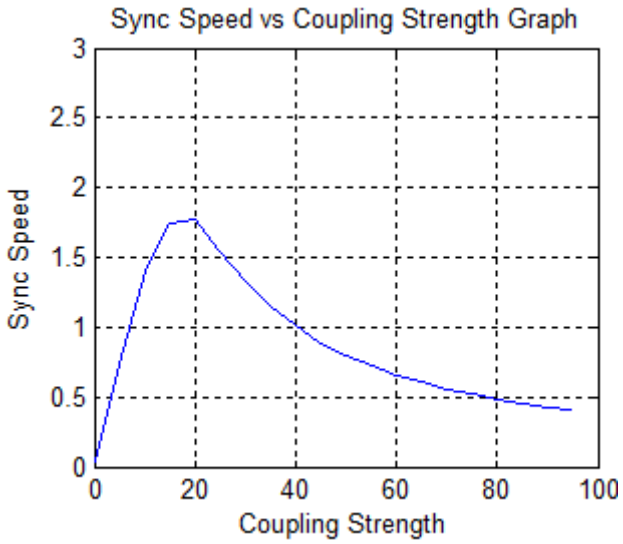

Figure 4.61: “Synchronization speed vs. coupling strength” plot for graph type: tree, coupling function: linear, w=10 rad/sec.

Between Figure 4.58 and Figure 4.61, the coupling graph is chosen as “tree”. In these plots, we almost have the same scenario like in the case of “all-to-all” coupling graph plots. In all plots, we see that there is a coupling strength value where the synchronization speed reaches the peak. As the coupling strength is moving away from the peak value, speed starts to decrease in either direction.

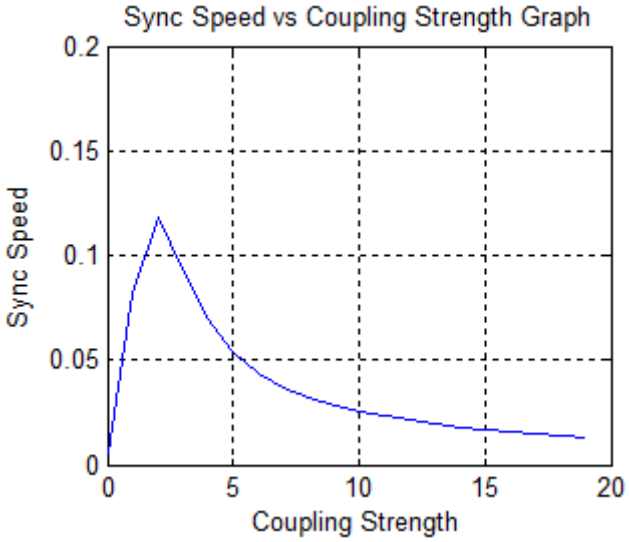

Figure 4.62: “Synchronization speed vs. coupling strength” plot for graph type: ring, coupling function: saturation, w=1 rad/sec.

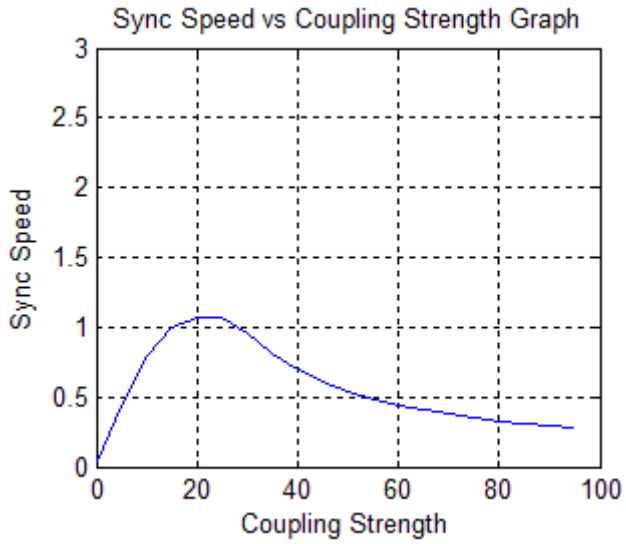

Figure 4.63: "Synchronization speed vs. coupling strength" plot for graph type: ring, coupling function: saturation, w=10 rad/sec.

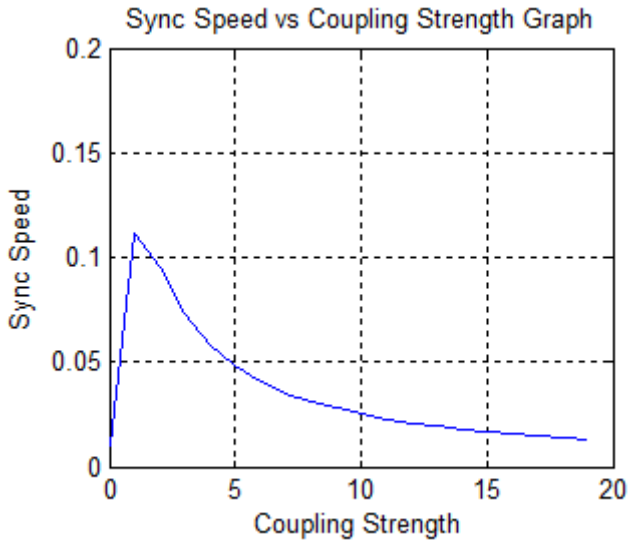

Figure 4.64: "Synchronization speed vs. coupling strength" plot for graph type: ring, coupling function: linear, w=1 rad/sec.

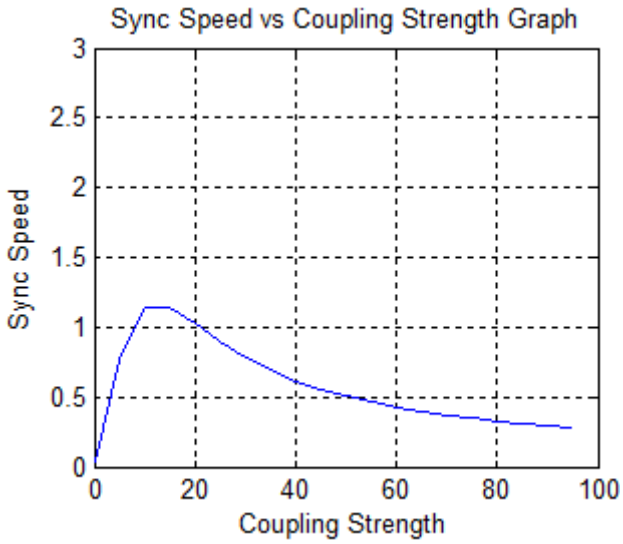

Figure 4.65: "Synchronization speed vs. coupling strength" plot for graph type: ring, coupling function: linear, w=10 rad/sec.

Between Figure 4.62 and Figure 4.65, coupling graph is chosen as "ring". These plots have almost the same shape with plots between Figure 4.54 and Figure 4.61. Therefore, we can say that coupling graph type has no significant effect on the shape of the speed vs. coupling strength plot. However, it affects the coupling strength value where the synchronization speed reaches the peak. Frequency and coupling function are other two parameters which affect the coupling strength value where the peak speed occurs.

To wrap up, coupling strength is an important parameter which directly affects the synchronization speed. Keeping the frequency of the system at a constant value, there is almost a linear relation between synchronization speed and coupling strength until the synchronization speed reaches its peak value. We will call the coupling strength value where the peak speed is reached as the *limit coupling strength value*. After the limit coupling strength value is exceeded, a quick decrease starts in the synchronization speed. As the coupling strength increases, the decrease on the synchronization speed slows down, but the decrease does not stop. Moreover, as the coupling strength goes to ∞ (infinity), the synchronization speed goes to 0 (zero).

4.2.3 Synchronization Speed vs. Frequency Relation

In this section we study the effect of frequency on synchronization speed. The simulations are run for

-graph types: all-to-all and tree, and ring,

-coupling function: linear, saturation and x^3,

-coupling strength: 1 and 10.

In this section, for each figure we obtain ten different results according to ten randomly chosen initial conditions in the region of [0, 20]. Then, we take the average of the results and plot the average result. Moreover, in each figure we present both the original plots (a) and the zoomed version of the plots (b). The simulation results are as follows:

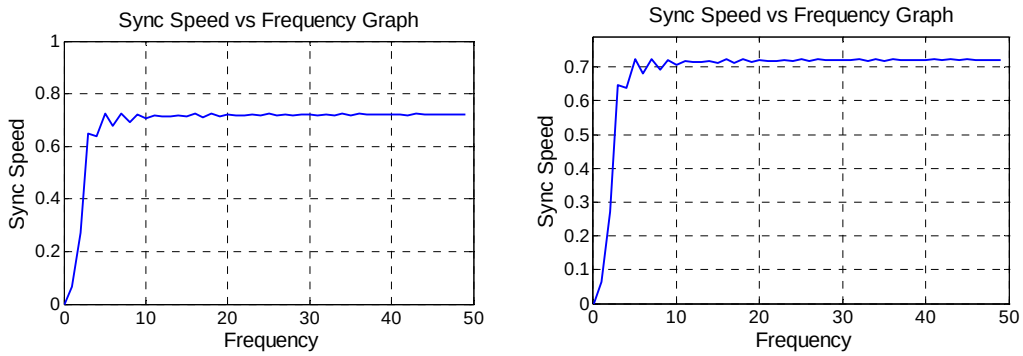

a) b)

Figure 4.66: "Synchronization speed vs. frequency" plot for graph type: all-to-all, coupling function: linear, s=1.

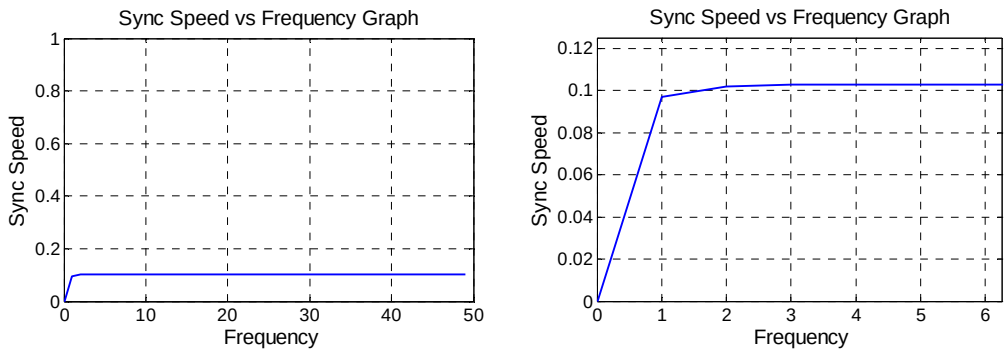

a) b)

Figure 4.67: "Synchronization speed vs. frequency" plot for graph type: tree, coupling function: linear, s=1.

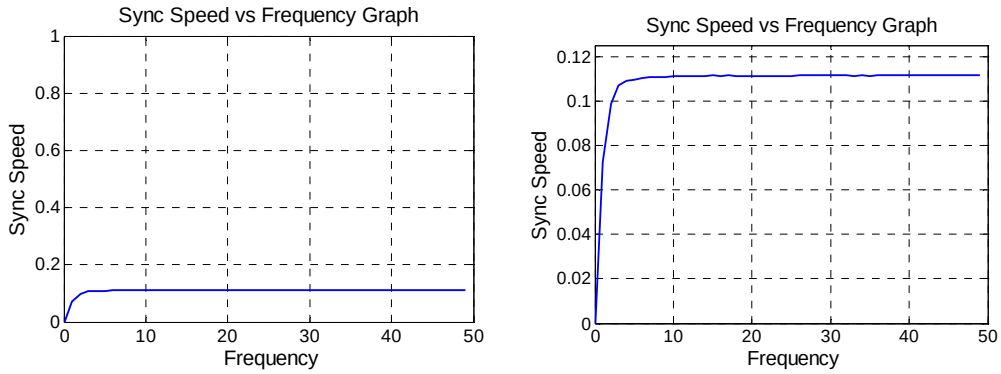

a) b)

Figure 4.68: "Synchronization speed vs. frequency" plot for graph type: ring, coupling function: linear, s=1.

In Figure 4.66, Figure 4.67 and Figure 4.68 the synchronization speed vs. frequency relation is shown for "linear" coupling function and different coupling graph types. All three plots give the same result from the behaviour point of view independent of the coupling graph type. The synchronization speed increases up to an upper limit value, at this limit value the speed reaches to the saturation. We can call the frequency value where the saturation starts as "saturation frequency". For frequency values larger than saturation frequency the synchronization speed stays in the upper limit value. For frequency values lower than saturation frequency, speed limiting factor is frequency. Therefore, as frequency increases the speed increases, as well. However, when the frequency of the agents is larger than the

saturation value, the limiting factor is the coupling function, coupling graph or coupling strength. Therefore, after the saturation value is reached, synchronization speed of the harmonic oscillators saturates and does not change unless the coupling parameters, such as coupling function or coupling strength, between the agents changes.

If we compare the plots shown between Figure 4.66 and 4.68 according to synchronization speed versus coupling graph type, we see that all-to-all coupling results in a faster speed than ring and tree graph types. Tree and ring graph types have almost the same speed values.

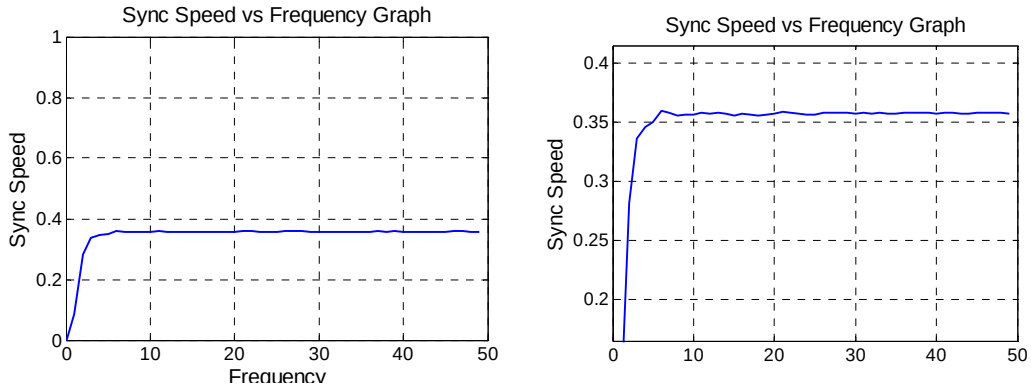

a) b)

Figure 4.69: "Synchronization speed vs. frequency" plot for graph type: all-to-all, coupling function: saturation, s=1.

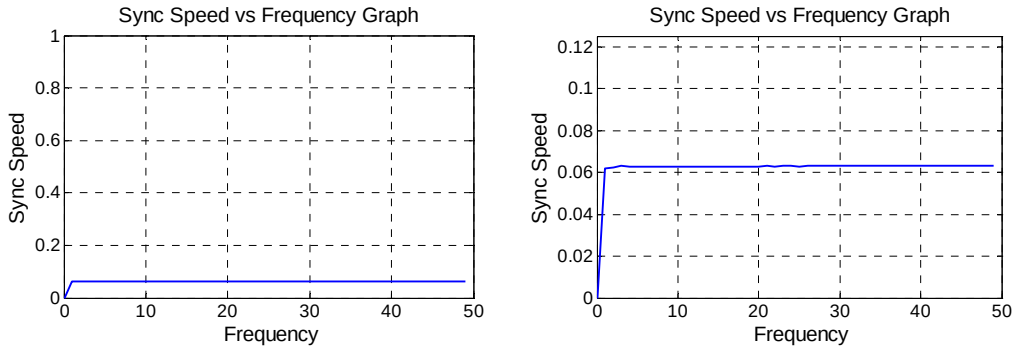

a) b)

Figure 4.70: "Synchronization speed vs. frequency" plot for graph type: tree, coupling function: saturation, s=1.

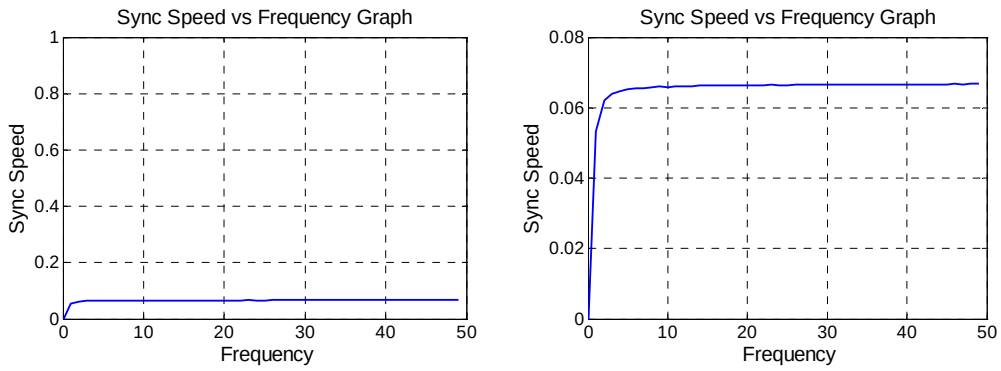

a) b)

Figure 4.71: "Synchronization speed vs. frequency" plot for graph type: ring, coupling function: saturation, s=1.

In Figure 4.69, Figure 4.70, and Figure 4.71 the synchronization speed vs. frequency relation is shown for "saturation" coupling function and different coupling graphs. All three plots give the same result independent of the coupling graph. The plots are very similar to the plots of "linear" coupling function case shown in Figure 4.66, Figure 4.67, and Figure 4.68. The synchronization speed increases up to a saturation value, then it stays fixed for larger frequency values. In the saturation region, the speed limiting factor is either the coupling strength or any other coupling parameter such as coupling function. Only difference between "linear" and "saturation" coupling functions is synchronization speed of linear function type is faster than the saturation function type.

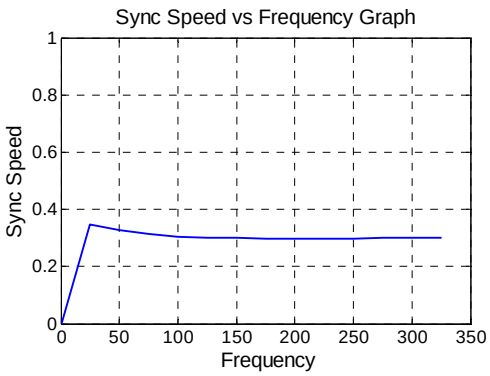

a)

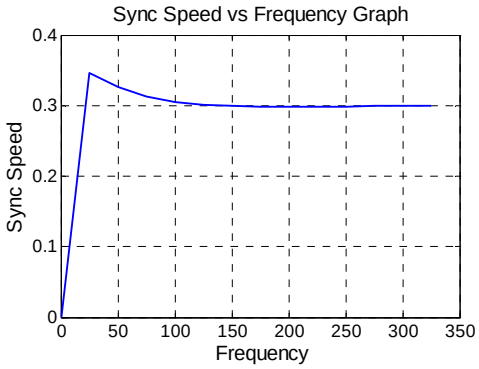

b)

Figure 4.72: "Synchronization speed vs. frequency" plot for graph type: all-to-all, coupling function: x^3, s=1.

In Figure 4.72, synchronization speed vs. frequency plot is given for "all-to-all" coupling graph and "x^3" coupling function. In this plot we observe a different characteristic from the plots shown between Figure 4.66 and Figure 4.71. After speed reaches a peak, it does not saturate but it decreases up to a point, and then speed saturates. Moreover, synchronization speed shown in Figure 4.72 saturates at a higher frequency value than the plots shown between Figure 4.66 and Figure 4.71.

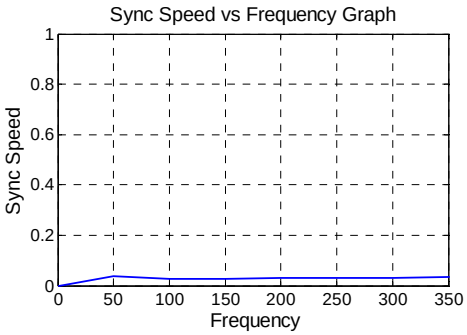

a)

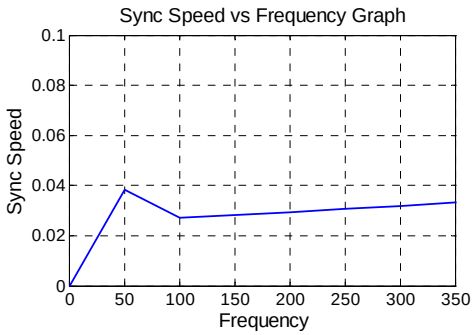

b)

Figure 4.73: "Synchronization speed vs. frequency" plot for graph type: ring, coupling function: x^3, s=1.

In Figure 4.73, synchronization speed vs. frequency plot is given for ring coupling graph and "x^3" coupling function. The result of coupling graph "ring" case is a bit

different from the other plots shown for “synchronization speed vs. frequency”. In Figure 4.73, we do not observe the saturation, but we observe a small increase for high frequency values. However, we expect that as frequency goes to ∞ (infinity) synchronization speed reaches to the saturation.

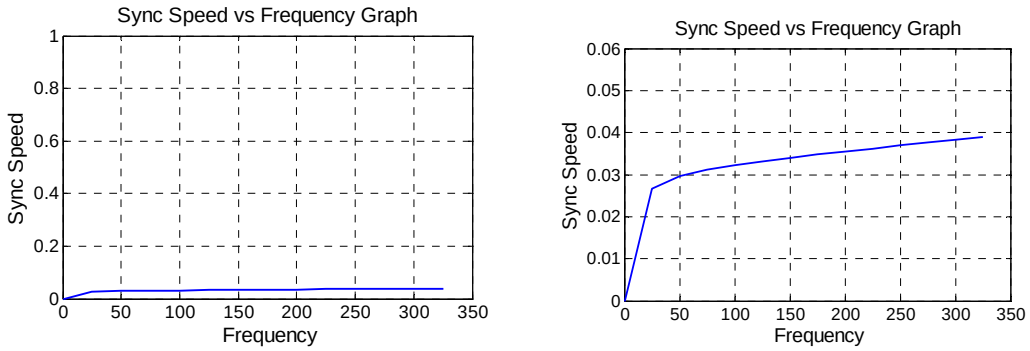

a) b)

Figure 4.74: “Synchronization speed vs. frequency” plot for graph type: tree, coupling function: x^3, s=1.

In Figure 4.74, two different “synchronization speed vs. frequency” plots are given for tree coupling graph and “x^3” coupling function. The result of coupling graph tree case is the same with ring coupling function type. In Figure 4.74, we do not observe the saturation, but we observe a small increase for high frequency values. However, we expect that as frequency goes to ∞ (infinity) synchronization speed reaches to the saturation.

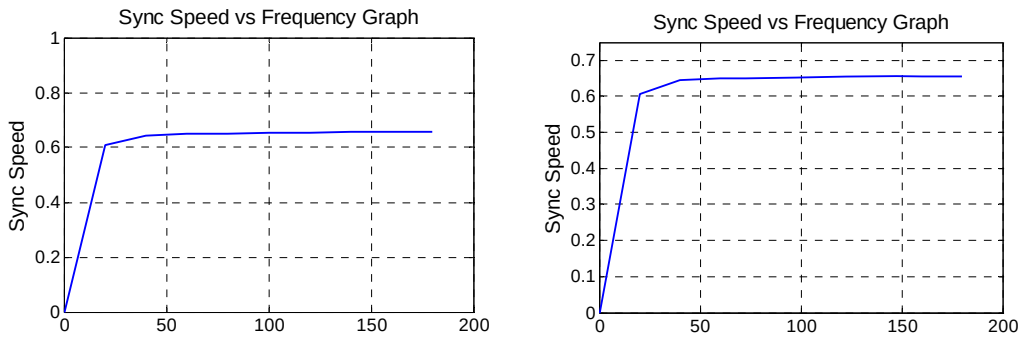

a) b)

Figure 4.75: "Synchronization speed vs. frequency" plot for graph type: ring, coupling function: saturation, s=10.

In Figure 4.75, the coupling strength is chosen as s=10 and the effect of coupling strength on synchronization speed vs. frequency relation is investigated. Figure 4.71 and Figure 4.75 have the same coupling graph and coupling function types. The only different parameter is the coupling strength. The shapes of the two plots are almost same. However, there is one difference between the plots: frequency value where the saturation occurs. The two plots tell us that when the coupling strength increases the saturation frequency value increases, as well. This result is not surprising. We know that after saturation is reached, one of the speed limiting factors is the coupling strength. Therefore, if we increase the coupling strength, synchronization speed also increases and the frequency value, where saturation occurs, shifts to a larger value.

To wrap up, for linear and saturation coupling functions as frequency increases synchronization speed increases up to a saturation value and after the saturation is reached, speed stays fixed at this saturation value. For x^3 coupling function we could not achieve to a definite generalization. However, we expect that as frequency goes to infinity, synchronization speed saturates for x^3 coupling function, as well.

4.2.4 Synchronization of Non-identical Harmonic Oscillators

In this section non-identical harmonic oscillators will be studied. The simulations are run for

- graph type: all-to-all,

- coupling function: linear, saturation, and x^3,

- coupling strength: 1 and 10,

- frequency: 1 rad/sec,

- Δw=2%, 5%, 10%, and 25%.

The simulation results are as follows:

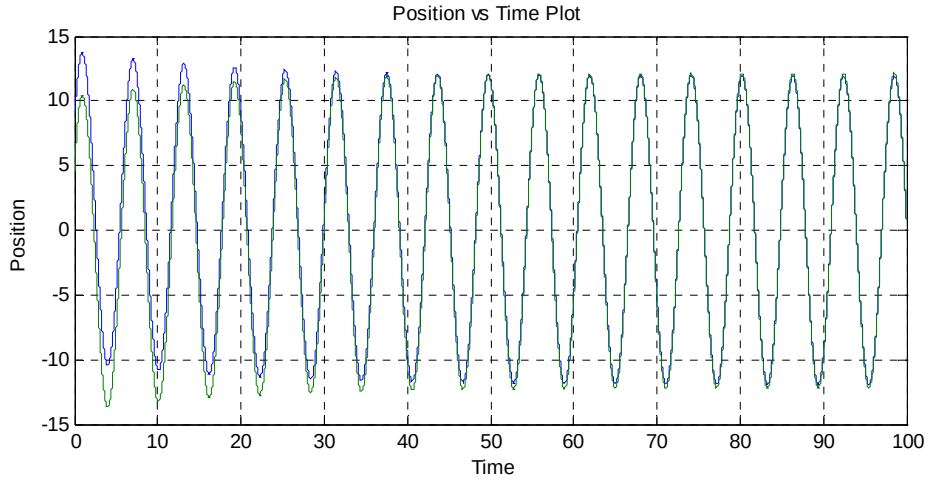

Figure 4.76: "Position vs. time" plot for graph type: all-to-all, coupling function: saturation, s=10, agent number=2, Δw=5%.

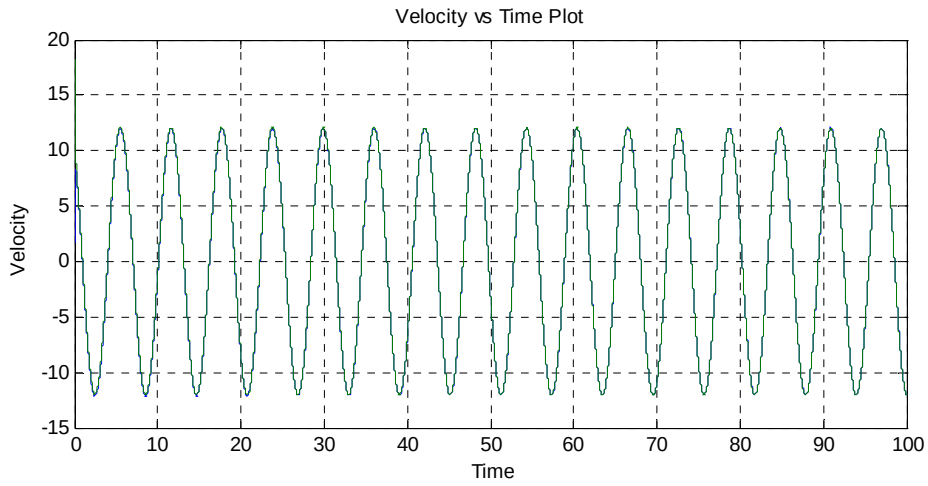

Figure 4.77: "Velocity vs. time" plot for graph type: all-to-all, coupling function: saturation, s=10, agent number=2, Δw=5%.

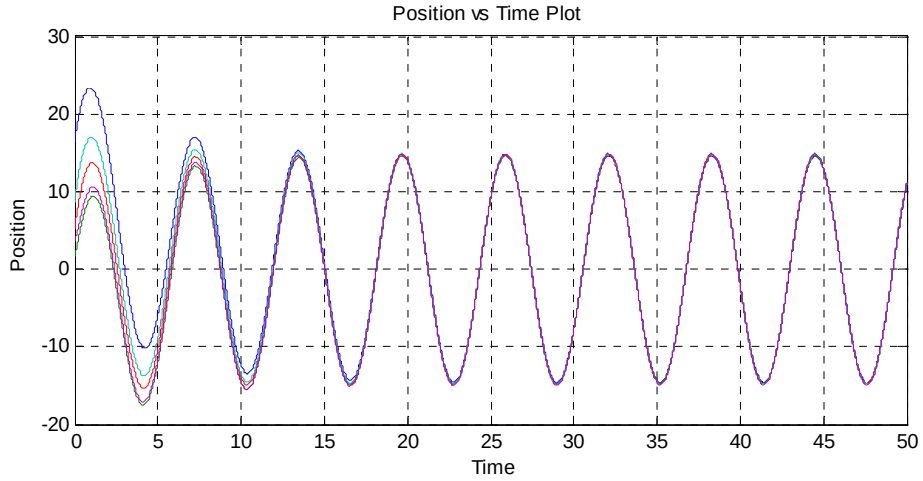

Figure 4.78: "Position vs. time" plot for graph type: all-to-all, coupling function: saturation, s=1, agent number=5, Δw=2%.

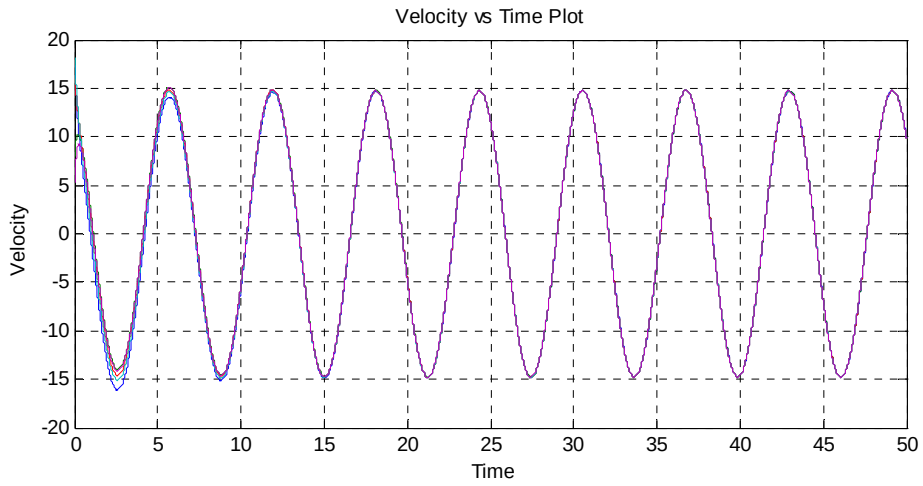

Figure 4.79: "Velocity vs. time" plot for graph type: all-to-all, coupling function: saturation, s=1, agent number=5, Δw=2%.

In Chapter 1, we have already talked about linearly coupled non-identical harmonic oscillators provided that frequency detuning is small. In Figure 1.9 and Figure 1.10, we see that if the frequency difference of the harmonic oscillators is small enough, linearly coupled oscillators synchronize to a common frequency. In other words, harmonic oscillators are locked at the same frequency. Secondly, even though phases of the agents did not become the same, the agents are locked at a certain phase difference.

In this chapter, the simulations are run for nonlinear coupling. In Figure 4.76 and Figure 4.77, the agent number is 2, w_1=1 rad/sec, w_2=1.05 rad/sec and coupling function is saturation. In Figure 4.78 and Figure 4.79, the agent number is 5, w_1=1 rad/sec, w_2=1.05 rad/sec, w_3, w_4 and w_5 are selected randomly between 1 and 1.05 rad/sec and coupling function is saturation. The simulation results of nonlinearly coupled non-identical harmonic oscillators are very similar to the case of linear coupling. Analyzing the Figure 4.78 and Figure 4.79 we understand that the synchronization is achieved which means their frequencies became equal and the phase difference is fixed to a constant value.

The previous simulation results showed that when the difference between the frequencies of the harmonic oscillators is small, harmonic oscillators synchronize

in both linear and nonlinear case. In the rest of the section, we will analyze what happens if the frequency detuning is high.

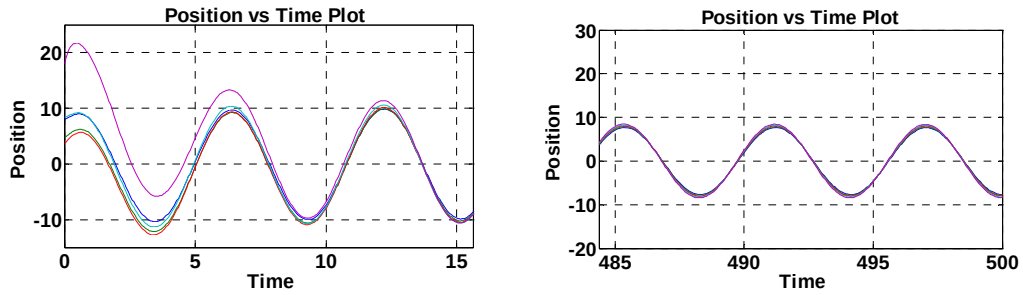

Figure 4.80: "Position vs. time" plots for graph type: all-to-all, coupling function: linear, N=5, s=1, Δw=10%.

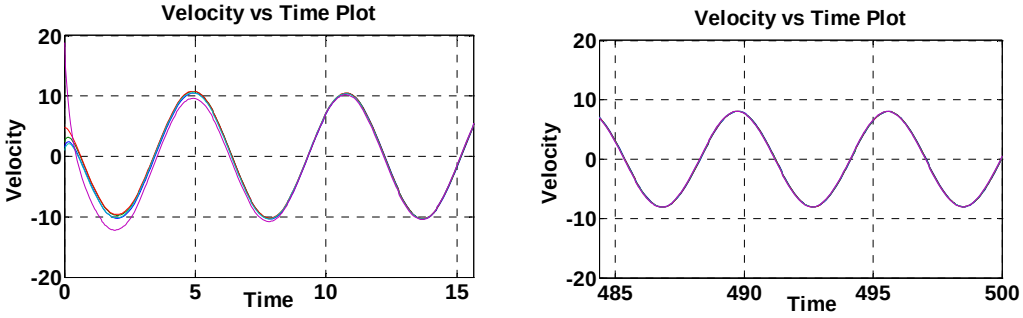

Figure 4.81: "Velocity vs. time" plots for graph type: all-to-all, coupling function: linear, N=5, s=1, Δw=10%.

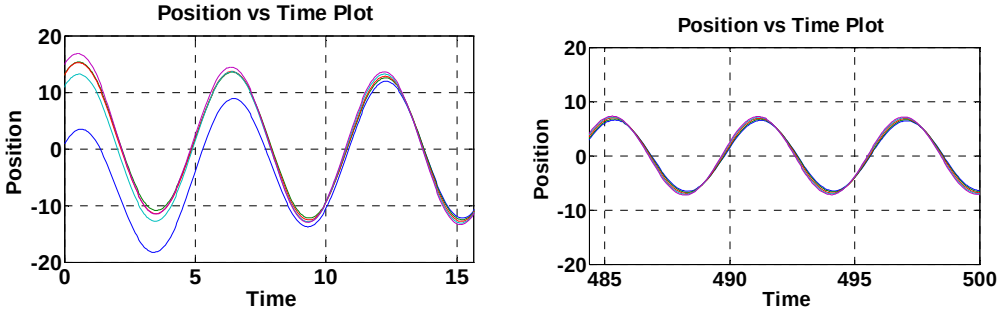

Figure 4.82: "Position vs. time" plots for graph type: all-to-all, coupling function: x^3, N=5, s=1, Δw=10%.

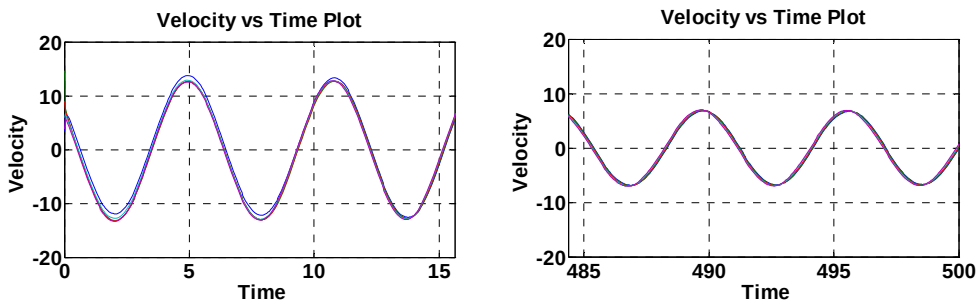

Figure 4.83: "Velocity vs. time" plots for graph type: all-to-all, coupling function: x^3, N=5, s=1, Δw=10%.

Between Figure 4.80 and Figure 4.83, the plots of both linearly and nonlinearly coupled harmonic oscillators of which coupling graph is all-to-all and the frequency detuning between each oscillator is 10% are illustrated. In both plots, we observe that synchronization is not achieved. However, as time goes to infinity, the states of the harmonic oscillators dissipate their energies and converge to zero. Since the frequency and phase values are different for each harmonic oscillator, until harmonic oscillators converge to zero, there is no synchronization between the coupled harmonic oscillators. However, when they converge to the origin, it is not wrong to say that they are synchronized.

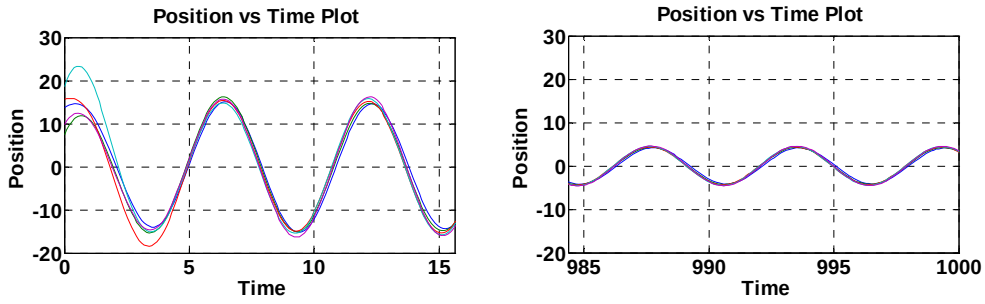

Figure 4.84: "Position vs. time" plots for graph type: ring, coupling function: linear, N=5, s=1, Δw=10%.

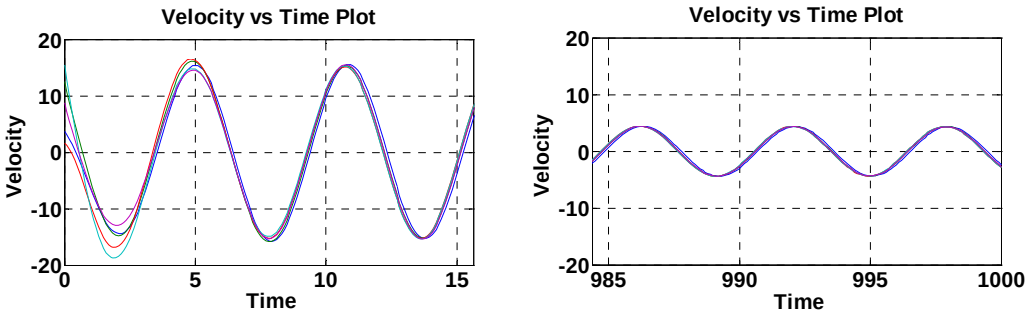

Figure 4.85: "Velocity vs. time" plots for graph type: ring, coupling function: linear, N=5, s=1, Δw=10%.

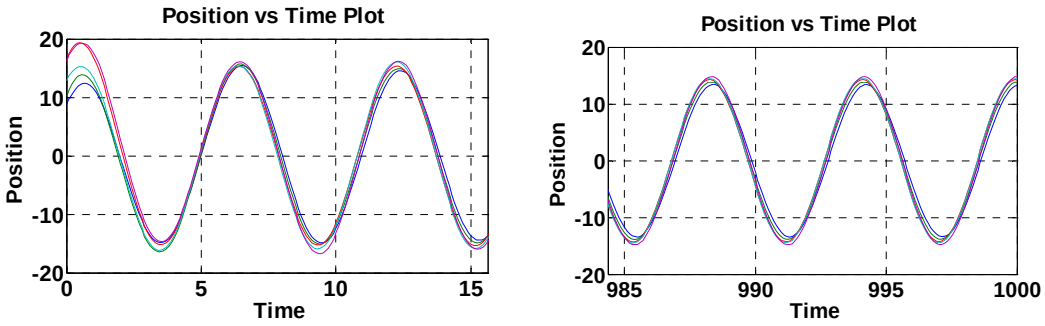

Figure 4.86: "Position vs. time" plots for graph type: ring, coupling function: x^3, N=5, s=1, Δw=10%.

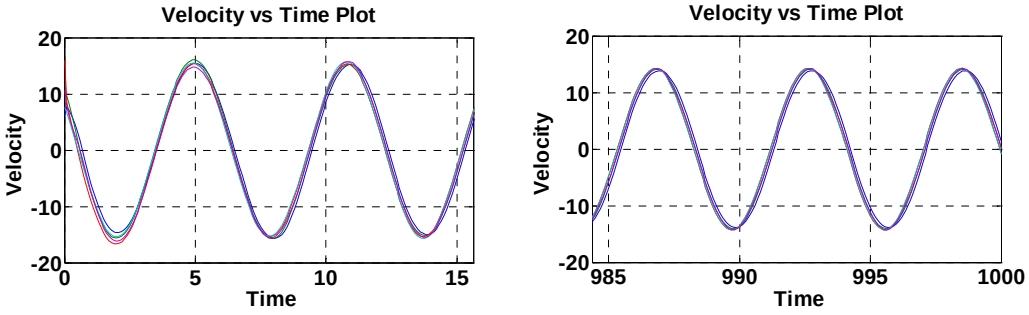

Figure 4.87: "Velocity vs. time" plots for graph type: ring, coupling function: x^3, N=5, s=1, Δw=10%.

In Figure 4.84 and Figure 4.87, the plots of both linearly and nonlinearly coupled harmonic oscillators of which coupling graph is ring and the frequency detuning between each oscillator is 10% are illustrated. The result is the same as in the case of all-to-all coupling graph. The agents do not synchronize until they converge to origin.

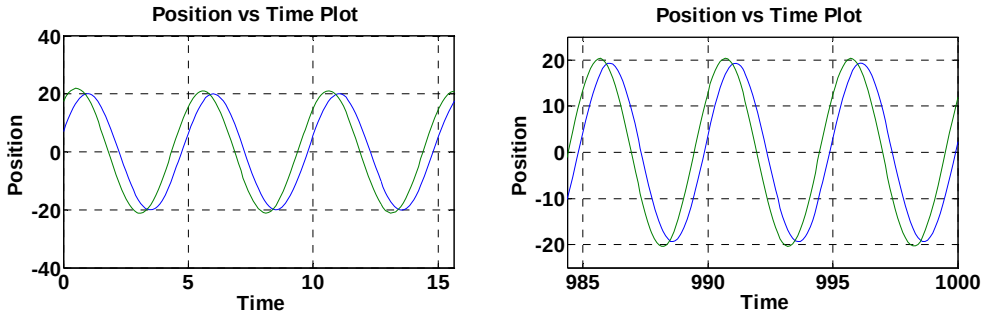

Figure 4.88: "Position vs. time" plots for graph type: tree, coupling function: linear, N=2, s=1, Δw=25%.

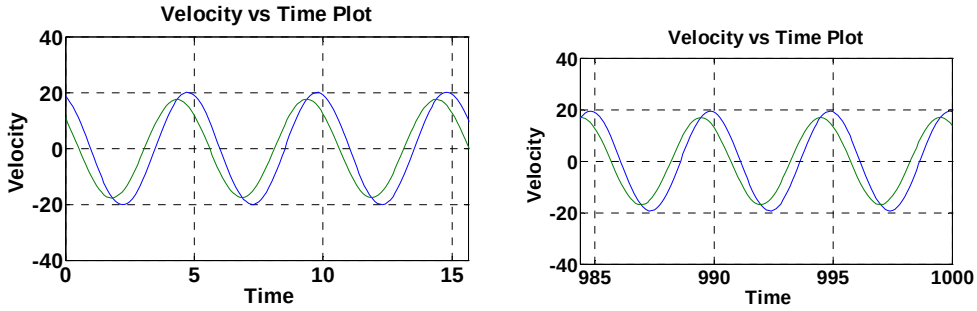

Figure 4.89: "Velocity vs. time" plots for graph type: tree, coupling function: linear, N=2, s=1, Δw=25%.

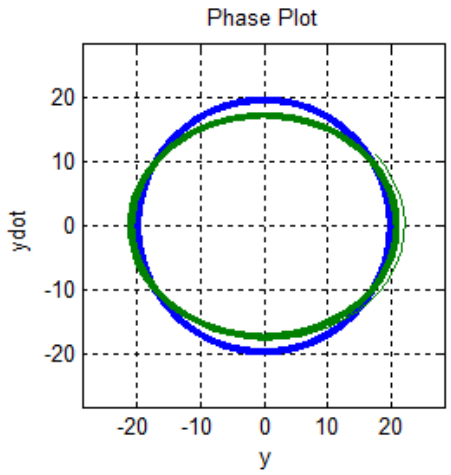

Figure 4.90: Phase plot for graph type: tree, coupling function: linear, N=2, s=1, Δw=25%.

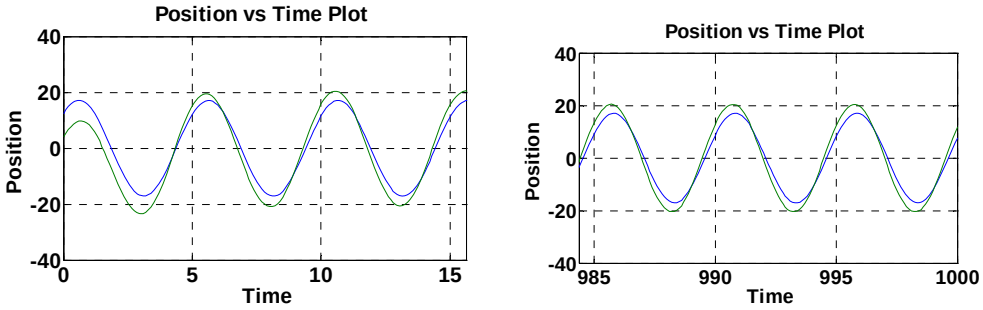

Figure 4.91: "Position vs. time" plots for graph type: tree, coupling function: x^3, N=2, s=1, Δw=25%.

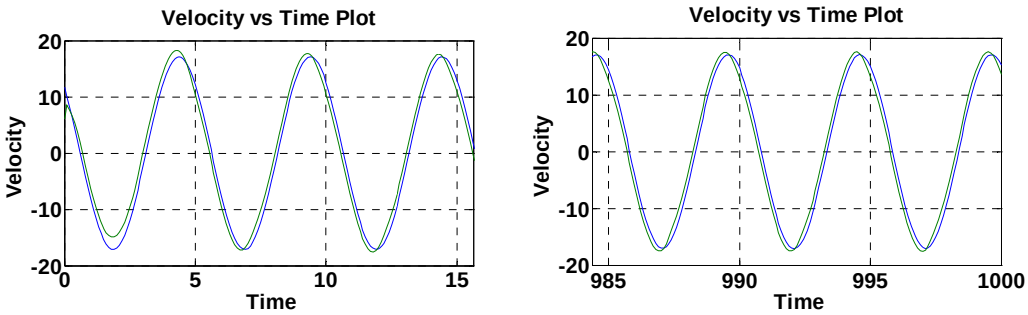

Figure 4.92: "Velocity vs. time" plots for graph type: tree, coupling function: x^3, N=2, s=1, Δw=25%.

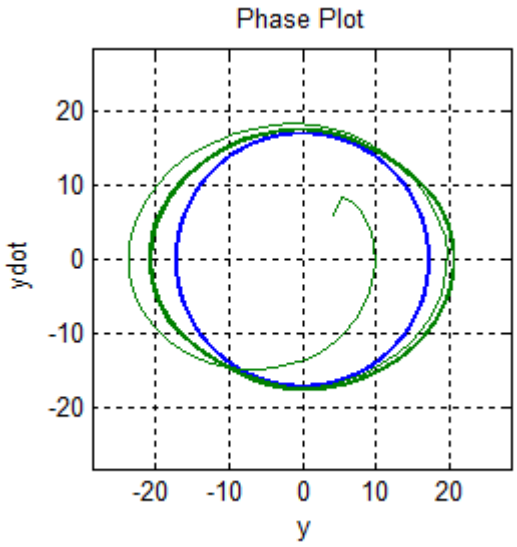

Figure 4.93: Phase plot for graph type: tree coupling function: x^3, N=2, s=1, Δw=25%.

Between Figure 4.88 and Figure 4.93, the plots of both linearly and nonlinearly coupled harmonic oscillators of which coupling graph is tree and the frequency detuning between the oscillators is 25% are illustrated. The results of these simulations, which are run for coupling graph "tree", are different from all-to-all and ring coupling graphs. When the coupling graph is tree, there is one leader agent and all other agents are affected by the leader agent. Therefore, in the plots between Figure 4.88 and Figure 4.93, the agents do not converge to zero. Moreover, the phase plots show that while the leader agent rotates according to its frequency independent of the other agent, rotation of the other agent depends not only to its internal frequency, but also to the coupling relation with the leader agent. Although leader agent affects the rotation of the other agent, synchronization does not occur due to high frequency tuning.

The last simulations in this section will be about effect of coupling strength on frequency detuning.

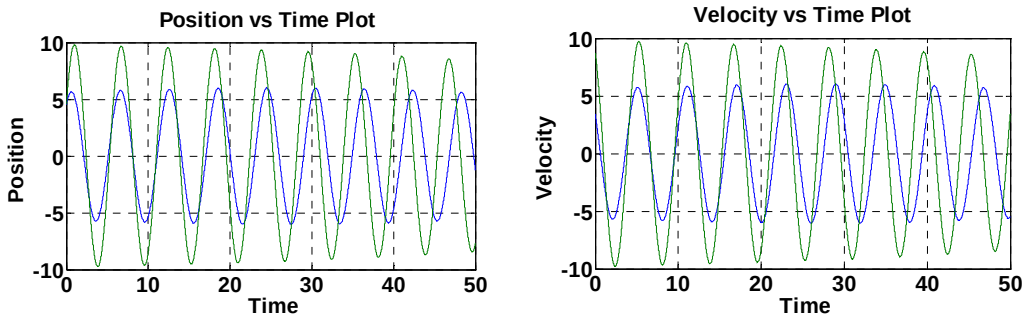

Figure 4.94: “Position vs. time” and “velocity vs. time” plots for graph type: all-to-all, coupling function: linear, N=2, s=0.01, Δw=5%.

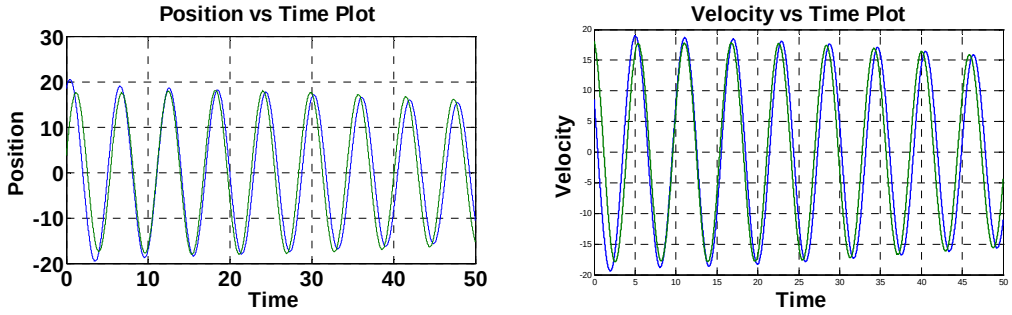

Figure 4.95: “Position vs. time” and “velocity vs. time” plots for graph type: all-to-all, coupling function: linear, N=2, s=0.1, Δw=5%.

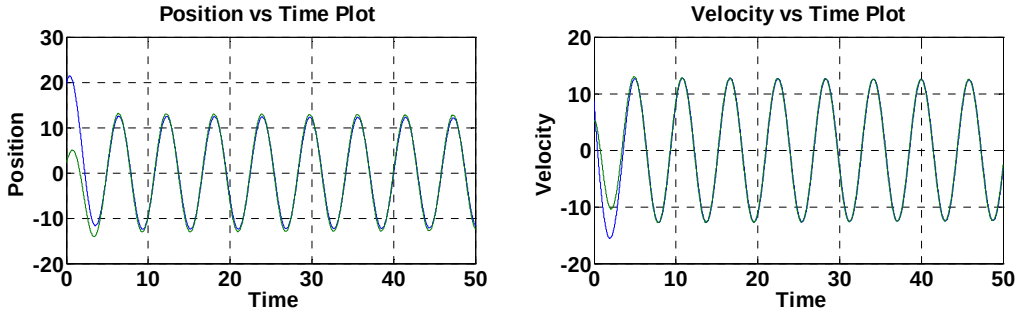

Figure 4.96: “Position vs. time” and “velocity vs. time” plots for graph type: all-to-all, coupling function: linear, N=2, s=1, Δw=5%.

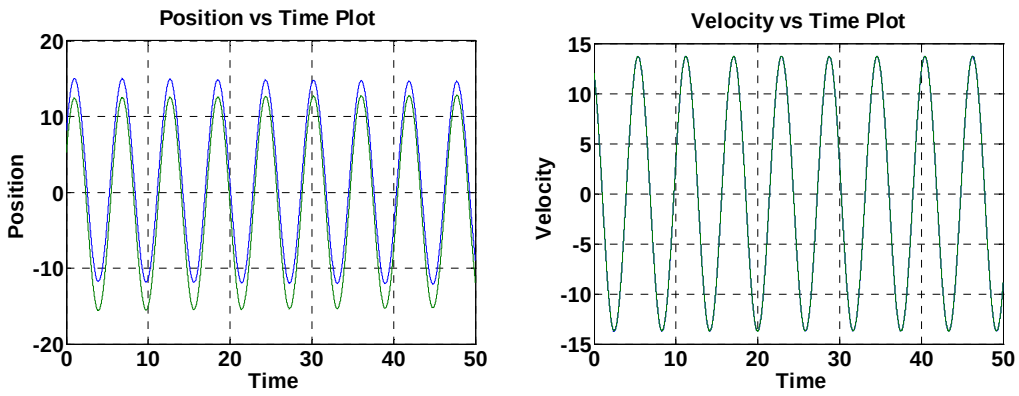

Figure 4.97: “Position vs. time” and “velocity vs. time” plots for graph type: all-to-all, coupling function: linear, N=2, s=100, Δw=5%.

In Figure 4.94, Figure 4.95, Figure 4.96, and Figure 4.97, the plots of linearly coupled harmonic oscillators of which coupling graph is all-to-all and the frequency detuning between oscillators is 5% are illustrated. The simulation results show that as the coupling strength increases, synchronization probability of the coupled non-identical harmonic oscillators increase, as well. However, when the coupling strength is very high, the synchronization speed is too slow. Therefore, even though synchronization is achieved, we can not observe it by the simulations, see Figure 4.97.

To sum up, in this chapter we have first introduced the simulator GUI user interface of MATLAB and the algorithms running behind the GUI. In the rest of the chapter, we have given the simulation results about synchronization of coupled harmonic oscillators. First, we have studied the synchronization vs. frequency relation for both linear and nonlinear coupling. In the next section, we have shown the simulation results about synchronization speed vs. coupling strength relation. Next, we have given the simulations results of synchronization speed vs. frequency relation. Finally, we have investigated synchronization of non-identical harmonic oscillators.

CHAPTER 5

CONCLUSION AND FUTURE WORK

5.1 CONCLUSION

In the thesis, we have worked on the synchronization of both linearly and non-linearly coupled harmonic oscillators for various coupling graphs, coupling functions, coupling strength values, and frequencies. The aim of thesis is to compare theoretical results with simulation results and present an extensive analysis about behavior of coupled harmonic oscillators for various different conditions.

The thesis consists of two main stages. The first one is the theoretical part. The theoretical part is given in the first three chapters. In Chapter 1, the very basics and historical evolution of the synchronization is explained and a brief information about linearly and nonlinearly coupled harmonic oscillators are introduced. In Chapter 2, linearly coupled harmonic oscillators are studied from theoretical point of view and in Chapter 3 theoretical concept of nonlinearly coupled harmonic oscillators is given in detail.

The second stage consists of the simulation results. The simulation results are given in Chapter 4. In this chapter, initially the user interface, GUI, and the algorithms are introduced. Then, the simulation results for the following list are given:

- ✓ Effect of frequency on the synchronization of both linearly and nonlinearly coupled harmonic oscillators.
- ✓ Effect of coupling strength on the synchronization speed of both linearly and nonlinearly coupled harmonic oscillators.

- ✓ Effect of coupling graph on the synchronization speed of both linearly and nonlinearly coupled harmonic oscillators.
- ✓ Synchronization of non-identical harmonic oscillators.

As a result, the simulation results have shown us that if the coupling graph is connected, the harmonic oscillators synchronize for both linear and nonlinear coupling and for any frequency.

Secondly, we have observed that coupling strength plays an important role on the synchronization of the harmonic oscillators. As coupling strength increases, the synchronization speed also increases until it reaches a peak speed value for a limit coupling strength value. Once the peak speed is reached, as coupling strength further increases, the synchronization speed decreases.

Thirdly, we have seen that when the frequency of harmonic oscillators increase, the synchronization speed increases until it reaches a saturation value, for higher frequency values synchronization speed stays constant.

Finally, frequency detuning and non-identical harmonic oscillators are studied. The simulations about frequency detuning have shown us that there are two important parameters affecting the synchronization of non-identical harmonic oscillators: Coupling strength and difference between the frequencies of the oscillators. In the case of low frequency detuning and high coupling strength, harmonic oscillators synchronize. However, if the coupling is weak or the frequency detuning is high, harmonic oscillators do not synchronize until they converge to the origin.

5.2 FUTURE WORK

As extensions of this thesis, the following future work can be recommended:

- In the thesis, there are some simulation results, which are not theoretically proved, such as synchronization of nonlinearly coupled harmonic oscillators for $w \approx 1$ and convergence of the non-identical harmonic oscillators to the origin. In a later study, one can try to give the theoretical proof of the simulation results which are not proved in this thesis.

- Synchronization of any other type of oscillators like Van Der Pol and integrate-and-fire oscillators or nonlinear coupling models such a Kuramoto model are also worth to study.
- The simulations can be realized by experimentally with the oscillator circuits in a laboratory. In this way, the simulation results and real life results can be compared.

REFERENCES

[1] A. Pikovsky, M. Rosenblum, and J. Kurths, *Synchronization: A Universal Concept in Nonlinear Sciences*. New York: Cambridge University Press, 2001.

[2] G. S. Balaraman and N. Ananthkrishnan, "Synchronization: A Heuristic Approach," *Resonance,* pp. 14-25, May 2005.

[3] S. H. Strogatz, *Sync: The Emerging Science of Spontaneous Order*, First ed. New York: Hyperion, 2003.

[4] S. H. Strogatz and I. Stewart, "Coupled Oscillators and Biological Synchronization," *Scientific American,* vol. 269, pp. 102-109, Dec 1993.

[5] L. Scardovi and R. Sepulchre, "Synchronization in networks of identical linear systems," *Automatica,* vol. 45, pp. 2557-2562, 2009.

[6] H. Su, X. Wang, and Z. Lin, "Synchronization of coupled harmonic oscillators in a dynamic proximity network," *Automatica,* vol. 45, pp. 2286-2291, 2009.

[7] L. Glass, "Synchronization and rhythmic processes in physiology," *Nature,* vol. 410, pp. 277-284, Mar 8 2001.

[8] S. J. Aton and E. D. Herzog, "Come together, right...now: Synchronization of rhythms in a mammalian circadian clock," *Neuron,* vol. 48, pp. 531-534, Nov 2005.

[9] N. Price-Lloyd, M. Elvin, and C. Heintzen, "Synchronizing the Neurospora crassa circadian clock with the rhythmic environment," *Biochemical Society Transactions,* vol. 33, pp. 949-952, Nov 2005.

[10] R. E. Mirollo and S. H. Strogatz, "Synchronization of Pulse-Coupled Biological Oscillators," *Siam Journal on Applied Mathematics,* vol. 50, pp. 1645-1662, Dec 1990.

[11] S. H. Strogatz, "Spontaneous synchronization in nature," *Proceedings of the 1997 IEEE International Frequency Control Symposium,* pp. 2-4, 1997.

[12] L. O'Hanlon. *Fireflies Blink in Sync*. Available: http://news.discovery.com /animals/fireflies-syncronize-flash.html [Last visited on 02/01/2011]

[13] Title: Wikipedia, Oscillation, Available: http://en.wikipedia.org/wiki/ Oscillation [Last visitd on 22/11/2010]

[14] J. M. González-Miranda, "Dynamics of coupled and driven harmonic oscillators," in *Synchronization and Control of Chaos*, First ed. London: Imperial College Press, 2004.

[15] B. Linares-Barranco and A. Rodríguez-Vázquez, "Harmonic Oscillators," in *Encyclopedia of Electrical and Electronics Engineering*. vol. 8, J. G. Webster, Ed., John Wiley & Sons, Inc, 1999, pp. 632-642.

[16] Title: Wikipedia, Graph (mathematics), Available: http://en.wikipedia.org/ wiki/Graph_(mathematics) [Last visited on 12/01/2011]

[17] Title: Wolfram Mathworld, Projection Matrix Available: http://mathworld. wolfram.com/ProjectionMatrix.html [Last visited on 10/12/2010]

[18] S. E. Tuna. (2008). Conditions for synchronizability in arrays of coupled linear systems. Available: http://arxiv.org/PS_cache/arxiv/pdf/0811/0811.3 530v1.pdf [Last visited on 25/03/2011]

[19] Y. Liu and F. X. Yang, "Some theoretical results of synchronization of a linearly coupled dynamical system with random perturbation on a network," *Journal of Physics a-Mathematical and Theoretical*, vol. 42, pp. , Feb 2009.

[20] I. Belykh, V. Belykh, and M. Hasler, "Generalized connection graph method for synchronization in asymmetrical networks," *Physica D-Nonlinear Phenomena*, vol. 224, pp. 42-51, Dec 2006.

[21] C. W. Wu and L. O. Chua, "Synchronization in an Array of Linearly Coupled Dynamical-Systems," *IEEE Transactions on Circuits and Systems I-Fundamental Theory and Applications*, vol. 42, pp. 430-447, Aug 1995.

[22] W. W. Wang and J. D. Cao, "Synchronization in an array of linearly coupled networks with time-varying delay," *Physica A-Statistical Mechanics and Its Applications*, vol. 366, pp. 197-211, Jul 2006.

[23] L. L. Bonilla, C. J. P. Vicente, and R. Spigler, "Time-periodic phases in populations of nonlinearly coupled oscillators with bimodal frequency distributions," *Physica D*, vol. 113, pp. 79-97, Feb 1998.

[24] J. A. Acebron, L. L. Bonilla, C. J. P. Vicente, F. Ritort, and R. Spigler, "The Kuramoto model: A simple paradigm for synchronization phenomena," *Reviews of Modern Physics*, vol. 77, pp. 137-185, Jan 2005.

[24] J. A. Acebron, L. L. Bonilla, C. J. P. Vicente, F. Ritort, and R. Spigler, "The Kuramoto model: A simple paradigm for synchronization phenomena," *Reviews of Modern Physics,* vol. 77, pp. 137-185, Jan 2005.

[25] G. M. He and J. Y. Yang, "Adaptive synchronization in nonlinearly coupled dynamical networks," *Chaos Solitons & Fractals,* vol. 38, pp. 1254-1259, Dec 2008.

[26] M. Arcak, "Passivity as a design tool for group coordination," *IEEE Transactions on Automatic Control,* vol. 52, pp. 1380-1390, Aug 2007.

[27] C. Cai and S. E. Tuna, "Synchronization of nonlinearly coupled harmonic oscillators," presented at the 2010 American Control Conference, Baltimore, MD, USA, 2010.

[28] L. Moreau, "Stability of multiagent systems with time-dependent communication links," *IEEE Transactions on Automatic Control,* vol. 50, pp. 169-182, Feb 2005.

[29] V. I. Arnold, *Geometrical Methods in the Theory of Ordinary Differential Equations*, second ed. Springer, 1988.